OCT 8 1946

THE JOURNAL OF CHEMICAL PHYSICS

VOLUME 14 NUMBER 9

SEPTEMBER, 1946

Published by the

AMERICAN INSTITUTE OF PHYSICS

Lancaster Press, Inc. New York, N. Y.

JOURNAL OF CHEMICAL PHYSICS

BOARD OF EDITORS

Editor

Associate Editors

Terms ending December 31, 1947

Terms ending December 31, 1948

Subscription Rates

The United States and Possessions, Canada and Mexico $10.00

Elsewhere 11.00

Back Numbers

Complete set: Vol. 1, 1933—Vol. 13, 1945 ..... $130.00

Yearly rate: $11.00.

Single copies: $1.00 each.

Subscriptions and orders for single copies should be addressed to Prince and Lemon Streets, Lancaster, Pennsylvania, or to the American Institute of Physics, 57 East 55 Street, New York 22, New York.

Changes of address should be sent to the Business Manager, American Institute of Physics.

Prince and Lemon Streets, Lancaster, Pennsylvania.

Entered December [illegible], 1932, at the Post Office at Lancaster, Pa., under the Act of August 24, 1912. Acceptance for [illegible], provided for in the Act of February 28, 1925, embodied in paragraph 4, Section 538, P. L. & R.: authorized

cated exponents. The solidus (/) should be used wherever possible for fractions.

All illustrations should accompany manuscript and should always be referred to in the text. Line drawings must be made with India ink on plain white paper or on tracing cloth. Coordinate paper is not desirable, but if used must be blue-lined with all coordinates to be reproduced drawn with India ink. Lettering should be of sufficient size to be legible after reduction.

Proof and all correspondence concerning papers in the process of publication should be addressed to the Publications Manager, American Institute of Physics, 57 East 55 Street, New York 22, New York.

THE JOURNAL
OF
CHEMICAL PHYSICS

VOLUME 14, NUMBER 9 SEPTEMBER, 1946

The Heats of Solution of Hexamethylbenzene, Cetyl Alcohol, and Dicetyl in Related Liquids; Heats of Fusion by an Extrapolation Process

GEORGE S. PARKS AND ROBERT D. ROWE
Department of Chemistry, Stanford University, Stanford University, California

(Received May 6, 1946)

The heats of solution of crystalline hexamethylbenzene, cetyl alcohol, and dicetyl in various related liquids have been obtained at 25°C. Benzene, toluene, xylene, and mesitylene have been used as solvents for hexamethylbenzene, and a value for the heat of fusion of this substance has been deduced from these heats of solution by an extrapolation process. Similarly, a series of alcohols (methyl, ethyl, *n*-butyl, *n*-heptyl, and *n*-dodecyl) have been used for the solution of cetyl alcohol. Solubility limitations, however, made it impractical to employ any liquid paraffin except *n*-heptane in the case of dicetyl. The heats of fusion at 25°C, as estimated from the present solution experiments, are per gram: hexamethylbenzene, 29.0±0.3 cal.; cetyl alcohol, 48.2±0.7 cal.; and dicetyl (dotriacontane), 58.7±1.2 cal.

INTRODUCTION

THE heat of solution of a crystalline substance in a liquid with which it forms an ideal or "perfect" solution is theoretically its heat of fusion at the temperature of the solution process.[1] Accordingly, the calorimeter which the authors[2] previously developed for measuring the heats of solution of various forms of glucose in water has now been used to measure the heats of solution of hexamethylbenzene, cetyl alcohol, and dicetyl (dotriacontane) in some related liquids at about 25°C, and particularly in the case of the first two substances to obtain a fairly accurate value for the heat of fusion at this temperature by an extrapolation process. Fusion data of this sort can then be combined with the heats of combustion, entropies, and free energies of the crystalline substances so as to yield corresponding values at 25° for the hypothetical liquid state. Such a procedure is frequently advantageous, since regularities are more pronounced in any homologous series, or related group, of organic compounds if the comparisons are based upon the liquid state rather than upon the more individualistic crystalline forms.

APPARATUS AND METHOD

The essential features of the calorimetric assembly have been described in our previous paper.[2]

The experimental procedure involved the dissolving of suitable amounts of the crystalline solute (hexamethylbenzene, cetyl alcohol, or dicetyl, as the case might be) in 250 ml portions of related liquids. The initial temperature of these liquids was around 25°, and the amount of crystalline solute employed generally gave a subsequent temperature lowering of about two degrees. The various values for the heats of

[1] J. H. Hildebrand, *Solubility* (Reinhold Publishing Corporation, New York, 1936), second edition, p. 57.
[2] R. D. Rowe and G. S. Parks, J. Chem. Phys. **14**, 383 (1946).

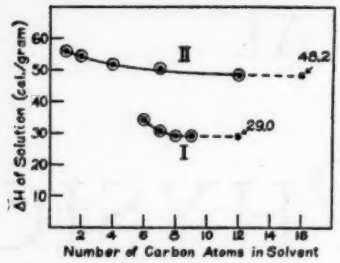

FIG. 1. Graph I shows the mean results for the heats of solution of crystalline hexamethylbenzene in benzene, toluene, xylene, and mesitylene with an extrapolation to a hypothetical value of 29.0 cal./g for the fusion process at 25°C. Likewise, Graph II shows the heats of solution of crystalline cetyl alcohol in a series of normal aliphatic alcohols with an extrapolation to a value of 48.2 cal./g for the fusion process.

solution thus obtained were then adjusted to the reference temperature of 25° by use of Kirchhoff's law with a suitable value for ΔC_p, the difference between the heat capacity of the dissolved and crystalline solute.

The most desirable application of this solution procedure to obtain a value of the heat of fusion of the crystalline solute involves the employment of a series of liquid solvents which approach progressively the chemical formula of the solute. With the aid of the corresponding data for the heats of solution, an extrapolation process to the solute itself can thus yield an accurate value for the heat of fusion. In the present measurements this method gave fairly satisfactory results both for hexamethylbenzene and for cetyl alcohol. However, the very limited solubility[3] of dicetyl in paraffinic hydrocarbons above *n*-heptane rendered such an extrapolation impractical with this particular substance.

SOLUTION DATA FOR HEXAMETHYLBENZENE

The heats of solution of hexamethylbenzene were measured in a series of experiments with benzene, toluene, *m*-xylene, and mesitylene as solvents. The resulting solutions were in all cases 0.287 (±0.003) molal. In this work Eastman's crystalline hexamethylbenzene was used without further purification and the four solvents were high grade C.P. materials. The necessary data for the heat capacities of crystalline and liquid hexamethylbenzene and for liquid benzene, xylene, and mesitylene were derived from the previous investigations of Parks and co-workers[4]; likewise, specific heat values for liquid toluene were deduced from the calorimetric studies of Kelley[5] and of Vold.[6] The various heats of solution were finally adjusted to the standard temperature of 25°C by the assumption of 0.035 calorie per gram per degree for the temperature coefficient of these solution processes.

The enthalpy data so obtained are summarized in Table I and the mean values are also represented graphically in Fig. 1. The values found with xylene and mesitylene as solvents indicate that these heats of solution are rapidly approaching a limiting value as additional methyl groups are introduced into the benzene ring. Accordingly, from our plot we have taken 29.0±0.3 calories as the heat of fusion for a gram of hexamethylbenzene at 25°.

By use of Kirchhoff's law with a value of $\Delta C_p = 0.035$, deduced from the heat capacity data of Spaght, Thomas, and Parks,[4] we have also computed a value of 33.9±0.8 calories per gram for the heat of fusion of hexamethylbenzene at 165.5°C, the normal melting point. Actually Spaght, Thomas, and Parks, by means of their radiation calorimeter, found a heat of fusion of 30.4 cal. per g at the melting point together with a heat of transition of 2.6 cal. per g at 110°C, or thus a total transition-fusion effect of about 33.0±0.8 cal. per g.

SOLUTION DATA FOR CETYL ALCOHOL

The heats of solution of cetyl alcohol were also measured in a series of experiments with methyl, ethyl, *n*-butyl, *n*-heptyl, and *n*-dodecyl alcohols

TABLE I. Heats of solution of crystalline hexamethylbenzene in related liquids at 25°C.

Experiment No.	ΔH_{298} of solution (calories per gram) in Benzene	Toluene	Xylene	Mesitylene
1	34.23	30.89	29.14	29.14
2	34.17	30.64	28.86*	29.20
3	—	—	29.22	—
Mean result	34.20	30.76	29.18	29.17

* This value was omitted in deriving the mean result.

[3] W. F. Seyer, J. Am. Chem. Soc. **60**, 827 (1938).

[4] M. E. Spaght, S. B. Thomas, and G. S. Parks, J. Phys. Chem. **36**, 882 (1932); H. M. Huffman, G. S. Parks, and A. C. Daniels, J. Am. Chem. Soc. **52**, 1547 (1930); H. M. Huffman, G. S. Parks, and M. Barmore, *ibid.* **53**, 3876 (1931).

[5] K. K. Kelley, J. Am. Chem. Soc. **51**, 2738 (1929).

[6] R. D. Vold, *ibid.* **59**, 1515 (1937).

as solvents. Here the resulting solutions were 0.130 (±0.005) molal except in the first experiment with ethyl alcohol, where a 0.210-molal solution was the product. In this work Eastman's cetyl alcohol (m.p. 48–49°) was used without further purification, as previous investigations in this Laboratory had demonstrated that its purity was quite adequate for the present purpose. The first four alcohol solvents were C.P. materials which were further purified by dehydration over quicklime and fractional distillation. The sample of dodecyl alcohol, which had been prepared in this laboratory by Dr. Martin E. Synerholm, was estimated to contain about 90 percent of the normal alcohol with 10 percent of related alcohols. It boiled at 150°–155° at a pressure of 21 mm; its melting point was 17.3°C; and it had a density of 0.8290 at 25°.

The necessary data for the heat capacity of crystalline cetyl alcohol and the first four solvent liquids were obtained from previous studies[7] which had been carried out in our Stanford Laboratory. The specific heat of the liquid dodecyl alcohol was estimated by extrapolation of the data for these lower alcohols.

The various experimental heats of solution were adjusted to 25°C by assuming 0.13 calorie per gram per degree for the temperature coefficient of these solution processes. The enthalpy data so obtained are summarized in Table II and are represented graphically in Fig. 1. Of the several sets of results, those with the dodecyl alcohol are unfortunately the least reliable, partly because of the impurities in this particular preparation and the estimate of its specific heat by extrapolation and partly because the cetyl alcohol samples tended to float on the surface of the solvent liquid and required at least two minutes for the solution process even though the rate of stirring was increased from 505 to 650 r.p.m. In view of these elements of uncertainty only moderate weight was given to the results with dodecyl alcohol in extrapolating the curve in Fig. 1 to yield an ideal value of 48.2 cal. per g for the heat of solution of crystalline cetyl alcohol in a hypothetical liquid cetyl alcohol at 25°C. This value, therefore, represents the heat of fusion at 25°.

[7] G. S. Parks, J. Am. Chem. Soc. **47**, 338 (1925); and an unpublished investigation by G. S. Parks, W. D. Kennedy, and G. E. Moore, dealing with *n*-heptyl and cetyl alcohols.

TABLE II. Heats of solution of crystalline cetyl alcohol in related liquids at 25°C.

Experiment No.	ΔH_{298} of solution (calories per gram) in Methyl alcohol	Ethyl alcohol	*n*-Butyl alcohol	*n*-Heptyl alcohol	*n*-Dodecyl alcohol
1	56.38	54.33	52.27	51.01	48.96
2	55.52	54.28	51.77	50.82	48.12
3	—	54.45	51.12	50.28	48.30
4	—	54.42	51.65	50.19	—
5	—	54.05	—	50.27	—
Mean	55.95	54.30	51.70	50.51	48.46

By Kirchhoff's law with the assumption of $\Delta C_p = 0.13$ cal. per g for the fusion process, we also computed initially a value of 51.3 cal. per g for the heat of fusion at 49.3°, the normal melting point of cetyl alcohol crystals.[8a] This fusion estimate is considerably larger than the experimental result of Tammann, 33.8 cal. per g, which is quoted by the *International Critical Tables*[8b] and the very early result of 29.2 cal. per g obtained by Favre and Silbermann.[9] At first we were at a loss to explain such a great discrepancy, especially as our higher value fitted in well with entropy data for the series of normal aliphatic alcohols in the liquid state. Later Baker and Smyth,[10] however, pointed out that crystalline cetyl alcohol undergoes an important transition at 32–35°C; and from a time-temperature heating curve, made in our laboratory by Dr. George E. Moore, we now estimate that this heat of transition amounts to about 47 percent of the actual heat of fusion. Accordingly, when we divide our preceding fusion estimate for 49.3°, which was computed without reference to such a transition, by the factor 1.47, we thus obtain a revised fusion value of 34.9 cal. per g together with a heat of transition of 16.4 cal. per g. In view of such results, nevertheless, it still seems probable that these earlier experimental determinations of the heat of fusion are somewhat low, perhaps because of an inadequate allowance for premelting.

[8] *International Critical Tables*, (a) Vol. I, p. 260; (b) Vol. V, p. 134.

[9] Quoted in the Landolt-Bornstein-Roth Scheel *Tabellen* (Verlagsbuchhandlung Julius Springer, Berlin, 1923), p. 1472.

[10] W. O. Baker and C. P. Smyth, J. Am. Chem. Soc. **60**, 1229 (1938).

TABLE III. Heat of solution of crystalline dicetyl in *n*-heptane at 25°C.

Experiment No.	Grade of solvent	ΔH_{298} of solution (in calories per gram)
1	"Practical"	58.5
2	"Practical"	56.6
3	"Practical"	59.1
4	"Practical"	60.0
5	"Practical"	60.3
6	"Highest purity"	57.6
7	"Highest purity"	58.7
Final mean value		58.7(±0.9)

SOLUTION DATA FOR DICETYL

Our original plan had been to measure the heats of solution of samples of crystalline dicetyl (dotriacontane) in several liquid normal paraffins, including the heptane, decane, and hexadecane. However, it was soon found that the limited solubility and slow rate of solution of the crystals in these two latter solvents at 25° rendered such a procedure experimentally impractical. Thus our present results pertain only to the formation of 0.030 molal solution with *n*-heptane as solvent. Even these are considerably less consistent than our previous results with hexamethylbenzene and cetyl alcohol, partly because the present solubility limitations made it necessary to use dicetyl samples which gave a temperature lowering of only about one degree and partly because the time of solution, in this case several minutes, necessitated larger and more uncertain corrections for heat exchange between the calorimeter and its jacket.

The dicetyl and the *n*-heptane used herein were Eastman materials. The former melted at 68–69.5°. Two grades of solvent, "practical" and "highest purity," were employed without significant differences in the enthalpy values, although the solution process took place somewhat more readily in the "practical" material. The necessary data for the heat capacities of crystalline dicetyl and liquid *n*-heptane were derived from previous investigations of Parks and co-workers.[11]

[11] G. S. Parks, H. M. Huffman, and S. B. Thomas, J. Am. Chem. Soc. **52**, 1032 (1930); and an unpublished study on dicetyl by G. S. Parks and J. A. Hatton.

The results of seven determinations of the heat of solution are reported in Table III. The final mean of 58.7 cal. per g involves an average deviation of ±0.9 cal. Under the circumstances we now suggest this mean result as the best value for the heat of fusion of dicetyl at 25°, with an over-all uncertainty of perhaps 1.2 cal. when some allowance is made for departures from ideality in the dicetyl-heptane solution. From the solubility studies of Seyer,[3] we have also computed a value of 59.0 cal. per g for the ideal heat of solution at 40°. With the plausible assumption[11] of 0.06 cal. per g for the temperature coefficient of the solution process, this value yields 58.1 cal. at 25°, which is in reasonable agreement with our present mean result.

By use of Kirchhoff's law with the assumption of $\Delta C_p = 0.06$ cal. per g for the fusion process, we now estimate from our mean result a value of 61.4 cal. per g for the heat of fusion of dicetyl at 70.2°C, the normal melting point.[3] The literature apparently contains no experimental value for the heat of fusion of this hydrocarbon, but Garner, Van Bibber, and King[12] have reported the following heats of fusion per gram for two closely related paraffins at their respective melting points:

n-$C_{30}H_{62}$	59.6 cal. per g,
n-$C_{34}H_{70}$	63.9 cal. per g.

The mean of these, 61.8 cal. per g, is thus in very good agreement with our present computed value for n-$C_{32}H_{66}$. Of course, it should be noted here that such fusion values really include the heat of transition for the $\alpha-\beta$ transformation of the crystalline hydrocarbon, which takes place a few degrees below the normal melting point.

ACKNOWLEDGMENT

Before concluding, the authors wish to acknowledge their indebtedness to Mr. John A. Hatton, who made the measurements of the heats of solution of dicetyl in *n*-heptane for this study.

[12] W. E. Garner, K. Van Bibber, and A. M. King, J. Chem. Soc. **1931**, 1533.

THE JOURNAL OF CHEMICAL PHYSICS VOLUME 14, NUMBER 9 SEPTEMBER, 1946

The Near Ultraviolet Absorption Spectrum of Toluene Vapor

NATHAN GINSBURG AND W. W. ROBERTSON
Department of Physics
AND
F. A. MATSEN
Department of Chemistry,
The University of Texas, Austin, Texas

(Received May 16, 1946)

The experimental work of Savard and the theoretical work of Sponer on the absorption spectrum of toluene vapor is extended. A spectrum of 209 bands was observed with partial resolution of the fine structure. A tentative analysis is given based on ground state frequencies 514, 620, 785, 1003, 1012, 1176, and 1209, which correlate completely with Raman data; on excited state frequencies, 456, 528, 751, 932, 964, and 1186; and on difference frequencies 59 and 178 cm^{-1}. Assuming C_{2v} symmetry, all frequencies below 1300 cm^{-1} of symmetry class A_1 appeared in $1-0$ transitions and with one exception in $0-1$ transitions. In addition, a vibrational frequency of symmetry class B_1, deriving from an ϵ_g^+ vibration in benzene, appeared strongly both in the ground and excited state.

INTRODUCTION

THIS investigation is a continuation of the study of the effect of substituents on the near ultraviolet absorption spectrum of the benzene nucleus. The substituents previously studied, Cl,[1] NH_2,[2a] OH,[2b] and F,[3] all possess an unshared pair of electrons which can resonate with the nucleus to modify rather markedly the electronic structure; in addition to this, an inductive effect of smaller magnitude operates.[4] It was of interest, therefore, to investigate the effect of the substitution of the CH_3 group, which does not possess an unshared pair of electrons to resonate with the ring. However, Mulliken, Rieke, and Brown[5] have pointed out the possibility of resonance due to hyperconjugation of the methyl group with the benzene nucleus. It is expected that this resonance will modify the electronic structure of the benzene nucleus to a lesser extent than that mentioned above.

Sponer[6] has discussed the theory and has analyzed Savard's[7] data on toluene assigning a large number of fundamental vibration frequencies in the excited state. Masaki[8] who also investigated the absorption of toluene, reported only the wave numbers of the $0-0$ and four $1-0$ bands. The Raman data have been summarized by Kohlrausch and Wittek[9] and by Pitzer and Scott,[10] the latter having completely classified the Raman frequencies.

In the present investigation the absorption spectrum of toluene was studied under higher dispersion and with greater resolving power than previously. A partial resolution of the fine structure, as well as the observation of a number of new bands resulted. Further, it was possible to obtain additional fundamental vibration frequencies in both the ground and excited states, to make a number of additional assignments, and to associate the fundamental frequencies with definite modes of vibration, this latter resulting from a complete correlation with Raman data.

EXPERIMENTAL

The absorption spectrum of toluene lies in the region 2390–2760A. All measurements were made in the second order of a spectrograph of the Eagle type, with a 3-meter grating ruled 15,000 lines per inch. The light source was a 5000-volt,

[1] H. Sponer and S. H. Wollman, J. Chem. Phys. **9**, 816 (1941).
[2a] N. Ginsburg and F. A. Matsen, J. Chem. Phys. **13**, 167 (1945).
[2b] F. A. Matsen, N. Ginsburg, and W. W. Robertson, J. Chem. Phys. **13**, 309 (1945).
[3] S. H. Wollman, J. Chem. Phys. **14**, 123 (1946).
[4] A. L. Sklar, Rev. Mod. Phys. **14**, 232 (1942).
[5] R. S. Mulliken, C. A. Rieke, and W. G. Brown, J. Am. Chem. Soc. **63**, 41 (1941).
[6] H. Sponer, J. Chem. Phys. **10**, 672 (1942).
[7] J. Savard, Ann. de Chimie **11**, 287 (1929).
[8] K. Masaki, Bull. Chem. Soc. Japan **11**, 346 (1936).
[9] K. W. F. Kohlrausch and H. Wittek, Monatsh **74**, 1 (1941).
[10] K. S. Pitzer and D. W. Scott, J. Am. Chem. Soc. **65**, 803 (1943).

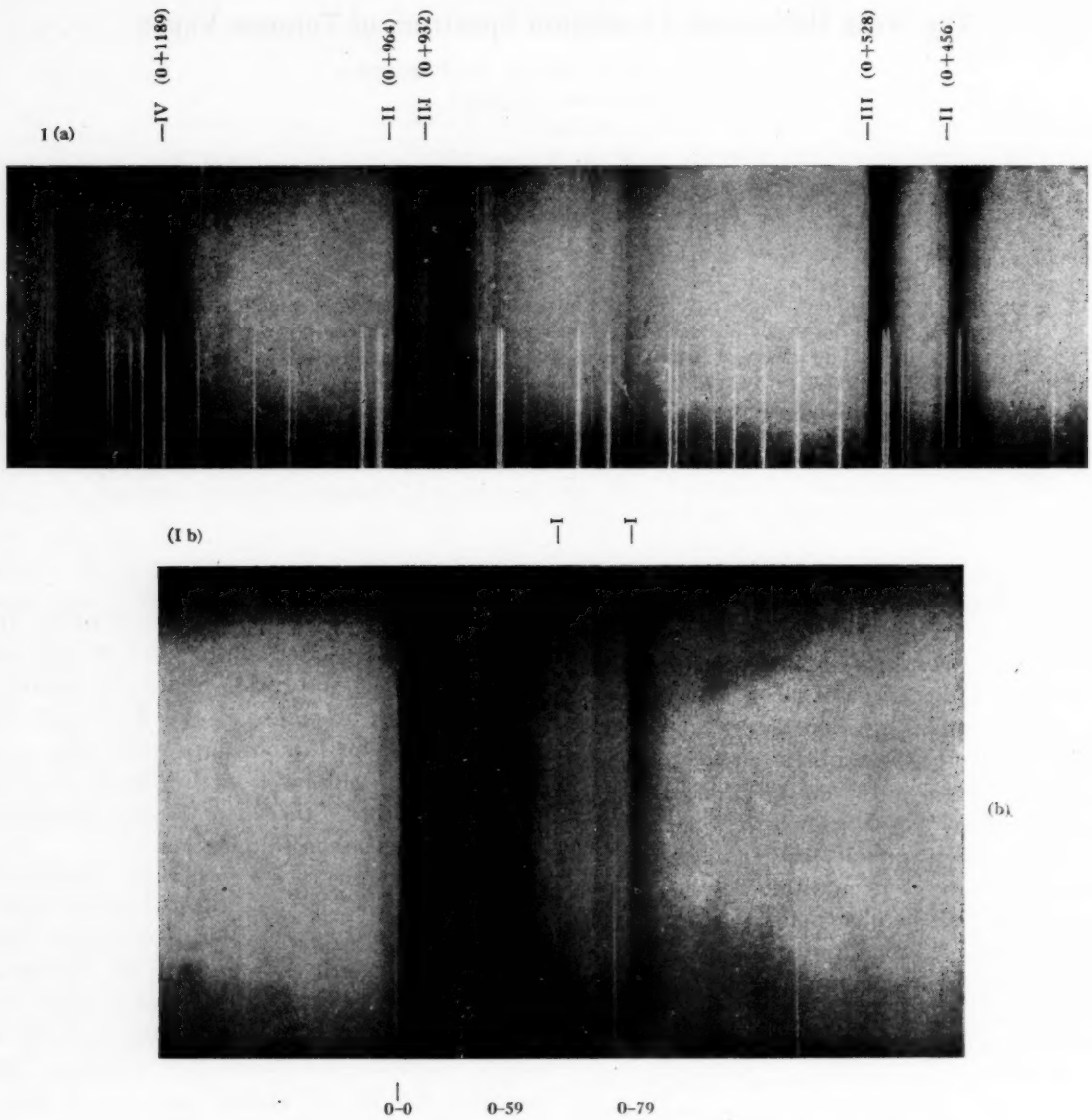

FIG. 1. The four different types of bands in the absorption spectrum of toluene, (a) in the region 2585–2635A and (b) in the region 2667–2680A.

2.5-kva hydrogen discharge tube, and the spectrum was photographed on Eastman 103−0 and 103−0 UV-sensitized plates.

Two absorption cells were used, one of 12-cm length, the other 70-cm, both all quartz. The shorter cell was used in almost all exposures, the long cell being necessary only for extreme development of the spectrum. The amount of toluene vapor introduced into the cells was controlled by variation of the temperature of the reservoir containing the toluene liquid. This was varied between −20° and 24°C for the short cell and between 0°C and 50°C for the long cell. The cell was heated to the same temperature as the reservoir when the reservoir was above room temperature.

Sulfur-free toluene with a 1°C boiling range was obtained from Eastman Kodak. It was redistilled in a meter-long, packed, adiabatic column. A number of cuts were taken and the cut with the highest refractive index ($n_D^{20°} = 1.4952$, BP. = 109.7°C at 745 mm) was retained for this investigation.

The 209 bands observed were measured to an

accuracy of 0.3 cm^{-1} for the very sharp bands, with the accuracy diminishing to 3 cm^{-1} for the extremely diffuse bands. Four types of band structure were observed: (I) doublets with the components of equal intensity; (II) doublets with a strong, long wave-length component and weak, short wave-length component; (III) bands with sharp heads with no apparent doublet structure and degraded toward the red; and (IV) diffuse bands with no sharp heads and most intense in the center (Fig. 1). This varied character made it necessary to set the cross-hair of the comparator at different relative positions for the different types of bands. The first two types were measured at the centers of gravity of the components of the doublets. The last two types were measured to the sharp head and the apparent head, respectively. Types II and IV were not found in aniline[2a] and phenol.[2b] The roman numeral in Table I indicates the type of band.

THEORY

Sponer[6] has pointed out that the spectrum of toluene, like that of other mono-substituted benzenes, possesses certain features of the benzene spectrum as well as other features arising from the reduction of the symmetry from type D_{6h} to a lower symmetry type. This reduction in symmetry makes allowed the forbidden (in benzene) 0−0 and other transitions involving only totally symmetric frequencies.

Sponer assigned C_s symmetry to toluene. However, if one considers the effect of the methyl group on the benzene ring the same as that of a one-atom substitution, toluene may be assigned a symmetry C_{2v} as has been done by Pitzer and Scott in their discussion of the Raman data. Then, by analogy with the Sponer-Wollman treatment of chlorobenzene, the electronic transition is A_1-B_1, the electric moment lying in the y direction, that is in the plane of the ring perpendicular to the z axis, which lies along the CH_3-C bond. This transition is allowed as are transitions involving vibrational states of symmetry class A_1. This transition is also allowed when vibrational states of symmetries B_1 and A_2 are excited. Such vibronic transitions, however, give rise to moments in the x and z directions, which are not believed to participate strongly. Hence, vibrations of symmetry class B_1 and A_2 should appear only weakly if at all, since for a single quantum excitation the symmetry of the vibrational state is the same as that of the vibration.

When vibrations of symmetry class B_2 are superposed on the electronic transition A_1-B_1, the transition integral is not invariant for any of the three moments and these vibrations should not appear at all. 1−1 transitions for vibrations of any symmetry class are allowed.

It is to be expected, however, that some aspects of the benzene spectrum are to be carried over into the spectrum of toluene, since the methyl group perturbation on the benzene ring cannot be very great. Hence the analog of the relatively strong absorbing ϵ_g^+ vibration which made the $A_{1g}-B_{2u}$ transition allowed in benzene, should appear strongly in the toluene spectrum. This in benzene is a degenerate vibration, whose degeneracy is removed as the symmetry of the molecule is reduced.

For C_{2v} symmetry the degenerate ϵ_g^+ vibration, 6*a* and 6*b*,[11] of D_{6h} symmetry divides, the 6*a* vibration becoming a member of symmetry class A_1, while 6*b* becomes a member of B_1. Hence 6*b* should yield a strong band more intense than the other members of class B_1.

DISCUSSION

The strongest band in the spectrum, the Type II doublet at 37,477 and 37,480 cm^{-1}, was taken to be the 0−0 band. Savard[7] reports 37,473 cm^{-1} for this band, while Masaki[8] reports 37,477 cm^{-1}. In addition to the 0−0 doublet, there appears a satellite doublet nine wave numbers to the red, similar to the diffuse satellite observed in chlorobenzene, aniline, and phenol.

The frequencies of the bands on the long wave-length side of the 0−0 band which correspond to reported Raman frequencies are given in Table II. The characterization numbers are those from Pitzer and Scott[9] and correspond to the usual numbering of the benzene frequencies. Six out of twelve possible non-totally symmetric frequencies were observed which could be correlated with reported Raman frequencies. The five starred in the table are of doubtful correlation. Of these five, two (*M*6 and 17*a*) are correlations

[11] A. Langseth and R. C. Lord, Kgl. Danske Vid., Sels. Math.-fys. Medd. **16**, No. 6 (1938).

TABLE I. The absorption spectrum of toluene. The intensities are designated as *vvw* = extremely weak, *vw* = very weak, *w* = weak, *m* = medium, *ms* = medium strong, *s* = strong, *vs* = very strong, *vvs* = extremely strong, *B* = broad, and *D* = diffuse. Primed intensities indicate measurements to the head of the band. (*S*) = satellite.

Wavelength (Angstroms)	Wave number	Intensity	Type	Assignment
2756.4	36,268	*vvw'*	III	0 −1209
2754.0	36,301	*vvw'*	III	0 −1004 −178 0 −1176
2745.3	36,415	*vvw'*	III	0 −1003 −59
2741.5	36,465	*vvwBD*		0 −1012
2740.9	36,474	*vwBD*		0 −1003
2739.5	36,493	*vvwBD*		
2737.6	36,517	*vvwBD*		0 −785 −178
2735.7	36,543	*vvwBD*		
2733.6	36,571	*vvwBD*		
2732.1	36,591	*vvw*		
2729.06	36,631.8	*vvw*	I	0 −785 −59
2728.69	36,636.8	*vvw*		
2725.95	36,673.2	*vvw*	I	0 −620 −178
2725.77	36,676.0	*vvw*		
2724.56	36,692.3	*w*	I	0 −785
2724.25	36,690.5	*vw*		
2723.6	36,705	*vvwBD*		
2721.9	36,729	*vvw*		0 −1209 +456
2721.4	36,735	*vvw*		
2719.3	36,763	*vvw'*	III	
2717.71	36,784.8	*vw'*	III	0 −514 −178
2716.9	36,796	*vw*		0 −620 −59
2715.82	36,810.4	*vvw*	I	
2715.56	36,813.9	*vvw*		
2712.35	36,857.5	*w'*	III	0 −620
2711.3	36,872	*vwB*		
2709.28	36,899.2	*vvw*	I	0 −514 −59
2709.00	36,903.1	*vvw*		
2704.59	36,963.2	*w'*		0 −514
2693.1	37,121	*vvw*		0 −2 ×178
2690.9	37,151	*vvw*		0 −785 −456
2688.0	37,191	*vvw*		
2686.9	37,206	*vvw*		
2684.1	37,245	*vw*	IV	0 −178 −59
2681.42	37,282.6	*vw*	I	
2681.20	37,285.7	*vw*		
2680.87	37,290.3	*vw*	I	
2680.62	37,293.7	*vw*		
2680.21	37,299.4	*ms*	I	0 −178
2680.01	37,302.2	*ms*		
2679.9	37,304	*vw*		0 −3 ×59
2679.04	37,315.7	*vw*	I	
2678.76	37,319.6	*vw*		
2678.31	37,325.9	*vw*	I	
2678.09	37,329.0	*vw*		
2677.1	37,343	*vvw*		
2676.10	37,356.7	*w*	I	0 −2 ×59
2675.80	37,360.9	*w*		
2674.30	37,381.9	*w*	I	0 −620 +528
2674.12	37,384.4	*w*		
2673.76	37,389.4	*vvw*	I	
2673.49	37,393.2	*vvw*		
2671.72	37,418.0	*ms*	I	0 −59 0 −514 +456
2671.48	37,421.3	*ms*		
2670.7	37,432	*vvw*		0 −1012 +964
2668.28	37,466.2	*s*	I	0 −0 −9 (*S*)
2667.96	37,470.7	*s*		
2667.48	37,477.4	*vvs*	II	0 −0
2667.27	37,480.4	*s*		
2666.3	37,495	*vw*		
2663.2	37,538	*vw*		
2655.3	37,649	*vw*		
2651.3	37,706	*vvw*		0 −520 +751
2648.4	37,748	*vvw*		
2647.5	37,760	*vw*		0 +456 −178
2645.8	37,785	*vwBD*		0 −620 +931
2644.1	37,823	*w*		0 +964 −620
2642.71	37,828.7	*w*	I	0 +528 −178
2642.51	37,831.6	*w*		
2641.3	37,850	*vwBD*		
2640.6	37,859	*vw'*	III	
2639.7	37,872	*vw*		
2639.5	37,875	*vw*		0 +456 −59
2636.8	37,913	*mBD*		
2636.1	37,924	*mBD*		0 +964 −520 0 +456 −9 (*S*)
2635.40	37,933.6	*s*	II	0 +456
2635.17	36,936.9	*m*		
2634.35	37,948.7	*w*	I	0 +528 −59
2634.05	37,953.1	*m*		
2632.0	37,982	*vwD*		
2631.65	37,987.7	*w*	I	
2631.43	37,992.3	*w*		
2631.25	37,993.4	*s*	I	0 +528 −9 (*S*)
2630.88	37,998.8	*s*		
2630.45	38,005.0	*vs*	I	0 +528
2630.23	38,008.2	*vs*		
2630.10	38,010.0	*vs*		
2629.5	38,019	*vvwD*		
2625.3	38,080.1	*vvwBD*		
2623.6	38,104	*vwBD*		
2618.9	38,173	*vvw*		0 +751 −59
2616.2	38,212	*wD*		
2615.08	38,228.3	*m*	I	0 +751
2614.87	38,231.4	*m*		
2614.76	38,233.0	*m'*	III	0 +932 −178
2612.93	38,259.8	*w*	I	0 +964 −78
2612.70	38,263.2	*w*		
2611.4	38,282	*vw*		
2610.63	38,293.5	*vw'*	III	0 +932 −2 ×59
2608.99	38,317.6	*vvw*	I	0 +964 −2 ×59
2608.73	38,321.4	*vvw*		
2607.3	38,342	*vwD*		
2606.71	38,351.1	*m*	II	0 +932 −59
2606.48	38,354.8	*w*		
2606.1	38,361	*vvw*		
2604.6	38,382	*mBD*		0 +964 −59
2604.0	38,391	*vw*		0 +2 ×456

TABLE I.—*Continued.*

Wavelength (Angstroms)	Wave number	Intensity	Type	Assignment
2603.2	38,402	*mBD*		0+932−9 (*S*)
2602.76	38,409.3	*vs*	I	0+932
2602.60	38,411.6	*vs*		
2602.46	38,413.7	*m'*	III	
2601.3	38,431	*mBD*		0+964−9 (*S*)
2601.0	38,435	*msD*		
2600.59	38,441.3	*s*	II	0+964
2600.36	38,444.7	*m*		
2599.6	38,456	*vwBD*		
2597.6	38,486	*vwBD*		0+1189−178
2596.1	38,508	*vvwBD*		
2595.9	38,512	*vw*		
2594.0	38,539	*vvw*		0+2×528
2593.4	38,547	*vvwBD*		0+1189−2×59
2592.7	38,559	*vvwBD*		
2592.3	38,565	*vvw*		
2591.5	38,577	*vwD*		
2591.1	38,582	*vw*		
2589.9	38,601	*wBD*		
2589.3	38,610	*wBD*		0+1189−59
2585.5	38,666	*s'*	IV	0+1189
2585.05	38,672.4	*ms'*	III	
2582.86	38,705.2	*vw'*	III	
2580.62	38,738.8	*m'*	III	
2579.9	38,749	*wBD*		0+751+528−9 (*S*)
2579.41	38,757.0	*m*	I	0+751+528
2579.24	38,759.5	*m*		
2577.0	38,794	*vw'*	IV	
2576.2	38,805	*vwBD*		
2575.5	38,815	*vwBD*		
2574.3	38,834	*vvw*		
2573.4	38,840	*m*		
2571.92	38,869.8	*m'*	III	0+932+457
2571.2	38,881	*w*		
2567.75	38,932.9	*w'*	III	0+932+528−9 (*S*)
2567.17	38,941.7	*s'*	III	0+932+528
2565.9	38,960	*wBD*		0+964+528−9 (*S*)
2565.17	38,972.1	*s'*	III	0+964+528
2564.4	38,984	*w*		0+2×751
2560.0	39,051	*vvw*		
2559.0	39,065	*vvw*		0+3×528
2556.9	39,099	*vw*		
2556.3	39,107	*vw*		
2555.2	39,124	*wBD*		0+1189+457
2553.87	39,144.5	*vw*	I	0+2×457+751
2553.66	39,147.7	*vw*		
2552.7	39,162	*m*		0+932+751
2550.0	39,204	*s'*	IV	0+1189+528 0+964+751
2541.45	39,335.8	*vw'*	III	0+2×932−9 (*S*)
2541.11	39,341.1	*m*	I	0+2×932
2540.96	39,343.4	*m*		
2539.5	39,367	*mBD*		0+932+964−9 (*s*)
2538.90	39,375.3	*msD'*	III	0+932+964
2538.8	39,377	*w*		
2537.9	39,391	*wB*		
2536.92	39,406.0	*m'*	III	0+2×964
2534.0	39,452	*vw*		
2531.6	39,489	*vvw*		
2530.1	39,513	*vwBD*		0+2×751+528
2528.8	39,532	*vvwBD*		
2528.1	39,543	*vw*		
2526.8	39,563	*vvw*		
2524.4	39,602	*ms'*	IV	0+1189+932
2522.2	39,636	*s'*	IV	0+1189+964
2520.6	39,662	*vw*		
2519.9	39,672	*vwBD*		
2518.60	39,692.7	*m'*	III	0+528+751+932
2517.5	39,712	*wB*		
2516.6	39,725	*w*		0+528+751+964 0+2×528+1189
2513.0	39,782	*vw'*	IV	
2511.80	39,800.1	*w'*	III	0+457+2×932
2511.1	39,811	*vwD*		
2509.59	39,835.2	*w'*	III	0+457+932+964
2508.5	39,853	*wD*		0+2×1189
2507.22	39,872.8	*m'*	III	0+528+2×932
2505.28	39,903.7	*s'*	III	0+528+932+964
2503.6	39,930	*wD*		0+2×964+528
2502.7	39,945	*vwBD*		0+2×751+964
2490.8	40,135	*w'*	IV	0+751+932+964 0+528+932+1189
2488.9	40,166	*w'*	IV	0+2×751+1189
2480.3	40,306	*wBD*		0+2×931+964
2479.3	40,322	*wD*		
2478.4	40,337	*wBD*		0+2×964+932
2477.6	40,349	*vvwBD*		0+751+932+1189
2475.5	40,384	*vvwBD*		0+528+2×1189 0+964+1189+751
2465.03	40,555.2	*s'*	III	
2464.5	40,565	*vw*		0+932+964+1189
2449.3	40,816	*vw*		0+2×1189+964
2446.7	40,859	*vvw*		
2436.5	41,030	*vvw*		
2421.9	41,278	*vw*		
2409.3	41,494	*vw*		
2395.3	41,736	*vvw*		

TABLE II. The fundamental frequencies of toluene. Raman frequencies beyond 1212 are not reported. * Indicates doubtful correlation.

Characterization No.	Ground State: Raman Masaki	Ground State: Pitzer Scott	Ground State: Kohlrausch Wittek	Ultraviolet absorption: Masaki	Ultraviolet absorption: This research	Excited State: This research	Excited State: Savard (Sponer)
Symmetry A_1							
6a	520	521	521 (6)	517	514 *w*	456 *s*	466
12	786	785	786 (9)	781	785 *vvw*	751 *m*	—
1	—	1002	1004 (12)	—	1003 *vw*	932 *vs*	930
18a	—	1030	1030 (8)	—	1012 *vvw*	964 *s*	964
9a	—	1175	1177 (1)	—	1176 *vvw*		
7a	—	1210	1208 (5)	—	1212 *vvw*	1189 *s*	1193
Symmetry B_1							
18b	333	340	344 ($\frac{1}{2}$)	334	—		
6b	622	622	623 (4)	623	620 *w*	528 *vs*	527
M6	—	1060	1085 (0)	—	*1062 *vvw*		
9b	—	1155	1155 (2)	—	—		
Symmetry A_2							
16a	—	405	405 (0)	—	—		
10a	—	842	843 (1)	—	*845 *vvw*		
17a	—	(985)	977 ($\frac{1}{2}$)	—	*988 *vvw*		
			933 ($\frac{1}{2}$)				
Symmetry B_2							
11	—	216	216 (5*b*)	—	—		
16*b*	—	467	—	—	—		
10*b*	—	730	730 (1)	—	*714 *vvw*		
17*b*	—	890	897 (1*b*)	—	*886 *vvw*		
M6	—	1190	1189 (00)	—	—		
Difference Frequencies					59 *ms*		
					178 *ms*		

with rather doubtful Raman frequencies. 10*a* has a reasonable assignment in terms of symmetric frequencies. 10*b* and 17*b* may also be coincidences since vibration 11 (216 cm^{-1}), which is in the same symmetry class, B_2, is five times as intense in the Raman spectrum and has a large Boltzmann factor, does not appear. This leaves only the frequency 6*b* (620 cm^{-1}) as the one non-totally symmetric vibration which can be definitely assigned. Further, the fundamental frequency, 528, of the excited state could not be correlated with any ground state frequency other than 620. If this correlation is correct, the 6*b* frequency was the only non-totally symmetric fundamental frequency observed in the excited state. The absence of the non-totally symmetric vibrations (except 6*b*) is in accord with the theory given in the previous section. Vibrations of class B_2 are definitely forbidden. Vibrations of classes A_2 and B_1 (except 6*b*) may occur weakly according to the theory. The intensities of the corresponding Raman bands are very low and it is often found that very weak Raman frequencies do not appear in ultraviolet absorption.

The 6*b* vibration appears relatively strongly as 620 cm^{-1} (Raman 622 cm^{-1}) in the ground state and very strongly as 528 in the excited state. Sponer did not list the ground-state frequency, but gave 527 for the excited state. This vibration is the B_1 component resulting from the removal of the degeneracy of the ϵ_g^+ vibration (606 cm^{-1} in benzene) upon the substitution of the methyl group. The 528 frequency combines strongly with all totally symmetric vibrations analogous to the situation in benzene. The band $0+2\times528$ appears only weakly in this spectrum. According to Herzberg and Teller[12] and Sponer and Teller,[13] non-totally symmetric vibrations have their minima above one another; hence, on the basis of the Franck-Condon principle the doubly excited frequency should be weak. Wollman[3] has pointed out that the doubly excited frequency becomes stronger in the order of increasing perturbing effect of halogen substituents on the ring Br<Cl<F.

Two strong low frequency "red" bands, 59

[12] G. Herzberg and E. Teller, Zeits. f. physik. Chemie **B21**, 410 (1933).
[13] H. Sponer and E. Teller, Rev. Mod. Phys. **13**, 76 (1941).

and 178 cm^{-1}, which cannot be correlated with any single Raman frequency, appear. It must be concluded that these are 1−1 transitions. No assignment could be made for the 0−178 band on the basis of assigned fundamental frequencies. The 0−59 band may be interpreted as 0−514+457 since both 0−514 and 0+457 appear. Again, as in previous investigations, the presence of bands to which assignments 0−2×59 and 0−3×59 are made, may argue against such an assignment since 0−2×514 and 0−3×514 do not appear. Further, assuming that no change in transition probabilities is involved, the ratio of the intensities of the combination bands should be the ratio of the Boltzmann factors, $_e-514hc/kT:{}_e-2\times514hc/kT:{}_e-3\times514hc/kT$, or 1:0.083:0.0068. The ratio of intensities obtained microphotometrically was 1:0.25 with the third uncertain because it occurred on the shoulder of the strong 0−178 band.

However, 1−1 transitions are allowed even when the corresponding 0−1 and 1−0 transitions are forbidden. Thus, a 1−1 transition involving frequency 11 (216 cm^{-1}) or symmetry class B_2 might account for the 59 cm^{-1} series. It is to be noted that this vibration yields the most intense Raman band of all of the non-totally symmetric vibrations. The ratio of the Boltzmann factors for this vibration is 1:0.33:0.11. Consequently, 0−216+157 is a possible interpretation of the 0−59[14] band.

The fundamental frequencies of the excited state are given in Table II. Those all appeared as doublets for the 0−1 transitions. In addition there appeared a satellite band nine wave numbers toward the red for each of these transitions and for some of the combination bands similar to that mentioned above for the 0−0 band and reported for some of the previously investigated mono-substituted benzenes. All totally symmetrical frequencies below 1300 cm^{-1} have been identified in the excited state with the exception of 1176. This frequency yields a Raman band much less intense than yielded by any of the other totally symmetric frequencies.

In Table III are listed the differences between the Raman frequencies for benzene and toluene and between the Raman frequencies and excited state frequencies for the six totally symmetric frequencies identified in this research. Since the methyl group replaces a hydrogen atom it is expected that predominantly hydrogen vibrations will be more affected by the substitution than will the typically carbon vibrations. On the other hand, since the electronic excitation affects the π electrons localized in the carbon-carbon bonds, it is to be expected that the typically carbon frequencies will be affected more in the excitation process. This is borne out by Table III.

TABLE III.

Frequency	Frequency differences	
	Benzene Raman − Toluene Raman:	Toluene Raman − Toluene excited
7a	1837 cm^{-1}	21 cm^{-1}
12	226	34
6a	85	65
18a	7	66
1	−10	70
6b	−14	94

Most of the $0+1\times\nu_i'\times1\times\nu_j'$ [15] bands were present with the exception of $0+456+1\times\nu_j'$, of which series only $\nu_j'=932$ and 1189 appear. The only other missing band of this type was 0+751 +1189. Of the transitions in which three quantum numbers change, only about half of the possible bands were found with no series appearing to be better than any other.

It may be concluded that the substitution of the CH_3 group affects the spectrum of the nucleus in much the same way as the substituents Cl, F, NH_2, and OH. However, the toluene spectrum is not as well developed for the transitions involving the higher vibrational quantum numbers as are the spectra of the latter. This may be attributed to the absence of an unshared pair of electrons on the CH_3 group.

The authors wish to acknowledge several suggestions made by Professor R. S. Mulliken. They also wish to acknowledge the continued support of the University of Texas Research Institute.

[14] See the discussion of the corresponding frequency in chlorobenzene by Sponer and Wollman, reference 1.

[15] ν_i' and ν_j' represent frequencies (cm^{-1}) in the excited state.

THE JOURNAL OF CHEMICAL PHYSICS VOLUME 14, NUMBER 9 SEPTEMBER, 1946

Corresponding States in the Frozen Rare Gases

G. W. MURPHY AND O. K. RICE
University of North Carolina, Chapel Hill, North Carolina

(Received June 11, 1946)

A method is presented for extending the principle of corresponding states to solids at comparatively low temperatures, where quantum effects are appreciable. The method has been applied to solid neon, argon, krypton, and xenon. The principle of corresponding states, as applied to the liquid and vapor states, is used for calculation of the potential energies and interatomic distances of three of the substances in terms of the other. The quantum contribution to the energy is taken into account by assuming the Debye theory for all the solids, and this is related to the potential energy by means of a modified Grüneisen equation. The Debye Θ's for three of the solids are determined from that of the other by a dimensional analysis of the mechanical system. Using this information, C_p for neon, argon, and krypton have been calculated from the experimental data for xenon. Agreement of the calculated values with experiment is reasonably good; small deviations may be caused by breakdown of the Debye theory, or may be indications of inexactitude in the law of corresponding states.

1. INTRODUCTION

THE principle of corresponding states has been the subject of two recent papers. Pitzer[1] has given a list of assumptions required for a substance to behave as a "perfect liquid." All such substances will obey the law of corresponding states. He pointed out that the rare gas liquids argon, krypton, and xenon conform closely to this behavior with respect to a number of their properties, while neon shows appreciable deviations caused by quantum effects. More recently Guggenheim[2] has undertaken a critical analysis of Pitzer's assumptions and has called attention to several additional properties of argon, krypton, and xenon in conformity with the principle.

Aside from the comparison of the entropy of fusion and the expansion on fusion of these substances, no attempts have yet been made to extend the principle to the solid state. We shall show in this article that Pitzer's assumptions, when due account is taken of the quantum effects, lead to what may be considered to be an extension of the principle of corresponding states, which should be valid for the solid rare gases even at low temperatures. Furthermore, we shall show that neon may be included in the comparison as effectively as the others.

[1] K. S. Pitzer, J. Chem. Phys. **7**, 583 (1939).
[2] E. A. Guggenheim, J. Chem. Phys. **13**, 253 (1945).

2. THEORY

By setting up a phase integral for substances conforming to his five assumptions, Pitzer has shown that the behavior of these substances will be the same when they are compared at equal values of T/A and V/r_0^3, where T is the absolute temperature, V the molar volume, and A and r_0^3 are constants characteristic of a given substance taken at some corresponding point. Since the critical point is a corresponding point, A may be taken as proportional to the critical temperature T_c and r_0^3 as proportional to the critical volume V_c.

We shall not consider all of Pitzer's assumptions in detail, but will comment on assumptions I and V, which are pertinent to our investigation. The former states that "classical statistical mechanics will be used." In this case we certainly do not have classical statistics alone operative, but we shall take into account quantum effects separately by assuming that they are taken care of by the Debye theory. Assumption V states: "The potential energy for a pair of molecules can be written $A\varphi(r/r_0)$, where r is the intermolecular distance, A and r_0 are characteristic constants, and φ is a universal function." If the potential energy of pairs is additive, as Pitzer has assumed, then a similar relation must hold for the total potential energy E_p of the solid. The A and r_0 of this assumption are the same as the A and r_0 of the preceding paragraph. Pitzer's and Guggenheim's

discussions of the rare gas liquids indicate that assumption V is justified. We will use it as one of the principal bases of our development. Since the Debye Θ will also depend on r_0, this assumption can also eventually be used to obtain a relation between E_p and Θ. (For a closer definition of E_p see page 290 of reference 4 below.)

The total energy E of a simple solid may be separated into three parts:

$$E=E_z+E_t+E_p,$$

where E_z is the zero point energy and E_t the "thermal energy." In the Debye theory $E_z=(9/8)R\Theta$, where $\Theta=h\nu_{\max}/k$ is the characteristic temperature. E_t/T is given in the Debye tables as a function of Θ/T.

We shall apply the principle of corresponding states to our case in the following manner: we select one of the four solids, xenon, as a standard, calculating E_p as a function of Θ by means of the experimental specific heat data and the Debye theory; since, for a given solid, both E_p and Θ are functions of r or the volume only, one can express E_p as a function of Θ only. We then calculate suitable factors for the conversion of the energy and interatomic distance of xenon to those of neon, argon, and krypton by using data at some corresponding point at a sufficiently high temperature so that all of Pitzer's assumptions, including the first, are fulfilled. We then extend the principle of corresponding states to low temperatures, where assumption I no longer holds, by keeping these same factors for E_p and r, and take into account quantum effects separately by calculating E_z and E_t from the Debye theory. This is done with the help of a factor to convert Θ of Xe to that of Ne, A, or Kr, which we obtain by a dimensional analysis of the mechanical system, using the energy and distance factors calculated above.

Following Pitzer, we take the critical point as a corresponding point. The energy factor f_e is then just $T_c(\mathrm{S})/T_c(\mathrm{Xe})$, where S stands for one of the solids other than xenon. The melting temperatures are found to be in the same ratio as the critical temperatures for argon and krypton, but not for neon. We can therefore take the melting points as corresponding points for the first two cases, and obtain the energy factor as the ratio of the heats of vaporization at the melting point.

TABLE I. Conversion factors.[a]

	f_e			
	from T_c	from L_v at M. P.	f_r	f_Θ
Ne	0.155	0.140	0.714	1.405
A	0.520	0.518	0.872	1.496
Kr	0.722	0.716	0.928	1.145
Xe	1.000	1.000	1.000	1.000

[a] For data see reference 2.

The energy factors calculated in both ways are shown in Table I. They agree very well; we have actually used 0.155 for Ne, 0.520 for A, and 0.720 for Kr.

The "volume factor" was obtained as the ratio of the critical volumes for neon, and the ratio of the volumes of the solid at the triple point for the other substances (the result in no case differs greatly from that obtained from the critical-volume ratio). The "distance factor" f_r is the cube root of the volume factor.

The "Θ-factor" is calculated as follows: Θ varies as the (limiting) frequency ν of vibration, which in turn varies as (force constant/mass)$^{\frac{1}{2}}$. A force constant has the dimensions of energy/distance,[2] whereas the mass is proportional to the molecular weight. Since we have already calculated the energy and distance factors, the Θ factor f_Θ reduces to

$$f_\Theta=\frac{1}{f_r}\left(\frac{f_e M(\mathrm{Xe})}{M(\mathrm{S})}\right)^{\frac{1}{2}}, \qquad (1)$$

the M's representing the molecular weights.

The various calculated factors have been collected and appear in Table I.

The specific heat at constant pressure for xenon[3] has been measured from 10°K up to temperatures near the melting point, 161.3°K. Following the procedure that Rice used in the case of argon[4] we can obtain the entropy as a function of T by integrating under the C_p/T curve, and, from this, Θ as a function of T from the Debye tables.[5]

We now make use of the Grüneisen equation,[6]

[3] K. Clusius and L. Riccoboni, Zeits. f. physik. Chemie **B38**, 81 (1937).
[4] O. K. Rice, J. Chem. Phys. **12**, 289 (1944).
[5] Landolt-Börnstein Tabellen, Supplement 1, pp. 702–707 (1927).
[6] E. Grüneisen, *Handbuch der Physik* (1926), Vol. X. See also below, reference 9, Appendix I.

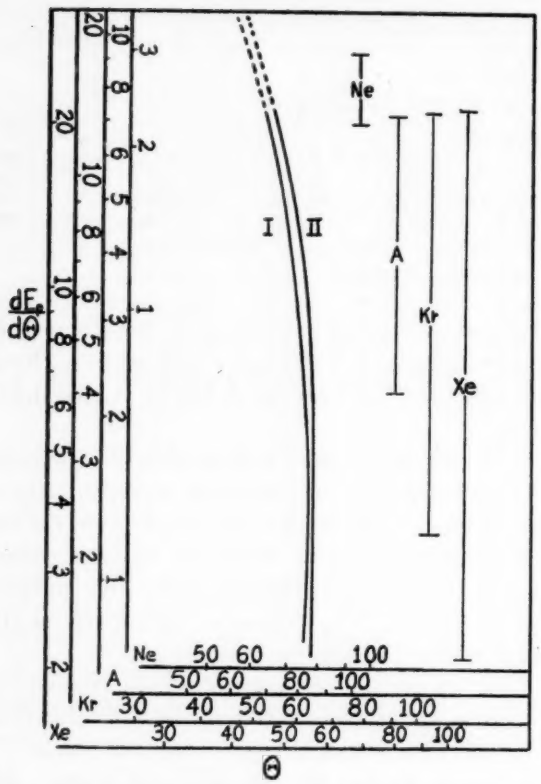

FIG. 1. $dE_p/d\Theta$ as a function of Θ. Θ in degrees, energy in cal./mole. Vertical lines indicate range of $dE_p/d\Theta$ values for each substance from 0°K to melting point. Curve I from xenon experimental specific heat data; Curve II is the assumed curve.

valid for the Debye solid, setting the pressure equal to zero for our process.

$$\frac{dE_p}{dV}=-\frac{E_t}{\Theta}\frac{d\Theta}{dV}-\frac{dE_z}{dV}. \tag{2}$$

Multiplying through by $dV/d\Theta$ and substituting $dE_z/d\Theta=E_z/\Theta$, we obtain

$$\frac{dE_p}{d\Theta}=-\frac{E_t+E_z}{\Theta}=-\left(\frac{E_t}{\Theta}+\frac{9}{8}R\right). \tag{3}$$

The right-hand side of this expression is a function only of Θ/T, and its values are obtainable from the Debye tables. This relation thus enables us to determine $dE_p/d\Theta$ as a function of Θ for xenon, and by means of our energy and Θ-factors, likewise for the other rare gas solids. However, in the latter case, we do not know to what temperature these values correspond, and we must reverse the procedure by substituting $dE_p/d\Theta=-(E_t/\Theta+9R/8)$ for each substance back into the Debye tables to obtain the proper Θ/T, and hence T.

We may test our procedure by means of the experimentally determined specific heats of neon, argon, and krypton.[3] To do this we make use of a relation of Grüneisen,[6] relating C_p, C_v, and the variation of Θ with T,

$$C_p=C_v\left(1-\frac{d\ln\Theta}{d\ln T}\right), \tag{4}$$

which holds for any Debye solid. This relation permits a direct calculation of C_p from the data we have obtained.

3. PROCEDURE

A graphical method was used to obtain $dE_p/d\Theta$ as a function of Θ/T for neon, argon, and krypton, from the xenon data. $E_t/\Theta+9R/8$ was obtained from the Debye tables and plotted as a function of Θ/T on log-log paper. The particular values of $dE_p/d\Theta$ for xenon were plotted as a function of Θ on another sheet of log-log paper. On superposition of the sheets, a shifting of the ordinate of the latter by $\log f_e/f_\Theta$ (for a given substance) corresponds to a multiplication of $dE_p/d\Theta$ by that factor; and a changing of the zero of the abscissa by $\log f_\Theta$ amounts to multiplication of Θ by that factor. Intersection of the two curves then gives Θ/T at the particular Θ or T desired. After one has obtained several intersection points at different temperatures, obtained by horizontal displacement of the two curves relative to each other, he has Θ/T and hence Θ as a function of T. The derivative $d\ln\Theta/d\ln T$ was obtained by

TABLE II. Xenon. [Units: temperature in °K; C_p in cal. mole^{-1} deg.$^{-1}$; α in deg.$^{-1}$.]

	Curve I (graphical)		Curve II				
T	Θ	C_p	Θ	$-\frac{d\ln\Theta}{d\ln T}$	$\alpha\cdot10^3$	C_p	C_p (expt)
10	53.6	1.95	56.0g	0.00	—	1.81	1.98
20	54.8	4.06	56.0g	0.00	—	4.15	4.06
40	54.9	5.69	56.0g	0.015	0.085	5.50	5.72
60	53.1	6.19	55.95	0.068	0.26	6.10	6.16
80	51.6	6.46	54.57	0.112	0.32	6.46	6.41
100	50.4	6.75	52.95	0.166	0.38	6.86	6.76
120	48.7	7.10	51.13	0.234	0.46	7.29	7.23
140	47.1	7.75	49.19	0.303	0.49	7.73	7.73
160	44.4	8.55	46.95	0.380	0.54	8.18	8.5

Melting point at 161.3°K.

plotting Θ *vs.* T on log-log paper and determining the slope graphically.

The results were later checked and extended by direct numerical calculation. A series of Θ and $dE_p/d\Theta$ values for one of the solids were calculated from the standard, and tabulated according to integral values of Θ. E_t/Θ was then obtained from $dE_p/d\Theta$ by the subtraction of $9R/8$, and from this Θ/T and hence T from the Debye tables. The difference in successive tabular values of T is just $dT/d\Theta$ for an intermediate Θ value, and by interpolation we get $dT/d\Theta$ for each integral value of Θ. $d \ln \Theta/d \ln T$ is the reciprocal of $(\Theta/T)dT/d\Theta$.

4. RESULTS OF CALCULATIONS

It was found that the results obtained with neon, argon, and krypton from the $dE_p/d\Theta$ curve for xenon (Curve I of Fig. 1) calculated from Clusius' and Riccoboni's experimental specific heat data, left much to be desired, especially in the case of argon. There is an apparent discrepancy in the data, however, which might account for the unsatisfactory agreement. The entropy at the melting point which Clusius and Riccoboni obtained by integrating under the C_p/T curve is 14.93 e.u., checking within 0.1 e.u. with the value calculated statistically. Using the same data we get 15.64 e.u., the percentage deviation from Clusius and Riccoboni's results being far outside the possible errors of computation. We are unable to explain this discrepancy. Furthermore, Curve I leads to an impossible trend in Θ at low temperatures (see Table II).

We decided to seek a $dE_p/d\Theta$ curve for xenon so adjusted as to give the best results for all the solids. The curve chosen is shown as Curve II in Fig. 1. The empirical equation which fits our assumed curve is

$$dE_p/d\Theta = 18.75 - 1.51(\Theta - 48) + 0.0245(\Theta - 48)^2 - 0.00338(\Theta - 48)^3. \quad (5)$$

This equation fits less accurately at high values of Θ, or low temperatures, where we have purposely given an infinite slope to the $dE_p/d\Theta$ curve over a considerable range.

The effect of assuming this particular curve is to reduce our calculated entropy for xenon, though it still does not reach the value of 14.93 given by Clusius. In Table II are given the values of C_p calculated from each of these curves and compared with the experimental values. As we would expect, Curve I checks the specific heats almost exactly throughout the temperature range, while with Curve II we get deviations as great as 0.3 cal. per degree.

The calculated specific heats obtained from Curve II are given in Tables II–V. The two methods of calculation checked closely, except at the lowest temperatures, where the empirical Eq. (5) deviates somewhat from the curve as drawn. The numerical calculations are given in the tables over most of the temperature range, unless otherwise indicated, since they are the more accurate. At low temperatures graphical

TABLE III. Krypton.

T	Θ	C_p (calc)	C_p (expt)	$-\frac{d \ln \Theta}{d \ln T}$	$\alpha \cdot 10^3$
10	63.9*g*	1.39	1.36	0.00	—
20	64.0*g*	3.75	3.72	0.00	—
30	63.6*g*	4.92	5.00	0.02	0.15
40	64.02	5.55	5.65	0.056	0.32
60	61.95	6.30	6.30	0.114	0.43
80	59.31	6.92	6.81	0.194	0.55
100	56.17	7.60	7.53	0.296	0.67
110	54.48	7.96	8.10	0.352	0.73

Melting point at 116.0°K.

TABLE IV. Argon.

	$f_\Theta = 1.496$ (graphical)		$f_\Theta = 1.530$				
T	Θ	C_p	Θ	$-\frac{d \ln \Theta}{d \ln T}$	$\alpha \cdot 10^3$	C_p	C_p (expt)
10	82.9	0.75	85.1*g*	0.00	—	0.70	0.82
20	82.5	2.89	84.7*g*	0.01	0.11	2.82	2.84
30	81.6	4.40	83.89	0.053	0.40	4.38	4.40
40	80.2	5.35	82.20	0.092	0.52	5.30	5.28
50	78.3	5.97	80.12	0.140	0.64	6.00	5.90
60	75.9	6.60	77.68	0.202	0.76	6.60	6.40
70	73.0	7.27	74.90	0.276	0.90	7.18	7.00
80	69.7	7.79	71.87	0.342	0.97	7.70	7.70

Melting point at 83.8°K.

TABLE V. Neon (graphical).

T	Θ	C_p (calc)	C_p (expt)	$-\frac{d \ln \Theta}{d \ln T}$	$\alpha \cdot 10^3$
10	65.9	1.36	1.43	0.045	1.02
14	64.7	2.64	2.58	0.070	1.14
18	63.2	3.86	3.69	0.120	1.52
21	61.7	4.79	4.62	0.195	2.11
23	60.5	5.35	5.46	0.240	2.37

Melting point at 24.5°K.

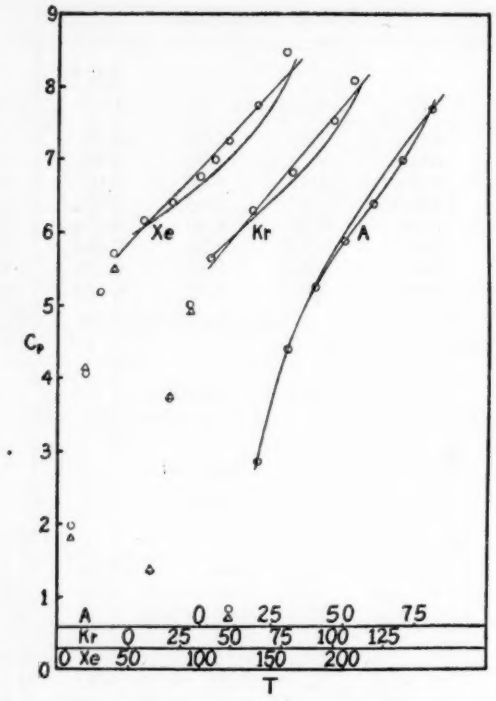

FIG. 2. Specific heats of the rare gas solids. Upper curves from Curve II, lower curves from argon $dE_p/d\Theta$ curve. ○ experimental points. △ calculated by graphical method from Curve II.

calculations are given and are denoted by the letter *g*.

It is seen that our attempt to find a $dE_p/d\Theta$ curve capable of explaining the experimental facts for the various substances is reasonably successful. Nevertheless, certain not entirely negligible differences remain, especially in the case of argon. Setting $f_\Theta = 1.530$ instead of 1.496 (without changing f_e), improves the results somewhat. This corresponds to an approximately 2 percent error in f_r, or a 6 percent error in the critical volume. This seems rather large; however, some such adjustment does seem to be necessary, since it brings the Θ's at the higher temperatures into agreement with those of Rice's earlier calculations.[4] Θ in Table IV, however, changes more rapidly with temperature than his calculations indicated. In view of the still remaining discrepancies, it seemed desirable, simply for comparison, to make some calculations based on the $dE_p/d\Theta$ curve for argon obtained from Rice's calculations. Actually the curve given by Rice in his latest paper[7] was very slightly modified, starting at about $\Theta = 74$. At $\Theta = 71$ the value of $dE_p/d\Theta$ has become a little over one-half percent, lower than that given by Eq. (7) of reference 7, thus increasing C_p at $\Theta = 71$ by about 1 percent. This was done to effect a better fit with the values of C_p at the highest temperatures. That such a slight change in $dE_p/d\Theta$ can produce this much change in C_p indicates that C_p is sensitive to small errors in calculation in this region of temperatures just below the melting point, and cannot be obtained with high accuracy in this region. It should be stated, however, that if all the values of $dE_p/d\Theta$ were changed uniformly only a small change in C_p would be caused; it is $d^2E_p/d\Theta^2$ which affects C_p.

The curve for xenon was obtained by reverse use of the f_e and f_Θ factors ($f_\Theta = 1.530$), and that for krypton then obtained from xenon in the standard way. This $dE_p/d\Theta$ curve, referred to xenon, is given by the empirical equation,

$$dE_p/d\Theta = 18.50 - 1.68(\Theta - 48) - 0.0125(\Theta - 48)^2 - 0.0014(\Theta - 48)^3. \quad (6)$$

We have not tabulated the results of the last mentioned calculation, but the results of both calculations are summarized in Fig. 2.

The experimental C_p values for krypton lie about midway between the values calculated from the assumed xenon $dE_p/d\Theta$ curve and the argon $dE_p/d\Theta$ curve. In the case of xenon a better fit is obtained with the assumed $dE_p/d\Theta$ curve. The experimental specific heats appear to show a gradual transition from one curve to the other as we go from argon to xenon.

Neon has not been included in this comparison, since most of the calculated C_p values must be obtained from an extrapolation of the $dE_p/d\Theta$ curve to higher values. It should be remarked, however, that the assumed $dE_p/d\Theta$ curve lends itself more readily to an extrapolation, which reproduces the experimental data for neon, than does the argon $dE_p/d\Theta$ curve. This will be discussed further in Section 6.

The quantity $-d \ln \Theta / d \ln T$ is a measure of the contribution of the thermal expansion to the specific heat. It can also be written

$$-\frac{d \ln \Theta}{d \ln T} = -\frac{d \ln \Theta}{d \ln V} \frac{T}{V} \frac{dV}{dT} = \gamma T \alpha, \quad (7)$$

[7] O. K. Rice, J. Chem. Phys. **14**, 321 (1946).

where $\gamma = -d \ln \Theta / d \ln V$, and α is the coefficient of thermal expansion. γ has been assumed by Grüneisen to be constant. Rice[7] has shown that $\Theta^{-1} d\Theta/dV = 0.18$ is consistent with the experimental data for argon. Using the molal volume for argon at the melting point, 24.5 cc/mole, we find the corresponding value of γ to be 4.40. Since the volume does not change much over the temperature range, γ as calculated by assuming $\Theta^{-1} d\Theta/dV$ to be constant will not vary by more than a few percent. Since the thermal expansion goes to zero in any event at low temperatures, we should get reasonably accurate results by the use of $\gamma = 4.40$ at all temperatures. This same value of γ will be used for the other solids; in effect we have already assumed this in the main part of the paper.

The coefficients of expansion for the four solids calculated in this manner appear along with the other data from Curve II in Tables II–V. The values are accurate to the extent that the Debye theory holds for the rare gas solids and to the extent that Curve II approximates the true $dE_p/d\Theta$ curve for each substance. The available experimental data on α are at present too scanty to make a useful comparison.

$d \ln \Theta / d \ln T$ should always be either zero or have a negative value, in order that α always remain positive. The values shown in this table correspond to this behavior. However, we must remember that at low temperatures these result from an assumed $dE_p/d\Theta$ curve, and at the lowest temperature our calculated C_p is generally less than the experimental value. This means that $d \ln \Theta / d \ln T$ would appear to become positive at very low temperatures, if the experimental data were followed exactly. This is connected with the Θ anomalies in argon at low temperatures already noted by Clusius,[8] and by Rice.[4,9] The available evidence does not enable us to decide between the various possible explanations for this anomaly.

5. EFFECT OF QUANTIZATION

The range of $dE_p/d\Theta$ values for the four solids indicated by the vertical lines of Fig. 1 provides an interesting study. The lower limit of these lines represents a temperature of absolute zero for that particular solid, and the upper limit the melting point. Xenon is seen to have a very wide range of $dE_p/d\Theta$ values, the range gradually decreasing as we go from xenon to krypton to argon to neon. Furthermore, the point on the $dE_p/d\Theta$ curve where melting occurs is about the same for argon, krypton, and xenon, but is considerably higher for neon.

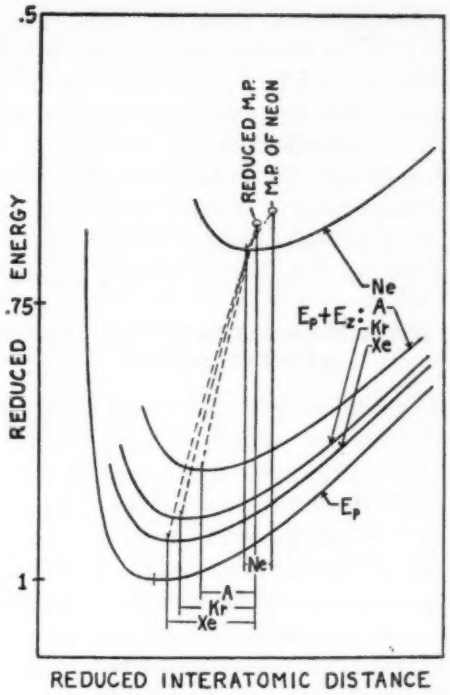

FIG. 3. Effect of zero point energy.

The difference in location of the absolute zero for the four solids is undoubtedly caused by the relative importance of the zero point energy. The situation can be visualized by considering the series of energy curves shown schematically in Fig. 3. The lowest curve is the "reduced" E_p curve for the four solids plotted against "reduced" interatomic distance. The other curves are the corresponding "reduced" E_p+E_z curves for xenon, krypton, argon, and neon. At the absolute zero the state of equilibrium is at the minimum of these E_p+E_z curves, not the E_p curve itself. As the relative importance of zero point energy becomes greater, this position of equilibrium is shifted more to the right of the E_p minimum. On heating the solid from absolute zero to the melting point the total energy will rise along some such path as is shown by the dotted lines.

We also see in Fig. 3 why the melting point is

[8] K. Clusius, Zeits. f. physik. Chemie **B31**, 459 (1936).
[9] O. K. Rice, J. Am. Chem. Soc. **63**, 3 (1941).

not a corresponding point for neon. The large relative effect of the zero point energy has shifted the minimum of the E_p+E_z curve so far to the right that neon has expanded beyond the "reduced" interatomic distance of melting before enough quantum levels have become excited to cause a breakdown of the lattice. Thus it must go to greater interatomic distances and consequently greater values of E_p before melting occurs.

6. DEVIATIONS BETWEEN CALCULATION AND EXPERIMENT

Although fairly good agreement is obtained in general between calculated and experimental values of C_p, one must try to explain the deviations which do occur. The deviations are of three types. (1) While there is a tendency for the C_p values of all the substances to rise rather sharply at temperatures near the melting point, there is difficulty in accounting for all the cases by the same curve. (2) We have noted that a change of 2 percent in f_Θ for argon improves the agreement, and indeed, appears to be required, though this corresponds to a 6 percent error in the critical volume. (3) There seems to be a definite difference in the character of the curvature of the experimental C_p *vs.* T curves of the different substances (see Fig. 2). To explain these deviations we may consider three possibilities, (A) experimental error, (B) failure of the Debye theory, and (C) failure of Pitzer's assumption V.

Let us first consider deviation (1). Near the melting point the experimental specific heats show a sharp rise for all four solids that is reproduced qualitatively, though not very exactly, for xenon, krypton, and argon, by calculation from the argon $dE_p/d\Theta$ curve, but not from Curve II. This rise in specific heat near the melting point is reflected in the $dE_p/d\Theta$ curve by a rapid change of slope, i.e., by a large $d^2E_p/d\Theta^2$ near the melting point. The calculated C_p's are very sensitive to the slope of the $dE_p/d\Theta$ curve. In the case of neon, we must pass through these high values of $d^2E_p/d\Theta^2$ long before melting occurs, and we must extrapolate the curve until the melting point is reached. The extrapolation on the assumed $dE_p/d\Theta$ curve is shown in Fig. 1. The specific heat calculated from this is higher than the experimental over most of the temperature range. If we make the straightest possible extrapolation of the argon $dE_p/d\Theta$ curve, the calculated C_p for neon is still higher, and an extrapolation with a uniform rate of change of the slope would be even worse. The situation could not be improved much by altering the energy and Θ factors for neon. It would be necessary to make a definite inflection in the $dE_p/d\Theta$ curve in the upper regions, giving an unreasonable appearance to the over-all curve, and it could be done only at the expense of the other solids, which require a high $d^2E_p/d\Theta^2$ near the melting point.

(A) In order to advance an explanation for these difficulties, we must ask why the sharply rising specific heats near the melting point occur. It may be caused, at least in part, by a pre-melting phenomenon, i.e., to a setting in of disorder before the melting temperature is reached, a rather special case of breakdown of the Debye theory. Rice[4] has concluded that the experimental data on solid argon are best explained by the assumption of no disorder in the solid, but a small amount may appear very close to the melting point. It may be possible, on the other hand, that the rise in experimental specific heat is greater than it should be because of experimental difficulties incident to specific heat measurements in this region. The fact that Clusius' experimental specific heats tended to be slightly erratic near the melting point lends some credence to this view. An experimental error could occur because melting was taking place on the faces of the crystals because of non-equilibrium temperature conditions. Disorder in the solid would mean that premelting was occurring throughout the interior of the crystal.

In general we hesitate to claim that deviations of type (2) or (3) are caused by errors in the specific heats, though the errors required would be of the order of only a few percent, and, as we have noted, some difficulties are apparent in the case of xenon (in fact the percentage difference between the two sets of Θ's shown in Table II is greater than the percentage difference between the two f_Θ's used in Table IV). It seems quite possible that explanations of the type (B) or (C) may hold the answer in these cases.

(B) The Debye theory itself rests on the theory of small vibrations in a molecular lattice; small vibrations are also implied in our method of calculating the Θ factor. Rice[4] has presented a

discussion of the failure of the theory of small vibrations in the case of argon, pointing out that the relatively large amplitudes deducible from experimental data should give rise to appreciable anharmonicities in the vibration. With this in view, it is not surprising that small changes are necessary in the Θ-factor; in fact the surprising thing is that our bold assumption that the Θ's can be obtained by a dimensional analysis of the mechanical system works as well as it does. This difficulty might also conceivably cause deviations of type (3).

(C) Pitzer's assumption V that the four substances have the same reduced E_p curve may not be strictly true. Guggenheim[2] noted that this assumption should be accurate for large values of r, where the intermolecular potential energy ϵ is proportional to $-r^{-6}$, but that there was good reason to suppose that it does not hold accurately in general. He further stated that many macroscopic properties were insensitive to the precise form of the relation between ϵ and r for small r. The fact that argon, krypton, and xenon obey the principle of corresponding states as liquids is consistent with these considerations. In the solid state, however, it seems likely that the properties are considerably more sensitive to the shape of the potential energy curve.

THE JOURNAL OF CHEMICAL PHYSICS VOLUME 14, NUMBER 9 SEPTEMBER, 1946

On the Ultraviolet Absorption Spectrum of Ozone†

W. H. EBERHARDT* AND W. SHAND, JR.
The Gates and Crellin Laboratories of Chemistry, California Institute of Technology, Pasadena, California
(Received April 1, 1946)

The absorption spectrum of ozone has been investigated in the near ultraviolet from λ3439 to 3850A at two temperatures. The bands observed have been interpreted as arising in part from transitions from the vibrationless ground electronic state and in part from transitions from excited vibrational levels of the ground electronic state. The distinction between the two groups is based primarily on the relatively large temperature sensitivity of the intensity of the bands ascribed to transitions from excited vibrational states. A partial analysis gives strong support to the assignment of the frequency 1043 cm^{-1} to a fundamental vibration of the molecule. Moreover, it appears quite unlikely that the frequency 710 cm^{-1} can be eliminated as one of the fundamental frequencies. No information concerning the third fundamental frequency was obtained.

THE spectroscopic evidence on the structure of ozone has recently been critically examined by Simpson,[1] who gives a new assignment of the fundamental vibration frequencies of the ozone molecule. This assignment leads to a configuration in which the oxygen atoms are arranged in the form of an obtuse isosceles triangle with apical angle 125° and bond length 1.17A, in fair agreement with the electron diffraction results[2] which give an apical angle of 127° and bond length 1.26A. However, the infra-red absorption spectrum of ozone has not been examined in sufficient detail under high enough dispersion to permit an unambiguous assignment of the three fundamental frequencies from among the four possibilities which seem most likely in view of the experimental data, namely,710, 1043, 1740, and 2105 cm^{-1}.[3-6]

An analysis of the effect of temperature on the vibrational structure of the band system in the ozone spectrum lying in the region λ3000–3850A offers hope of affording additional information as to the fundamental vibrational frequencies of the normal state of the molecule. Such analysis

† Contribution Number 1051.
* Present Address: Georgia School of Technology, Atlanta, Georgia.
[1] D. Simpson, Trans. Faraday Soc. **41**, 209 (1945).
[2] W. Shand, Jr. and R. A. Spurr, J. Am. Chem. Soc. **65**, 179 (1943).
[3] G. Hettner, R. Pohlmann, and H. J. Schumacher, Zeits. f. Elektrochemie **41**, 524 (1933).
[4] S. L. Gerhard, Phys. Rev. **42**, 622 (1933).
[5] A. Adel *et al.*, Astrophys. J. **89**, 320 (1939), **94**, 451 (1941); Phys. Rev. **49**, 288 (1936).
[6] R. S. Mulliken, Rev. Mod. Phys. **14**, 204 (1942).

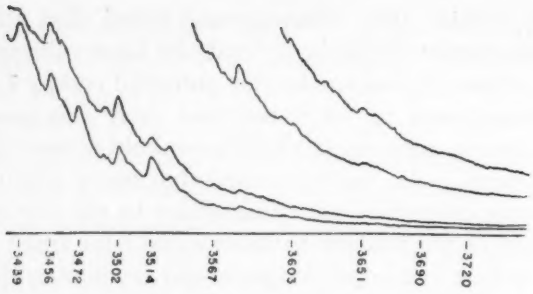

FIG. 1. Copy of microphotometer traces of a part of the near ultraviolet absorption spectrum of ozone at room temperature and at 90 degrees Centigrade. Complete description in text.

involves the finding and the interpretation of a number of bands, among the many members in the system, which originate in transitions from excited vibrational levels in the normal electronic state of the molecule. It should be possible to identify these bands by the pronounced increase with temperature of the intensity of their absorption.

The absorption spectrum of ozone in the region from λ3000–3650A[7–12] consists of a system of diffuse bands falling off rapidly in intensity with increasing wave-length which appear to overlie a background of continuous absorption. The intense bands in this region may be ordered in groups of partial progressions and interpreted in terms of transitions from a vibrationless ground state to an upper electronic state in which two vibrational frequencies are excited. A formula for these bands which has been suggested by Jakowlewa and Kondratjew[11] seems to fit the positions of the bands reasonably well:

$$\nu = 28447 + 636.3v_1' - 16.0v_1'^2 + 351.7v_2' - 4.5v_2'^2 - 0.17v_2'^3 - 12.0v_1'v_2' - 1.5v_2'v_1'^2 - 0.5v_1'v_2'^2 - 1058v'' + 11.5v''^2. \quad (1)$$

In addition to the bands described by this expression there exists, principally to longer wavelengths, a large number of weaker bands. These bands are strongly temperature-sensitive and may presumably be ascribed to transitions from excited vibrational levels in the ground state. If this is the case it is to be expected that these bands may be ordered in such a way as to form progressions homologous to the temperature insensitive bands but shifted toward the red from them by constant frequency differences corresponding to the energies of the excited vibrational levels of the ground state. Four bands of such a group, based upon the frequency 1043 cm^{-1}, have been observed in work at the temperatures −78°C, room temperature, and 100°C.[10,11] We have endeavored to extend the ultraviolet absorption spectrum of ozone to longer wavelengths in order to obtain more data on the temperature-sensitive bands, to ascertain that no temperature-insensitive bands lie beyond the proposed $(000)'' \rightarrow (000)'$ bands[8,11] at λ3514A, and to classify as many as possible of the temperature-sensitive bands in terms of vibrational frequencies of the ground state as indicated by observations in the infra-red.

The absorption was studied at room temperature and at 90°C in the region of weak absorption from λ3439 to 3850A by means of a Bausch and Lomb Littrow quartz spectrograph with a dispersion of about 7A per mm in this region. A 500-watt tungsten projection lamp was used as a light source. The absorption cell was an 8-meter glass tube enclosed in a stainless steel jacketing tube which could be heated electrically. The ozone was prepared by passing a continuous stream of tank oxygen through two Siemens type ozonizers and then through the cell. Dry-ice traps were provided to condense N_2O_5, which catalyzes the decomposition of ozone at the higher temperature, and might contribute to the absorption in this region if its partial pressure were not kept sufficiently low.[13] The concentration of ozone in the cell was estimated by means of the absorption coefficients of Ny and Choong[14] at λ3439A to be about 6 percent. The positions and relative intensities of the bands were determined from microphotometer traces; the weakness of the bands and the intensity of the continuous background made measurements with a visual comparator impractical. A large number

[7] A. Fowler and G. Strutt, Proc. Roy. Soc. **93**, 729 (1917).
[8] O. R. Wulf and E. H. Melvin, Phys. Rev. **38**, 330 (1931).
[9] D. Chalonge and L. Lefebvre, Comptes rendus **197**, 444 (1933).
[10] L. Lefebvre, Comptes rendus **199**, 456 (1934).
[11] A. Jakowlewa and K. Kondratjew, Phys. Zeits. Sowjetunion **9**, 106 (1936).
[12] D. Melcher, Helv. Phys. Acta **18**, 72 (1945).
[13] E. J. Jones and O. R. Wulf, J. Chem. Phys. **5**, 873 (1937).
[14] T. Z. Ny and S. P. Choong, Chinese J. Phys. **1**, 38 (1933).

of bands was observed, including all of those indicated by Chalonge and Lefebvre,[9] and other bands at longer wave-lengths. In all, seventy-four bands were recorded, although some of these were very weak and longer ozone paths or higher concentrations would be necessary to confirm their existence and to determine their exact positions. The positions of the bands could be estimated to an accuracy of only about ± 1A in the region λ3439 to 3600A and ± 2A in the region λ3600 to 3850A.

A copy of microphotometer traces of a part of the spectrum is presented in Fig. 1. Two sets of traces are given which differ in the technique of microphotometering employed. The lower two traces were prepared with a narrow microphotometer slit and show the stronger bands clearly and with high resolution. The upper set of two traces was made with a wider slit for reasons of greater sensitivity in regions of the plate where the photographic density was higher. In each set the lower of the two traces corresponds to the spectrum at room temperature; the higher corresponds to that at 90 degrees C. Both traces are referred to the same base line. The wave-length of some readily identified bands is indicated on the figure. The figure does not present adequately the data at longer wave-lengths were enlarged traces made with wider microphotometer slits allow greater accuracy in measuring the bands. Moreover, comparison of measurements from several plates also lends greater confidence in the existence and position of these very weak bands than is suggested by the single figure presented. The figure shows clearly the relatively low temperature sensitivity of the bands at λ3439, 3472, and 3514A.

An approximate estimate of the absorption coefficients of the bands was made using the optical density of the photographic plate as indicated by the photometer traces and the Hurter and Driffield curves for the plate. The ratio of these calculated coefficients for the two temperatures, 90 degrees and 25 degrees C, was used as an indication of the temperature sensitivity of the bands. Only rough quantitative significance should be attached to this ratio for the following reasons: First, the concentration of ozone at the lower temperature was known only approximately and no estimate whatsoever was made of that at the higher temperature; most likely, it was appreciably less because of thermal decomposition. In the calculations it was assumed that these concentrations were equal. Second, the estimates were based only on the absorption of the maxima of diffuse bands and not on the integrated intensity of the bands. Moreover, since it was not possible to separate the bands from the background of overlapping bands, the estimate of the absorption coefficient depends not only on the particular band system for which it was calculated, but also on the underlying, very temperature-sensitive background. It was found that the ratio of the absorption coefficients at the two temperatures for bands assigned to transitions of the type $(000)''\rightarrow(v_1v_20)'$ was considerably less than that for bands believed to be caused by transitions from excited vibrational levels in the lower electronic state. That the "temperature-insensitive" bands vary at all with temperature is probably due to the overlapping of portions of adjacent temperature-sensitive bands. In particular, of all the bands here studied, only those at λ3439, 3472, and 3514A were relatively insensitive to temperature change; all other bands in this spectral region increased more rapidly in intensity on heating than these. Thus, the data seem to confirm quite well the assignment of the band at λ3514A to the transition $(000)''\rightarrow(000)'$.

An attempt was made to classify the remaining temperature-sensitive bands in the following fashion. The intense bands previously reported[8,12] and arranged in array of partial progressions were assumed to be caused by transitions from the vibrationless ground state. (A convenient tabulation of these bands is given by Melcher, reference 12.) Energies corresponding to assumed vibrational levels were subtracted from the energies associated with these temperature-insensitive bands, and the tabulated data were searched for bands with frequencies corresponding to those calculated by this method. Because of the diffuse character of the bands, the accuracy of the measurements limited the precision obtainable in matching the calculated and observed frequencies, and agreement to within about 15 cm^{-1} was considered acceptable. Attempts were made to classify the bands in terms of the assumed fundamental frequencies

TABLE I. Summary of the bands observed and their possible assignment $\nu_1'' = 1043$, $\nu_2'' = 710$, $\nu_3'' = 2105$.

Upper state			$(v_1' v_2' 0)$			$(v_1' v_2' 0)$			$(v_1' v_2' 0)$			$(v_1' v_2' 0)$		$(v_1' v_2' 0)$	
Lower state			$(v_1'' 0\ 0)$			$(0\ v_2''0)$			$(0\ 0\ v_3'')$			$(1\ 1\ 0)''$		$(1\ 2\ 0)''$	
Band		$\frac{\alpha_{90}^{**}}{\alpha_{25}^{\circ}}$	v_1''	v_1'	v_2'	v_2''	v_1'	v_2'	v_2''	v_1'	v_2'	v_1'	v_2'	v_1'	v_2'
3439A	29070±5 cm^{-1}	1.07	0	1	0										
3448	28994	1.24				1	1	2							
3452	28960	1.25	1	1	3										
3456	28927	1.24	1	2	1	1	2	0							
3463	28868	1.22				2	2	2							
3472	28794	1.16	0	0	1										
3481	28719	1.34													
3486	28678	1.48	1	1	2	1	1	1							
3488	28662	1.46													
3495	28604	1.40	1	2	0	2	1	3	1	4	0				
3498	28580	1.43				2	2	1							
3502	28547	1.53				3	2	3						4	1
3506	28514	1.48										2	2		
3509	28490	1.50	3	4	3										
3514	28442	1.23	0	0	0							3	0		
3518	28417	1.37	1	0	3	1	0	2							
3526	28353	1.44	1	1	1	1	1	0						3	2
3529	28329	1.44				2	1	2							
3533	28297	1.44												4	0
3537	28265	1.40	3	4	2	2	2	0				1	3		
3538	28256	1.42	2	2	2	3	2	2							
3545	28201	1.59										2	1		
3553	28137	1.51												2	3
3560	28082	1.69	1	0	2	2	0	3;	1	3	0			3	1
						1	0	1							
3567	28027	1.47	1	1	0	2	1	1							
3571	27995	1.42	3	4	1										
3575	27964	1.47				3	1	3				1	2		
3580	27925	1.53	2	2	1	3	2	1							
3583	27902	1.52										2	0		
3590	27847	1.45												2	2
3596	27801	1.40	3	3	2										
3603	27747	1.36	1	0	1	2	0	2;						3	0
						1	0	0							
3606	27724	1.32	3	4	0										
3608	27708	1.34				2	1	0				0	3		
3614	27662	1.31	2	1	2	3	1	2							
3620	27616	1.36	2	2	0	3	2	0							
3624	27586	1.40	3	2	3							1	1		
3627	27563	1.37				4	3	0	1	2	0			1	3
3630	27541	1.47													

710, 1043, 1740, and 2105 cm^{-1}, which appear as reasonable possibilities in the light of previous investigations of both the ultraviolet and the infra-red spectrum of ozone.[1,6]

Table I summarizes the positions of the bands observed and the transitions assigned to them. Only two frequencies were employed in the upper state, according to Eq. (1), since the data did not seem to justify the assumption of a third. Because of the lack of resolution, the two frequencies 1740 cm^{-1}, assumed as a possible fundamental, and 1753 cm^{-1}, corresponding to (710 +1043) cm^{-1}, are tabulated together; the data do not allow of a distinction between these two possibilities.

Table II was prepared to show the comparative number of bands which can be fitted by various assumed combinations of fundamental frequencies. The assumed lower state frequencies and their combinations are indicated at the head of the columns of the table, namely, 1043, 710, 1740, 1043+710, 1043+2×710, and 2105 cm^{-1}. From the columns of Table I it is readily possible to count the number of bands fitted by each of these frequencies. The maximum number of bands fitted by the frequency at the head of the column is given in the last row of the table regardless of whether it is possible to account for some of the bands by other assumed frequencies. However, since some of the bands may be described in more than one way, it is necessary in evaluating the assignment of vibrational fre-

TABLE I.—*Continued.*

Band		$\frac{\alpha_{30}^{\circ *}}{\alpha_{25}^{\circ}}$	v_1''	v_1'	v_2'	v_2''	v_1'	v_2'	v_3''	v_1'	v_2'	v_1'	v_2'	v_1'	v_2'
3633A	27518±5 cm^{-1}	1.41	3	3	1									2	1
3637	27487	1.47													
3648	27405	1.35	1	0	0	2	0	1							
3651	27381	1.37										0	2		
3655	27352	1.33	2	1	1	4	1	3;							
						3	1	1							
3657	27337	1.35				4	2	1				1	0		
3664	27285		3	2	2									1	2
3667	27262														
3672	27225	1.36												2	0
3674	27211		3	3	0										
3676	27196														
3678	27181														
3681	27159														
3683	27144	1.32													
3688	27107														
3690	27093		2	0	2	3	0	2							
3693	27071					4	1	2;							
						3	1	0;							
						2	0	0							
3700	27019	1.32	3	1	3;	4	2	0				0	1	0	3
			2	1	0										
3706	26976		3	2	1										
3708	26961								1	1	0			1	1
3718	26889														
3720	26874														
3725	26838					4	0	3							
3734	26773	1.31				4	1	1;							
						3	0	1							
3738	26745		2	0	1										
3743	26709		3	1	2							0	0	0	2
3750	26659		3	2	0										
3753	26638													1	0
3760	26587														
3777	26469		3	0	3										
3782	26434					4	1	0;							
						3	0	0							
3786	26406		3	1	1;	4	0	2							
			2	0	0										
3795	26343	1.33							1	0	0			0	1
3824	26143													0	0
3840	26034		3	0	2	4	0	1							

* Since the ratio of absorption coefficients for bands at λ greater than λ3650A differed so little from that of the background, this ratio was not calculated for individual bands at wave-lengths greater than λ3680A. The values given are for the region of the spectrum, not individual bands.

quencies to consider the relative value of various sets of assumed frequencies in fitting the entire band system. Accordingly, certain sets of frequencies have been chosen which are enumerated in the first column of the table. The number of bands described by each set is counted as follows:

Bands which can be accounted for by the first listed frequency of the set are tabulated in the column allocated to this frequency; then bands not already accounted for by the first frequency, but given independently by the second frequency are counted and entered in the corresponding frequency column, and similarly for the third frequency excluding bands ascribed to the first and second. Finally bands accounted for by combinations or other frequencies are listed in their respective columns, but always so that no band has been counted more than once. In the tabulation, bands arising from the vibrationless ground state have been omitted. The last column of the table gives the total number of bands fitted by any particular set of assumed frequencies. Not all of the bands which are listed in Table I have been fitted into any of the schemes of Table II; twelve bands are not accounted for by any transitions based on the frequencies assumed. These bands are almost all at the long wave-length end of the band system and are very weak. Uncertainties in the measurement of their positions are large, and they may actually

TABLE II. Number of bands fitted into scheme of frequency.

Frequencies excited in lower state / Order of use of frequencies	1043	710	1740 or 1043 +710	1043 +2 ×710	2105	Total
1043	33					
710		14	4	8	0	59
710		32				
1043	15		4	8	0	59
1740			12			
1043	29			8	0	59
710		10				
2105					5	
1043	31		4	6		59
710		13				
2105					5	
1043	31	—		—		43
1740			7			
Maximum number	33	32	12	8	5	

be spurious. It is however, not unreasonable to suppose that they arise from still higher levels in the ground state than have been employed in the calculations, and it is believed probable that these bands could be accounted for satisfactorily in that fashion. In addition, it should be pointed out that no value for ν_3' has been suggested, and it might indeed be profitable to examine the positions of the unassigned bands for such a possibility.

It will be noticed that the frequency 1043 cm^{-1} enters into all of the assumed schemes. The assumption of this frequency as a fundamental seems hardly disputable since the intensity of the bands based upon this frequency is greater by far than any other band arising from transitions of a similar type. The infra-red data[1] are also in support of this frequency as a fundamental. Transitions arising from levels of this set but higher than the first were fitted by adjusting the first anharmonic term in the expansion of the energy of the vibrational state so as to give as accurate a fit as possible to the positions of temperature-sensitive bands in the correct neighborhood. With both this frequency and that based on 710 cm^{-1} only the square term in the expansion is given, since it is not believed that the three infra-red frequencies involved in the bands associated with the 1043 cm^{-1} separation and the four infra-red frequencies involved in the bands associated with the 710 cm^{-1} separation justify the addition of higher terms. The energy (expressed in wave numbers) corresponding to higher levels of these two vibrations fitted in the way described are represented by the following two formulas:

$$\nu_1'' = 1066v_1'' - 23v_1''^2,$$
$$\nu_2'' = 727v_2'' - 17v_2''^2.$$

The point to which we wish to call particular attention is demonstrated by Table II, namely, that it is possible to ascribe almost all of the bands observed in the temperature-sensitive ultraviolet spectrum of ozone to the two fundamental frequencies 710 and 1043 cm^{-1}, and their harmonics and combinations. Some bands fit into schemes in which other fundamental frequencies are assumed, but these bands are just as well classified by the first two frequencies, which in addition explain many other bands. Moreover, the assumption of frequencies for the ground electronic state which do not include 710 cm^{-1} results in a scheme which is considerably inferior in classifying all of the bands. It accordingly seems very unlikely that 710 cm^{-1} can be eliminated as one of the fundamental frequencies of the ozone molecule.

The authors wish to express their appreciation to Dr. O. R. Wulf of the U. S. Weather Bureau for suggesting this problem, and for his encouragement and assistance in obtaining and interpreting the data. We also wish to thank Professor Badger for use of the spectrograph and for helpful criticism of the manuscript.

The Force Constants of Ozone

GEORGE GLOCKLER AND GEORGE MATLACK*
Department of Chemistry and Chemical Engineering, State University of Iowa, Iowa City, Iowa
(Received April 8, 1946)

A general valency force field treatment has been applied to the ozone molecule, in which it has been possible to obtain values for all four force constants. The values obtained, using a fundamental frequency assignment of Penney and Sutherland, are compared with values obtained from other assignments. In the light of present knowledge concerning the structure of the ozone molecule, the values used by Penney and Sutherland ($\omega_1=1043$, $\omega_2=710$, $\omega_3=1740$ cm^{-1}) are the most consistent, and the force constant of the oxygen-oxygen bond agrees better with the value predicted by Badger's rule than do the others. The oxygen-oxygen bond force constant in ozone lies in the range 0.75 to 0.99 megadyne.

INTRODUCTION

SINCE 1934, various assignments of the fundamental frequencies of the ozone molecule have been made in the attempt to evaluate its force constants.[1-5] The results obtained from these investigations do not seem satisfactory when compared with the value predicted by Badger's rule[6] and when the type of O−O bond is considered. This is partly caused by a questionable assignment of fundamental frequencies and partly caused by the fact that a simplified force field treatment was previously used in which some of the force constants were assumed to be zero. It is the purpose of this paper to show that force constants in fair agreement with the predicted values (by Badger's rule) can be obtained by treating the problem with a general valency force field in which none of the force constants is assumed to be zero.

APPLICATION OF THE GENERAL VALENCY FORCE FIELD

The theoretical considerations of the method have been explained in a previous paper.[7] In general, the six force constants of a triatomic molecule are reduced to four when the molecule is of the isosceles triangle model type. Since there are only three fundamental frequencies in a triatomic molecule, only three of the four force constants can be evaluated by a direct approach to the problem; the four force constants are: valence bond (c_1), angle bending (c_2), angle-bond interaction (c_3), bond-bond interaction (c_4). In the present method, c_4, which is nearly always small in magnitude, is assumed to have certain values; c_1, c_2, and c_3 may then be calculated from the three equations from the theory of small vibrations, using the three fundamental frequencies, the valence angle, and the value assumed for c_4 as known quantities. When a number of sets of values is thus calculated for c_1, c_2, c_3, and c_4, it is found that an elliptical relation exists between c_4 and c_3, between c_4 and c_2, and a linear relation between c_4 and c_1. The problem is thereby reduced to one of choosing the appropriate set from all the real sets thus calcu-

TABLE I. Force constants of O_3 calculated from Eq. (2).

Source	Assignment (cm^{-1})			Range of force constants (megadynes/cm)			
	ω_1	ω_2	ω_3	c_1	c_2	c_3	c_4
Simpson[a]	1740	1043	2105	2.030 1.242	0.312 0.588	0.378 0.136	0.432 −0.356
Hettner[b]	2105	1043	710	1.894 0.533	0.366 0.840	0.554 0.136	1.712 0.351
Adel *et al.*[c]	1043	710	2105	1.242 1.004	0.133 0.215	0.136 0.063	−0.356 −0.594
Penney and Sutherland[d]	1043	710	1740	0.988 0.751	0.133 0.215	0.136 0.063	−0.103 −0.341
—	1740	710	1043	1.427 0.401	0.207 0.565	0.378 0.063	1.035 0.009

[a] Reference 5. [c] Reference 3.
[b] Reference 1. [d] Reference 2.

* From a thesis submitted in partial fulfillment of the requirements for the degree of Master of Science, in the department of chemistry, in the Graduate College of the State University of Iowa.

[1] Hettner, Pohlman, and Schumacher, Zeits. f. Physik **91**, 372 (1934); Zeits. f. Electrochemie **41**, 524 (1935).
[2] Penney and Sutherland, Proc. Roy. Soc. **A156**, 654, 678 (1936).
[3] Adel, Slipher, and Fouts, Phys. Rev. **49**, 288 (1936).
[4] Mulliken, Rev. Mod. Phys. **14**, 204 (1942).
[5] Simpson, Trans. Faraday Soc. **41**, 209 (1945).
[6] R. M. Badger, J. Chem. Phys. **2**, 128 (1934); **3**, 710 (1935).
[7] G. Glockler and J. Y. Tung, J. Chem. Phys. **13**, 388 (1945).

TABLE II. Badger's rule.

Substance	State	ω_e (cm^{-1})	r_e (A)	c_1	$c_1^{-1/3}$
O_2	$^3\Sigma_g^-$	1580.36[a]	1.2076[a]	1.174	0.9479
O_2	$^1\Sigma_g^+$	1432.62[d]	1.223[d]	0.965	1.012
O_2	$^3\Sigma_u^-$	710.14[d]	1.599[d]	0.237	1.616
H_2O_2		877[b]	1.47[c]	0.361	1.405

[a] Herzberg, *Diatomic Molecules* (Prentice-Hall, Inc., New York, 1939).
[b] Herzberg, *Infrared and Raman Spectra of Polyatomic Molecules* (D. Van Nostrand Company, New York, 1945).
[c] Giguere and Schomaker, J. Am. Chem. Soc. **65**, 2025 (1943).
[d] W. Jevons, *Band Spectra of Diatomic Molecules*, (Physical Society, London, 1932).

lated. The range of real values can be found from the condition

$$dc_4/dc_2 = dc_4/dc_3 = 0. \tag{1}$$

The question may be immediately asked: How does one know the range of values to assign to c_4? Obviously, it is possible that the assumed value of c_4 may give imaginary values of c_2 and c_3. Glockler and Tung[7] have derived explicit relations which define the end-points of the ellipses:

$$\left.\begin{aligned}
c_1 &= \frac{\lambda_3}{2C} + \frac{C\lambda_1}{2(AC-B^2)} \\
&\text{or} \\
c_1' &= \frac{\lambda_3}{2C} + \frac{C\lambda_2}{2(AC-B^2)}, \\
c_2 &= \frac{\lambda_2}{2C} + \frac{B^2\lambda_1}{2C(AC-B^2)} \\
&\text{or} \\
c_2' &= \frac{\lambda_1}{2C} + \frac{B^2\lambda_2}{2C(AC-B^2)}, \\
c_3 &= \frac{B\lambda_1}{2(AC-B^2)} \\
&\text{or} \\
c_3' &= \frac{B\lambda_2}{2(AC-B^2)}, \\
c_4 &= c_1 - \frac{\lambda_3}{C} \\
&\text{or} \\
c_4' &= c_1' - \frac{\lambda_3}{C},
\end{aligned}\right\} \tag{2}$$

where $A = 1/\mu - \cos\alpha/M$; $B = \sin\alpha/M$; $C = 1/\mu - \cos\alpha/M$; α = valence angle; M = atomic weight of oxygen; μ = reduced mass of two oxygen atoms; $\lambda_i = 4\pi^2\omega_i^2$, where ω_1 is the symmetrical vibration frequency, ω_2 is the deformation vibration frequency, and ω_3 is the antisymmetrical vibration frequency. The two sets (Eq. (2)) define the end-points of the ellipse where condition (1) holds. In other cases[7] it appeared possible to choose one of these two sets by the above condition and this set checked isotopic molecules satisfactorily. Up to this point in the argument it can only be said that the O–O bond force constant of ozone must lie within the range of real values (0.75 to 0.99 megadyne).

THE OZONE MOLECULE

Shand and Spurr,[8] by means of electron diffraction studies, have shown that the ozone molecule exists in the form of an isosceles triangle in which the apical angle is 127°±3° and the O–O distance is 1.26±0.02 angstroms. Using the above value for the apical angle, the four force constants were calculated for four different assignments of the fundamental frequencies. The

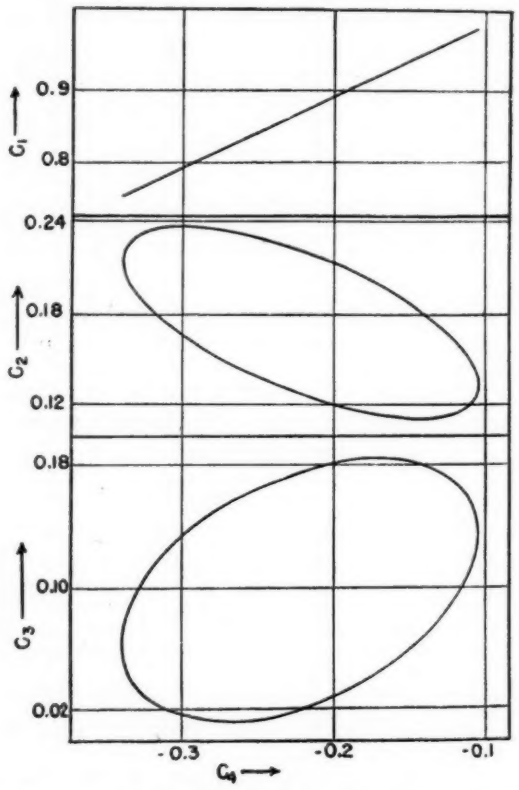

FIG. 1. Possible real values of the force constants of ozone (megadynes/cm).

[8] W. Shand, Jr., and R. A. Spurr, J. Am. Chem. Soc. 65, 179 (1943).

data are summarized in Table I. Figure 1 illustrates the relation between the force constants which were calculated from the assignment of Sutherland and Penney,[2] which appears to give results most consistent with the structure of the ozone molecule. The two values for the O—O force constant, 0.988 and 0.751 megadyne (see Fig. 1 and Table I) lie on either side of the value predicted by Badger's rule, or 0.87 (for an O—O distance of 1.26A), as illustrated in Table II and Fig. 2.

DISCUSSION

Simpson[5] has reported a value of 1.597 megadynes for the O—O bond force constant in ozone. This value seems too large in view of the presently accepted structure of the ozone molecule. The force constant may be expected to lie between 1.174 (oxygen molecule) and 0.361 (hydrogen peroxide) as can be seen from an inspection of Table II where it is noted that the O—O distance in ozone (1.26A) lies between the values for hydrogen peroxide and the oxygen molecule.

From Table I it appears that Simpson's assignment is the only one which will give real values for c_2 and c_3, if c_4 is assumed to be zero, since c_4 must be given some value lying between the two ranges for c_4 given in Table I in order that real values result from c_2 and c_3. This explains the imaginary values which result when the other assignments are treated by the simple valency force field in which c_4 is assumed to be zero.

The Penney and Sutherland assignment used above is consistent with the modern interpretation of the infra-red spectrum.[5] The range for c_1 (0.75 to 0.99 megadyne) can be supported by an examination of heats of dissociation.

This consideration which yields information concerning the relative strength of the O—O bonds in the three molecules discussed, concerns the dissociation energy of the three O—O bonds. From Table III it is seen that the ozone bond is intermediate between the O—O bonds of hydrogen peroxide and of oxygen molecule.

TABLE III. Heats of dissociation.

Reaction	D (electron volts)
$H_2O_2 \rightarrow 2OH$	1.48[a]
$\frac{1}{2}O_3 \rightarrow \frac{3}{2}O$	3.06[b, c]
$O_2 \rightarrow 2O$	5.08[c]

[a] L. Pauling, J. Am. Chem. Soc. **54**, 3570 (1932).
[b] F. R. Bichowsky and F. D. Rossini, *Thermochemistry of the Chemical Substances* (Reinhold Publishing Corporation, New York, 1936).
[c] G. Herzberg, *Diatomic Molecules* (Prentice-Hall Inc., New York, 1939).

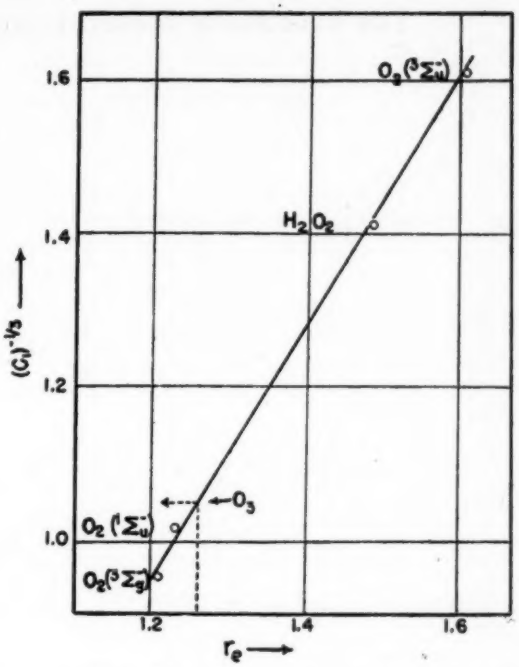

FIG. 2. Badger's rule applied to the O—O bond.

The O—O bond energy in ozone has been calculated as follows:

$$3O_2 \rightarrow 2O_3; \quad \Delta H = -3.00 \text{ ev}$$
$$6O \rightarrow 3O_2; \quad \Delta H = 15.24 \text{ ev}$$
$$6O \rightarrow 2O_3; \quad \Delta H = 12.24 \text{ ev}$$

or

$$1\tfrac{1}{2}O \rightarrow \tfrac{1}{2}O_3; \quad \Delta H = 3.06 \text{ ev}$$

The dissociation of the oxygen bond in ozone is intermediate between the dissociation energies of the oxygen bond in hydrogen peroxide and molecular oxygen. Therefore it should be reasonable to expect the force constant in ozone to lie between those in molecular oxygen and hydrogen peroxide. Hence the Penney and Sutherland assignment of fundamental frequencies yielding a force constant for the oxygen bond in ozone between 0.75 and 0.99 megadyne seems most acceptable at present.

THE JOURNAL OF CHEMICAL PHYSICS VOLUME 14, NUMBER 9 SEPTEMBER, 1946

The Reaction of Methyl Radicals with Butadiene and Isoprene*

H. E. GUNNING AND E. W. R. STEACIE
Division of Chemistry, National Research Laboratories, Ottawa, Canada

(Received June 24, 1946)

An investigation of the reaction of methyl radicals with butadiene and isoprene has been made by photolyzing admixed mercury dimethyl. In each case the amount of methane formed by the reaction

$$CH_3+RH\rightarrow CH_4+R$$

was small relative to the accompanying polymerization. For butadiene the activation energy of methane formation is 6.5 kcal. This value is, however, rather unreliable on account of the small amount of methane formation.

INTRODUCTION

THE reaction

$$CH_3+R-H\rightarrow CH_4+R- \qquad (I)$$

has been studied by H. S. Taylor and his coworkers,[1] with various hydrocarbons. The methyl radicals were generated, *in situ*, by the photolysis of admixed mercury dimethyl. One of the most interesting results of these investigations was that the activation energy of reaction (I) is low, if the hydrocarbon has a C−H bond in a β-position to a double bond. Thus, for example, propylene and methyl radicals form methane with an activation energy of 3.1 kcal. per mole, while with ethylene and benzene, E for reaction (I) is greater than 10 kcal. per mole.

Taylor and Smith[2] suggest that the low activation energy for the reaction of propylene with methyl radicals might be caused by the weak C−H bond in the methyl group of propylene. Since $E=8$ kcal. for ethane in reaction (I), they conclude that the weakest C−H bond in propylene has a bond strength 5 kcal. less than the C−H bond strength in ethane, or about 91–93 kcal. per mole.[3] The present work extends the study of reaction (I) to butadiene and isoprene.

EXPERIMENTAL

The mercury dimethyl used was prepared by the method of Gilman and Brown,[4] which yields a product of high purity. Traces of water were removed with fused calcium chloride, and the dried product was stored in a glass bulb, connected to the system through a Warrick-Fugassi valve.[5]

Owing to the high solubility of mercury dimethyl in stopcock grease, mercury valves were used exclusively in the system. The cell was similar in shape to the one used by Taylor and Smith,[2] and was made entirely of quartz except for the narrow neck which was made of Pyrex and sealed to the quartz portion by a graded seal. The cell was provided with a small thermocouple well, and a side tube with an internal glass tip for introducing the products of the reaction into the analytical unit. The cell had a volume of 252 cc, and was sealed off from the system after the introduction of the sample. The partial pressures of the mercury dimethyl and the hydrocarbon were measured with a constant volume manometer.

In making a run, the cell was sealed to the system by means of a short piece of 2-mm capillary tubing. After evacuation, the mercury dimethyl was admitted until the pressure reached 40 mm, which corresponds to the vapor pressure of mercury dimethyl at 18°C. 200 mm of hydrocarbon were then introduced, after which the cell was immersed in liquid air and sealed off from the system.

The reaction was studied at various temperatures by placing the cell in a small furnace which

* Contribution No. 1408 from the National Research Laboratories, Ottawa, Canada.

[1] See Hugh S. Taylor, Ann. N. Y. Acad. Sci. **41**, 231–240 (1941).

[2] H. S. Taylor and J. O. Smith, Jr., J. Chem. Phys. **8**, 543–546 (1940).

[3] D. J. LeRoy and E. W. R. Steacie, J. Chem. Phys. **10**, 683–685 (1942).

[4] H. Gilman and R. E. Brown, J. Am. Chem. Soc. 3314–3317 (1930).

[5] E. Warrick and P. Fugassi, Ind. Eng. Chem. Anal. Ed. **15**, 13 (1943).

TABLE I.

Furnace temperature °C	Butadiene			Isoprene		
	$k(CH_4)\times10^3$	$-\Delta P\times10^3$	$-\Delta P/k(CH_4)$	$k(CH_4)\times10^3$	$-\Delta P\times10^3$	$-\Delta P/k(CH_4)$
106	0.105±0.011	.0.61±0.03	5.8	0.17±0.012	7.2±0.2	42
140	0.245±0.015	7.2±0.2	29			
232	1.01±0.02	53±0.8	53			

contained a quartz window 4×4 cm through which the cell could be irradiated. The temperature of the cell was followed with the thermocouple in the cell.

The absorption spectrum of mercury dimethyl exhibits a continuum beginning at 2800A, and extending into the far ultraviolet. Since mercury vapor is always present in the cell, it was necessary to choose a mercury arc source in which the λ2537 resonance line was completely reversed. Otherwise mercury photo-sensitized decomposition of the reactants would occur. A Hanovia Alpine sun lamp proved to be a satisfactory source for photolyzing the mercury dimethyl. Plates taken of the radiation from the lamp with a large Hilger quartz spectrograph showed almost complete reversal of the λ2537 resonance line. Furthermore, there was no indication of mercury photo-sensitized decomposition when a cell containing ethylene and mercury vapor was exposed to the lamp for 12 hours.

After exposure, the cell was sealed to an analytical unit, similar to one previously employed.[6] After evacuation, the cell was immersed in liquid air and the glass tip broken by a small iron hammer, actuated by a solenoid. The gas, non-condensible in liquid air, was pumped into a gas burette, designed for the accurate measurement of small quantities of gas. After measuring its volume, the gas was burned to carbon dioxide and water, in a small combustion tube containing an electrically heated platinum spiral. By this means it was conclusively shown that the gas was pure methane.

At the end of each run, the pressure of residual hydrocarbon was determined, in order to obtain some indication of the extent of polymerization.

[6] H. E. Gunning and E. W. R. Steacie, J. Chem. Phys. 12, 484–493 (1944).

RESULTS

The quantities of methane formed were extremely small, and consequently the measurements were heavily influenced by experimental error. The results for butadiene and isoprene are summarized in Table I. Each value is the average of three determinations. $k(CH_4)$ and $-\Delta P$ the decrease in pressure, are expressed in cc per minute at 760 mm and 0°C. Above 100°C thermal polymerization of isoprene becomes appreciable.

The plot of $\log[k(CH_4)]$ *vs.* $1/T$ is roughly linear for butadiene. From the slope of this line the activation energy of methane formation is about 6.5 kcal. per mole.

In general the chain length of the polymer radical will be given by the expression

$$-d\frac{[R-CH=CH_2]}{dt}\Big/\frac{-d(CH_3)}{dt},$$

and the ratio $-\Delta P/k(CH_4)$ will represent a maximum value for the chain length, provided there is no other source of methane than the reaction under investigation. Consequently the quantity is of considerable interest.

The values of $-\Delta P/k(CH_4)$ for butadiene would suggest that, as in case of propylene, the chain length increases with temperature. The measurements made at 100°C on isoprene indicate a longer chain length than butadiene under the same conditions.

The activation energy of 6.5 kcal. for butadiene seems altogether too low. In view of the small amount of methane formed, and the large amount of polymerization, the possibility of complicating factors is considerable and too much reliance should not be placed on this value.

THE JOURNAL OF CHEMICAL PHYSICS VOLUME 14, NUMBER 9 SEPTEMBER, 1946

The Site of Reaction in Direct Photographic Development*

T. H. JAMES
Kodak Research Laboratories, Rochester, New York

(Received July 3, 1946)

The rate of the silver-catalyzed reduction of silver ions derived from soluble silver salts is directly proportional to the concentration of the hydroquinone when the latter is the reducing agent. The kinetics thus give no evidence that adsorption of hydroquinone by silver is a prerequisite for reaction. Similar results are obtained with catechol as reducing agent. The rate of development of silver bromide grains, on the other hand, varies approximately with the 0.6 power of the hydroquinone concentration (*p*H 8.0–8.9) and the 0.56 power of the catechol concentration (*p*H 7.7), indicating adsorption by the silver bromide or by the silver-silver bromide interface region prior to reaction. This result is in contradiction with the "electrode" mechanism of development, but is in accord with the concept of a direct reaction between the developing agent and silver halide at the triple interface.

IT is widely accepted[1–5] that the reduction of the major portion of the silver ions in normal "chemical" (direct) development takes place at or near the interface between silver halide and silver. The proposed reaction mechanisms, in general, can be assigned to one or the other of two distinct groups. In the first group, the latent-image nucleus is treated as an electrode which readily accepts electrons from the developer. The developing agent, in this view, can give up electrons to the silver nucleus at any point where the developer can reach its surface, but the site of the reduction of the silver ions is confined to the region of the interface between the silver halide and the silver. The reaction, accordingly, consists of at least two separate steps, which may be symbolized:

1. $n\text{Ag}+\text{developer}\rightarrow n\text{Ag}_\epsilon+\text{oxidized developer}$, (nucleus)

2. $$\text{Ag}^+ + n\text{Ag}_\epsilon \rightarrow (n+1)\text{Ag}.$$

Development can occur only if the transfer of electrons to silver and the subsequent transfer of electrons from silver to silver ions take place much more readily than the transfer of electrons directly to silver ions or to the silver halide crystal.

The second point of view is that the molecule or ion of the developing agent participates directly in the reduction of the silver ion in contact with the silver nucleus. Development can occur when the reaction between silver ions and developing agent at the interface requires considerably less activation energy than the reaction of silver ions and developing agent at any point out of contact with the silver, i.e., when the reaction:

$$\text{developer}+\text{Ag}^+(n\text{Ag})\rightarrow \text{oxidized developer}+(n+1)\text{Ag},$$

or

$$(\text{developer}\ldots\text{Ag}^+\ldots n\text{Ag})\rightarrow \text{oxidized developer}+(n+1)\text{Ag}$$

occurs with smaller activation energy than the direct transfer of electrons to Ag^+.

One of the fundamental postulates of the electrode mechanism is that the transfer of electrons from the developing agent to the silver nuclei can occur at any point on the silver surface along the interface between the silver and the solution. This postulate, however, appears to be inconsistent with the kinetics of development by hydroquinone. The active species in the hydroquinone developer is the bivalent ion, and the kinetics of development by this agent indicate that the bivalent ion is adsorbed prior to reaction.[6] However, both direct adsorption measurements[7]

* Communication No. 1090 from the Kodak Research Laboratories.

[1] S. E. Sheppard, Phot. J. **69**, 330 (1929).
[2] A. J. Rabinovich, Trans. Faraday Soc. **34**, 920 (1938).
[3] T. H. James and G. Kornfeld, Chem. Rev. **30**, 1 (1942).
[4] W. F. Berg, Trans. Faraday Soc. **39**, 115 (1943).
[5] Kh. S. Bagdasar'yan, J. Phys. Chem. U.S.S.R. **17**, 336 (1943).
[6] T. H. James, J. Phys. Chem. **44**, 42 (1940).
[7] E. S. Perry, A. Ballard, and S. E. Sheppard, J. Am. Chem. Soc. **63**, 2357 (1941).

and data on the silver-catalyzed reduction of silver ions derived from soluble silver salts[8] fail to indicate adsorption of hydroquinone by silver itself. It may be concluded, therefore, that the bivalent hydroquinonate ion is adsorbed by the silver bromide or by the silver-silver bromide interface. If this conclusion is correct, the electrode mechanism becomes untenable. Accordingly, it seems desirable to check further the kinetic evidence for adsorption of hydroquinone in development.

The kinetic experiments on development by hydroquinone, previously reported,[6] were carried out with solutions in the *p*H range of 8.0 to 8.9, using a simple motion-picture positive type of emulsion. At a fixed *p*H, the net rate of development of heavily exposed (but not solarized) film varied accurately as the 0.56 power of the hydroquinone concentration over the experimental concentration range of sixteen-fold. At a fixed total hydroquinone concentration and varying *p*H, the relation held over the sixty-four-fold range of concentration of the bivalent ion. These experiments have been repeated using dilute emulsions, and the general result has been confirmed.

Evidence from several sources has been adduced to show that, under the conditions employed, the individual grains were developed in a substantially parallel fashion, so that the gross kinetics did not differ significantly from the kinetics of development of a single grain. As a further check on the validity of interpreting the kinetic data in terms of development of the individual grain, some measurements were made according to the following procedure. A motion-picture positive type of emulsion having a narrow range of grain sizes[9] was given a heavy exposure and developed to a density of 0.15 in a hydroxylamine developer. The film was then rinsed in 0.5 percent dilute acetic acid, washed thoroughly, and dried. Photomicrographs of samples, after fixation, showed the presence of a large number of tiny nuclei which were all much smaller than the original grains. Samples of the film were developed further in a sulfite-free hydroquinone solution of *p*H 8.59 and containing 0.0167*M* potassium bromide. This concentration of bromide greatly inhibited development of any grains in which reaction had not already passed the induction period stage,[9] but the effect upon continued development of grains in which reaction has passed the induction period stage was much smaller. Photomicrographs of the film at various stages of the hydroquinone development showed that the number of silver particles per unit area did not change significantly, whereas their size progressively increased.

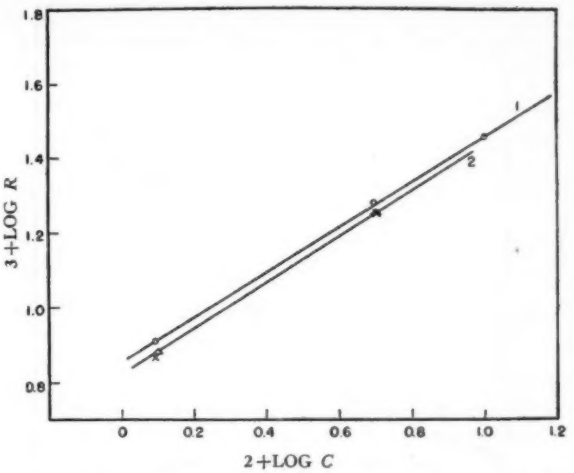

FIG. 1. Dependence of development rate upon hydroquinone concentration. 3+log *R* (ordinate) plotted against 2+log *C* (abscissa).

The data on the rate of development in the hydroquinone solutions of various concentrations are represented by the logarithmic plot in Fig. 1, Curve 1. The straight line has a slope of 0.60, showing that the rate varied with the 0.6 power of the hydroquinone concentration.

In the earlier work on the kinetics of development by hydroquinone, it was found[6] that addition of sodium sulfite to eliminate the influence of quinone on the development process changed the rate of development, but did not alter its relative dependence upon the hydroquinone concentration. In the present work, experiments were carried out using iso-ascorbic acid[10] in place of sulfite. This substance has the advantage that it does not exert a solvent action upon the silver bromide. It effectively removes the quinone,

[8] T. H. James, J. Am. Chem. Soc. **61**, 648 (1939); J. Phys. Chem. **45**, 223 (1941).

[9] See T. H. James, J. Frank. Inst. **240**, 89 (1945). Emulsion *G* was employed, but was diluted with gelatin to one-half normal silver halide concentration, and was coated at normal thickness.

[10] Cf. A. Weissberger, D. S. Thomas, and J. E. LuValle, J. Am. Chem. Soc. **65**, 1489 (1943).

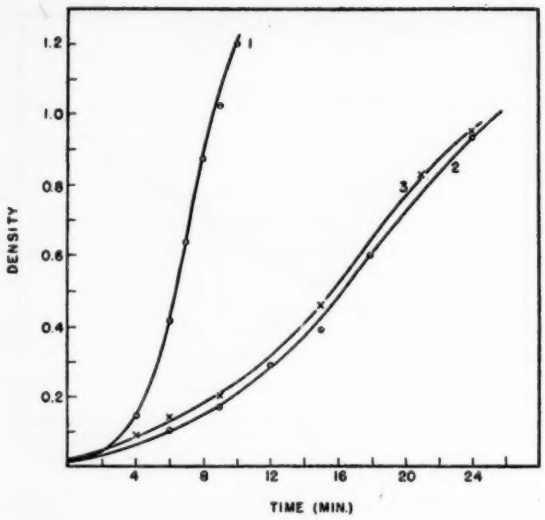

FIG. 2. Development by hydroquinone. pH = 8.78; log E = 2.05; Curve 1, no addition; Curve 2, sodium sulfite added; Curve 3, iso-ascorbic acid added.

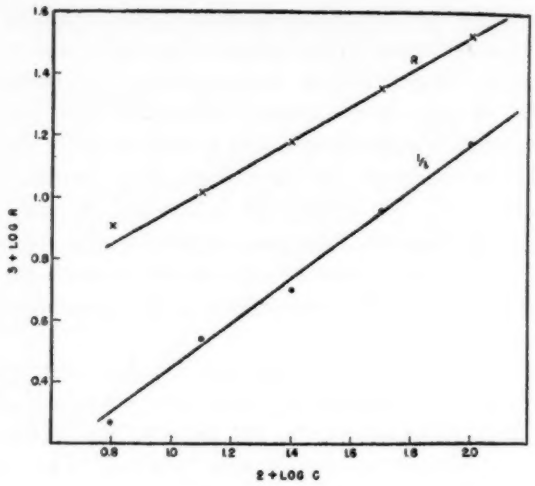

FIG. 3. Dependence of development rate on catechol concentration.

however, as shown by the development curves in Fig. 2. Curve 1 represents the course of development in bromide-free hydroquinone at pH 8.78, without addition of any quinone reactant. Curve 2 shows the effect of an optimum amount of sodium sulfite. Curve 3 shows the effect of adding iso-ascorbic acid.

Film developed initially to a density of 0.3 in the hydroxylamine solution and treated as before, was further developed in a hydroquinone solution containing iso-ascorbic acid and 0.0067M potassium bromide at pH 8.78. Blank runs were carried out to determine the rate of development by the iso-ascorbic acid in the absence of hydroquinone. This rate was much smaller than the hydroquinone development rate, but was significant. Accordingly, the measured rates were corrected for the iso-ascorbic acid development rate. The corrected rates are plotted in Fig. 1, Curve 2. The slope of the line is 0.61, in almost perfect agreement with results obtained in the absence of a quinone reactant.

The rate of development in a hydroquinone solution does not always vary with a fractional power of the hydroquinone concentration. Table I gives rate measurements for development in a solution containing 0.01M potassium bromide, 0.128M sodium sulfite, and 0.04M excess potassium hydroxide. The R values give the maximum rate of increase in density in terms of density units per minute. The t values give the time in minutes required to attain a density of 0.20. In this strongly alkaline solution, the development rate is roughly proportional to the hydroquinone concentration. The rate here very probably is controlled by the rate of diffusion of the hydroquinone through the electric double layer surrounding the grain.[11] The somewhat greater than first power dependence actually observed can be attributed to incomplete removal of the quinone by the sulfite, and consequent influence of the quinone (or more probably a decomposition product of quinone) upon the double layer.

Development by Catechol

Catechol is another example of a developing agent which, according to the indications of the development reaction kinetics, is adsorbed prior to reaction, but does not appear to be adsorbed by silver. The dependence of the development rates upon the concentration is shown in Fig. 3.

TABLE I. Development of Film G in hydroquinone solution at high pH. Solution: Hydroquinone, $x M$; Na_2SO_3, 0.128M; KBr, 0.01M; excess KOH, 0.04M.

Hydroquinone conc.	R	$1/t$
0.0025	0.0936	0.0719
.0050	.1875	.154
.0100	.426	.322
.0200	.999	.714

[11] T. H. James, J. Frank. Inst. **240**, 15 (1945).

The data were obtained for a solution at *p*H 7.70, buffered by a disodium phosphate-monosodium phosphate mixture. The R rates show almost exactly the same dependence upon catechol concentration (0.56 power) as upon hydroquinone concentration. The $1/t$ rates, which apply to the induction period region of development, vary with a somewhat higher power of the catechol concentration. The rate of the silver-catalyzed reaction of catechol with silver ions derived from a soluble silver salt, on the other hand *is directly proportional* to the catechol concentration. This, again, is the same result as that obtained previously in similar experiments with hydroquinone. The technique employed was the same as that described previously,[8] and the rate data are given in Table II.

TABLE II. Rate of silver-catalyzed reduction of silver ions from solution. Solution: *p*H 7.58; Na_2SO_3, 0.0555M; $AgNO_3$, 0.0111M; gum arabic, 0.55 percent; total volume, 90 ml.

Catechol conc.	0.0104	0.0208	0.0416	0.0832
Rate	0.0156	0.0310	0.0627	0.117

Thus, a marked difference is observed, both with hydroquinone and catechol, between the silver-catalyzed reduction of silver ions from solution and the development of silver bromide grains. Adsorption of the reducing agent is not indicated for the first reaction, but is indicated for the second. This is true under conditions such that the *p*H is equal in both types of reaction, and the silver-ion concentration of the solution in the first type is equal to or of the same order of magnitude as the equilibrium silver-ion concentration supplied by silver bromide.

THE JOURNAL OF CHEMICAL PHYSICS VOLUME 14, NUMBER 9 SEPTEMBER, 1946

The Mercury-Sensitized Reaction between Hydrogen and Nitrous Oxide

H. AUSTIN TAYLOR AND NORMAN ZWIEBEL
New York University, New York, New York

(Received June 20, 1946)

The mercury photo-sensitized reaction of nitrous oxide and hydrogen to produce nitrogen and water has been studied in the pressure range 10–500 mm. It is shown that hydrogen exerts only a minor influence on the rate. A mechanism has been postulated involving a sensitized decomposition of nitrous oxide into nitrogen and atomic oxygen at a rate roughly one thousand times the rate of reaction of hydrogen atoms with nitrous oxide. The atomic oxygen promotes chains by reaction with hydrogen, the chains are terminated by recombination of hydrogen atoms, on the wall at low pressure and mainly in the gas phase above 100 mm pressure under the experimental conditions.

DURING a study of the mercury-sensitized reaction between hydrogen and nitric oxide, Taylor and Tanford[1] concluded that nitrous oxide, if formed during the course of the reaction, could not accumulate in the system because of a rapid reaction with hydrogen atoms. This conclusion was contrary to the findings of Melville[2] in claiming an energy of activation for the reaction between nitrous oxide and hydrogen atoms of 15–20 kcal. Careful analysis of Melville's paper in conjunction with an earlier paper[3] on the thermal reaction and especially in the light of other work on nitrous oxide[4] showed inconsistencies which called for further study.

EXPERIMENTAL

A low pressure quartz-mercury arc in the form of a flat spiral energized by a 5000-volt transformer carrying about 4.8 amp. in the primary, was used as the source of the resonance radiation. The lamp had an estimated yield of about 90 percent of its energy at 2537A. The reaction vessel was a stoppered quartz flask of about

[1] H. A. Taylor and C. Tanford, J. Chem. Phys. **12**, 47 (1944).
[2] H. W. Melville, Proc. Roy. Soc. **A146**, 737 (1934).
[3] H. W. Melville, Proc. Roy. Soc. **A142**, 524 (1933).
[4] W. H. Manning and W. A. Noyes, Jr., J. Am. Chem. Soc. **54**, 3907 (1932); J. K. Dixon, *ibid.* **56**, 101 (1934).

TABLE I. Pressure change in mm.

Time (min.)	Run 19 P_{N_2O} 28.6 P_{H_2} 28.9	Run 20 249.7 253.9	Run 36 19.8 19.9	Run 119 120.1 81.3
0.5	−0.2	−2.4	0	0
1	0.5	−2.7	0.1	−0.8
2	1.7	−2.1	1.1	1.7
4	3.7	−0.1	2.8	5.2
6	5.2	3.0	4.0	7.7
8	6.9	6.2	4.7	8.6
10	7.9	10.0		8.8
15	10.2	17.7		9.8
20	11.9	24.3		10.7
25	13.0	30.9		
30		36.1		
40		48.6		
50		56.1		
60		61.3		

250-cc capacity, carrying in its neck, placed horizontally, a boat filled with P_2O_5 to remove the water produced by the reaction. The vessel was submerged in a water bath, maintained at 39°C during a run and was connected to reservoirs of reactants, manometer, and pump system as well as to a gas analysis apparatus. After every two runs the flask was detached from the rest of the apparatus, washed, dried, and supplied with fresh P_2O_5.

Nitrous oxide was prepared by decomposition of ammonium nitrate under atmospheric conditions, the water and nitrous oxide being collected at the temperature of liquid nitrogen and then pumped to a good vacuum. The nitrous oxide was later volatilized from the water at −78°C into a large evacuated vessel. It was stored in this reservoir which was always open to a dry-ice trap.

Tank hydrogen was purified from oxygen by passage over hot platinized asbestos and was saturated with mercury vapor by bubbling through two traps containing mercury, the first at 95°C, the second at room temperature.

The products from two experiments were analyzed by removal from the reaction vessel with a Toepler pump through a trap immersed in liquid nitrogen and thence to a gas burette. Nitrous oxide was thus frozen out along with other possible gases present except nitrogen and hydrogen. The total volume of these latter being determined, the hydrogen was burned over copper oxide at 350°C and the residual gas measured as nitrogen. The contents of the trap was then vaporized and its volume measured. No attempt was made to analyze this fraction further.

For a run, a known pressure of nitrous oxide and of hydrogen saturated with mercury vapor, was admitted to the reaction vessel and exposed to the lamp which had previously been allowed to attain its full intensity. The course of the reaction was followed by pressure readings on the manometer at suitable intervals.

RESULTS

In Table I are listed the pressure changes observed at various times in four typical experiments chosen to illustrate various characteristics. An induction period is characteristic of all runs. When the pressure of nitrous oxide is high, an initial increase in pressure is observed indicating that the initial slow pressure decrease in other runs is caused by a balancing of this increase by the normal decrease. When nitrous oxide containing mercury vapor but without hydrogen was exposed to the radiation under the same conditions a steady increase in pressure was observed. The initial pressure increase is thus accounted for and at the same time it should be noted that

TABLE II. Dependence of rate on total pressure.

Run	P_{N_2O} mm	P_{H_2} mm	Rate (mm/sec.)	Av. rate	K
27	10.0	11.3	0.0120		
21	9.5	10.7	0.0128	0.012_4	0.076
30	20.0	20.1	0.0152		
36	19.8	19.9	0.0151		
40	19.9	19.9	0.0146		
44	20.3	20.3	0.0157	0.015_2	0.091
17	28.0	28.9	0.0173		
19	28.6	28.9	0.0174		
24	26.1	26.0	0.0170		
25	26.8	25.3	0.0178		
46	26.9	25.8	0.0179	0.017_5	0.100
15	49.9	49.7	0.0186		
16	53.8	52.6	0.0196		
76	51.8	53.0	0.0206		
51	51.5	52.3	0.0212	0.020_0	0.111
22	99.1	106.8	0.0221		
C	100	100	0.0223	0.022_3	0.114
11	150.1	156.1	0.0236		
12	147.0	155.0	0.0230		
73	149.3	150.0	0.0236		
74	150.1	152.0	0.0237	0.023_5	0.106
7	247.3	248.8	0.0269		
20	249.7	253.9	0.0278	0.027_4*	0.108

* This value was corrected on the basis of a plot of rate as a function of total pressure to 0.025_8.

TABLE III. Dependence of rate on nitrous oxide.

Run	P_{N_2O}	P_{H_2}	Rate (mm/sec.)	Av. rate	K
57	10.1	100.9	0.0064	0.006_4	0.089
92	19.1	99.2	0.0095		
95	21.0	101.0	0.0094	0.009_5	0.088
56	30.7	100.4	0.0122		
88	29.9	102.0	0.0121		
89	29.5	103.8	0.0120		
94	31.1	99.1	0.0124	0.012_2	0.093
91	39.1	101.0	0.0147	0.014_7	0.103
87	49.1	100.2	0.0158	0.015_8	0.099
85	81.0	99.9	0.0208	0.020_8	0.113
C	100	100	0.0223	0.022_3	0.114
79	122.0	101.0	0.0240	0.024_0	0.116

the quenching efficiency of N_2O must be quite high. Again, when in a normal run with hydrogen present and the lamp turned off, there was observed a continued pressure decrease for from one to three minutes, it was obvious that the diffusion of water vapor to the drier was relatively slow when only small amounts were present. If therefore, the diffusion takes about two minutes it is to be expected that the pressure increase due to decomposition of nitrous oxide will evidence itself initially but with increasing amounts of water present a pressure decrease will predominate. The maximum rate of pressure change immediately following the induction period was taken as that most nearly representative of the water-forming reaction. This would of course be a minimum value.

A limitation on the amounts of nitrous oxide and hydrogen which could be used was observed and is illustrated partially by Run 119, a borderline case, where over 75 percent of the reaction (in terms of the final pressure change) is complete in five or six minutes. For still higher ratios of nitrous oxide to hydrogen an irregular pressure increase was observed for only one or two minutes after which no further pressure change occurred. Examination of the drier after such a run showed it to be densely caked and grey or black, quite unlike its appearance after a normal run. If this same drier were used again for a normal run, a rate was observed which was at least 15 percent below that of similar runs using fresh drier. The ratio of nitrous oxide to hydrogen had therefore to be maintained below 1.3.

Table II shows the dependence of the rate for a 1:1 ratio of the gases as a function of the total pressure varying from 20 to 500 mm.

Table III shows the variation of the rate at constant hydrogen pressure with change in the nitrous oxide pressure from 10 to 125 mm. Comparison of Tables II and III shows a great similarity between the effect of total pressure and of nitrous oxide indicating that the change in nitrous oxide pressure is much more significant than a change in hydrogen. This is borne out by the data in Table IV for the dependence of the rate on hydrogen at constant nitrous oxide. Because of the limitation mentioned previously it was impossible to go below 75-mm hydrogen, the nitrous oxide pressure being 100 mm. The last three runs in Table IV were made after the apparatus had been dismantled and reassembled. They are self-consistent, the trend with changing hydrogen reproduces that of the earlier runs and they differ only in the magnitude of the rates. This is probably caused by a change in the light intensity resulting from a change in position of the lamp.

In Table V are presented the data for several runs with the new lamp setting in which the total pressure was maintained constant at about 200 mm while the ratio of the partial pressures was varied. Again the similarity in the trend of these rates, as the nitrous oxide pressure is changed, with those in Table III shows the prime influence of the nitrous oxide on the over-all rate.

The results of the analyses of the products from two runs are given in Table VI. The first was at

TABLE IV. Dependence of rate on hydrogen.

Run	P_{N_2O}	P_{H_2}	Rate (mm/sec.)	Av. rate	K
97	100.8	74.0	0.0215	0.021_5	0.100
96	99.2	119.9	0.0222		
103	99.5	118.0	0.0223		
101	99.7	120.7	0.0222	0.022_2	0.118
C	100	100	0.0223	0.022_3	0.114
98	100.6	153.9	0.0210	0.021_0	0.119
109	99.2	100.0	0.0263	0.026_3	0.143
104	99.7	166.8	0.0246	0.024_6	0.153
108	100.5	200.4	0.0230	0.023_0	0.146

TABLE V. Dependence of rate on pressure ratio.

Run	P_{N_2O}	P_{H_2}	Rate (mm/sec.)	K
117	40.6	157.9	0.0178	0.154
112	60.0	139.7	0.0212	0.149
110	80.3	122.2	0.0241	0.148
111	99.5	102.6	0.0263	0.143
118	111.2	90.6	0.0268	0.139
119	120.1	81.3	0.0275	0.138

TABLE VI. Analysis of products.

	I		II	
$P^0_{N_2O}$	101.2		100.8	
$P^0_{H_2}$	100.7		101.1	
	Calc.	Obs.	Calc.	Obs.
N_2	25.1 cc	25.4	13.4	14.5
H_2	2.0	2.2	13.4	13.7
N_2O	—	—	13.4	15.2

about 93 percent reaction, the second at about 50 percent. The discrepancy between the observed and calculated values for nitrous oxide in the second analysis might indicate the presence of another gas in the nitrous oxide fraction. However, the fact that both the hydrogen and nitrogen are also high casts doubt on this possibility. In any event nitric oxide was not found since no brown fumes formed when the nitrous oxide fraction was mixed with air.

DISCUSSION

The following mechanism is suggested to account for the above observations:

$$Hg+h\nu=Hg^*, \quad (I)$$

$$Hg^*+H_2=Hg+2H, \quad (1)$$

$$Hg^*+N_2O=Hg+N_2+O, \quad (2)$$

$$O+H_2=OH+H, \quad (3)$$

$$H+N_2O=N_2+OH, \quad (4)$$

$$OH+H_2=H_2O+H, \quad (5)$$

$$2H+M=H_2+M. \quad (6)$$

Reactions (I) and (1) constitute the well-known mercury-sensitized dissociation of hydrogen. Melville[2] assumed that nitrous oxide merely deactivates excited mercury and assigned to it a quenching diameter the same as for hydrogen. The observation of a rapid reaction in mercury-sensitized nitrous oxide by Taylor and Marshall,[5] which has been repeated here, as well as in the work of Manning and Noyes,[4] is contrary to this assumption. Noyes shows that the quenching diameter expressed as $(R_{H_2}+R_{N_2O})$ is 10A, an exceedingly large value relatively. Noyes concludes that reaction (2) seems to be the most probable initial step and Stearn and Eyring[6] have calculated the activation energy for the nitrous oxide dissociation to yield $N_2(^1\Sigma)$ and $O(^3P)$ to be only 50 kcal.

The subsequent reactions of the oxygen atoms are those well-established by the interpretation of hydrogen-oxygen systems. As will become obvious later, reaction (2) is the principal mode of destruction of the nitrous oxide but does not quite account quantitatively for the observed rates. This is the main reaction, and requires that the removal of hydrogen atoms from the system occurs chiefly by recombination. In reaction (6) M designates the third body which could be another hydrogen atom, a hydrogen molecule, a nitrous oxide molecule, or the wall of the vessel. It is expected that at least in the higher pressure range a gas phase recombination would be more probable; a wall reaction predominant at low pressures. Concerning the relative efficiencies of hydrogen and nitrous oxide as third bodies little can be said definitely. Melville has suggested that the possible reaction

$$2H+N_2O=H_2O+N_2$$

might favor nitrous oxide as being the more efficient. This reaction would however add another mode of removal of nitrous oxide to those pictured above and it is doubtful that the data are sufficiently accurate to warrant its inclusion with the added rate constant. It is not unlikely on the basis of the resonance structure of nitrous oxide that a collision with a hydrogen atom would be 'sticky' thus favoring it as a third body. It has been assumed in the subsequent analysis that the concentration of M may be replaced by the total initial pressure in the higher pressure range.

The removal of nitrous oxide by reaction (4) with a hydrogen atom was used by Melville in interpreting both the thermal and the photo-

[5] H. S. Taylor and A. L. Marshall, J. Phys. Chem. **29**, 1140 (1925).

[6] A. E. Stearn and H. Eyring, J. Chem. Phys. **3**, 778 (1935).

chemical reactions. From his interpretation of the measured temperature coefficient he calculates the energy of activation to be 7.5 kcal. but promptly casts doubt on the value and suggests 15–20 kcal. as a more reliable value. Dixon[7] from a study of this reaction using hydrogen atoms from a discharge tube estimated a lower limit of the energy of activation as 10 kcal. Geib also found evidence[8] for a high E and it is found here that this reaction is slow. Some energy would however be available as residual energy in the production of hydrogen atoms from the excited mercury.

Evaluating the stationary concentrations of excited mercury, hydrogen, and oxygen atoms and hydroxyls, the over-all rate of disappearance of nitrous oxide is given by

$$-\frac{dP_{N_2O}}{dt}=\frac{k_2IP_{N_2O}}{k_1P_{H_2}+k_2P_{N_2O}}+\frac{k_4I^{\frac{1}{2}}P_{N_2O}}{(k_6P)^{\frac{1}{2}}}$$

$$=\frac{KP_{N_2O}}{P_{H_2}+(k_2/k_1)P_{N_2O}}+\frac{K'P_{N_2O}}{(P_{H_2}+P_{N_2O})^{\frac{1}{2}}}.$$

The ratio of the quenching efficiencies of nitrous oxide and hydrogen for excited mercury, namely k_2/k_1, has a value of 6.4 based on Noyes' value of $100A^2$ for the quenching area of nitrous oxide and $6A^2$ for hydrogen when due allowance is made for the reduced masses of the two molecules. With this ratio known, the rate equation contains two constants. When the pressures of the two gases are equal as in Table II the first term on the right of the equation is constant and hence K' can be deduced from the rate differences. For partial pressures above 50 mm K' has an average value of 0.001. Using this value for K' the values of K given in the previous tables were obtained. The constancy of K in the higher pressure ranges is good. The higher value of the constant in runs numbered 104 and higher is caused as previously mentioned by the changed position of the lamp. The general constancy is still good, all the pressures being above 50 mm.

That the failure of K to remain constant at lower pressures is probably caused by a wall recombination of hydrogen atoms is shown by the dependence of the rate differences in Table II between 10 and 20 mm, and between 20 and 25 mm, on the pressure of nitrous oxide rather than on its square root. For a wall combination, the rate of reaction (6) would not involve M and the second term on the right of the final rate equation would be $K''P_{N_2O}$. K'' thus found has a value 0.0003 and K has the constant value 0.070 at 10, 20, and 25 mm (Table II). On the other hand, the drop in rate at low pressure may be due to incomplete quenching since the effect is also observed (Table III) at low nitrous oxide pressures.

The mechanism suggested is thus capable of accounting for the observed results. From the relative magnitudes of K and K' it is apparent that reaction (2) the decomposition of nitrous oxide by excited mercury is much more effective than (4) the reaction with hydrogen atoms which Melville considered the principal reaction. The mechanism is essentially the same as that which Melville proposed for the thermal reaction and thus the thermal and photo-sensitized reactions become correlated. Finally the observations by Taylor and Marshall as also by Melville that the photo-sensitized nitrous oxide-hydrogen reaction proceeds faster than the oxygen-hydrogen reaction receive explanation since the quenching efficiency of nitrous oxide is so high and the chain steps, essentially the same in both reactions are thus initiated more rapidly by oxygen atoms from nitrous oxide. When the nitrous oxide to hydrogen ratio is high the reaction of the oxygen atoms with mercury becomes significant and HgO deposits, driven by the water vapor stream on to the drier causing the discoloration and caking observed.

[7] J. K. Dixon, J. Am. Chem. Soc. **56**, 101 (1934).
[8] See Geib, Ergeb. d. exakt. Naturwiss. **15**, 44 (1936).

THE JOURNAL OF CHEMICAL PHYSICS VOLUME 14, NUMBER 9 SEPTEMBER, 1946

The Mercury Photo-Sensitized Reactions of Isobutene*

H. E. GUNNING AND E. W. R. STEACIE
Division of Chemistry, National Research Laboratories, Ottawa, Canada

(Received June 25, 1946)

An investigation has been made of the reaction of isobutene with mercury ($^3P_1$) atoms at 30°C. The main products of the reaction are propylene, liquid polymer, and acetylene. Smaller amounts of a large number of other products are also formed. The over-all rate of consumption of isobutene, as well as the rates of formation of propylene, acetylene, and propane are independent of pressure in the region of complete quenching. Furthermore the rate of formation of propylene is just double the rate of formation of acetylene. The maximum quantum yield of consumption of isobutene is 0.59. The principal steps in the mechanism proposed for the reaction are

$$i\text{-}C_4H_8+Hg(^3P_1)\rightarrow C_4H_7+H+Hg(^1S_0),$$
$$H+i\text{-}C_4H_8\rightarrow C_4H_9,$$
$$C_4H_7+i\text{-}C_4H_8\rightarrow C_2H_2+C_6H_{13},$$
$$C_4H_9+i\text{-}C_4H_8\rightarrow C_3H_6+C_5H_{11},$$
$$C_5H_{11}+i\text{-}C_4H_8\rightarrow C_3H_6+C_6H_{12}.$$

On the above mechanism the initial step would be only about 16 percent efficient. Polymerization is considered to be initiated mainly by the C_6H_{13} radical. The average molecular weight of the polymer would then be approximately 240.

INTRODUCTION

THE investigation of LeRoy and Steacie on ethylene,[1] and of Gunning and Steacie on butadiene,[2] propylene,[3] and isoprene,[3] would seem to suggest that these molecules all react with mercury ($^3P_1$) atoms, at room temperature, mainly by an activated molecule mechanism of the type

$$C_xH_y+Hg(^3P_1)\rightarrow C_xH_y^*+Hg(^1S_0), \qquad (a)$$

TABLE I. Analysis of original isobutene.

Component	Mole, percent
Propylene	0.97
Propane	0.09
Isobutene	95.65
Butanes	2.39
Methyl butenes	0.14
Pentadienes	0.06
Neopentane	0.44
Cyclohexane	0.01
Methyl cyclohexenes	0.02
Dimethyl pentenes	0.06
Ethyl cyclohexenes	0.04
Di-isobutylene	0.13

$$C_xH_y^*+C_xH_y\rightarrow 2C_xH_y, \qquad (b)$$
$$C_xH_y^*\rightarrow C_xH_{(y-2)}+H_2, \qquad (c)$$

or

$$C_xH_y^*\rightarrow C_xH_{(y-1)}+H. \qquad (d)$$

The activated ethylene and butadiene molecules decompose by reaction (c) into hydrogen molecules and a more unsaturated hydrocarbon: while the activated propylene and isoprene molecules seem to split mainly into radicals by reaction (d). In a previous paper[3] the present authors suggested that the difference in behavior between ethylene and butadiene, on the one hand, and propylene and isoprene, on the other might be caused by the presence in the latter of weak C−H bonds in a position once-removed from a double bond.

Isobutene offers interesting possibilities for testing further the generality of the mechanism cited above, since it possesses six C−H bonds in positions once-removed from a double bond. The results of this investigation are reported below.

EXPERIMENTAL

For a general description of the apparatus employed, and the experimental technique, reference should be made to the paper of Gunning

* Contribution No. 1409 from the National Research Laboratories, Ottawa, Canada.

[1] D. J. LeRoy and E. W. R. Steacie, J. Chem. Phys. 9, 829 (1941).

[2] H. E. Gunning and E. W. R. Steacie, J. Chem. Phys. 12, 484 (1944).

[3] H. E. Gunning and E. W. R. Steacie, J. Chem. Phys. 14, 57 (1946).

TABLE II.

P_0 mm	$-\frac{\Delta p}{\Delta t}$ mm/min. $\times 10^2$	$\frac{A}{d[H_2]/dt}$ moles/min. $\times 10^6$	$\frac{B}{d[CH_4]/dt}$ moles/min. $\times 10^6$	A/B
1.49	0.95	0.0110	0.0344	0.32
5.05	1.05	0.0142	0.0140	1.0
9.50	1.23	0.0210	0.0101	2.1
11.94	1.05	0.0239	0.0077	3.1
14.29	1.15	0.0199	0.0104	1.9
18.14	1.28	0.0255	0.0100	2.6
26.63	1.17	0.0233	0.0083	2.8
45.90	1.20	0.0185	0.0079	2.3
51.28	1.15	0.0183	0.0081	2.3
69.93	1.20	0.0163	0.0080	2.0
83.91	1.32	0.0135	0.0059	2.3

TABLE III.

P_0 mm	$-\frac{d[i-C_4H_8]}{dt}$	$\frac{d[C_2H_2]}{dt}$	$\frac{d[C_3H_6]}{dt}$	$\frac{d[C_3H_8]}{dt}$
	Moles per min. $\times 10^6$			
1.49	0.82_5	0.036	0.077	0.0085
5.05	1.42	0.164	0.33_2	0.020
9.50	2.00	0.31_6	0.61	0.029
11.93	1.72	0.40°	0.77	0.031
14.29	1.98	0.51°	0.88	0.052
18.14	3.80	1.00	1.94	0.086
26.63	4.18	1.17	2.43	0.087
45.90	4.15	1.33	2.46	0.110
51.28	4.15	[0.59]	2.37	0.090
69.93	4.03	1.30	2.49	0.162
83.91	4.14	0.98	2.04	0.046

and Steacie on the mercury photo-sensitized reactions of butadiene.[2] The cylindrical quartz cell used had a volume of 240 cc. The cell was immersed in a water thermostat maintained at 30.00±0.01°C. The total volume of the system was 1052 cc.

In order to obtain more complete information about the products of the reaction and their variation with the initial pressure, arrangements were made with Dr. A. Keith Brewer, Chief of the Mass Spectrometry Section of the National Bureau of Standards, to have analyses of the products performed on the mass spectrometer. After considerable experimentation on gaseous mixtures of known composition, the following technique was finally adopted for obtaining a representative sample of the gaseous mixture of unreacted isobutene and products present in the system at the end of each run.

A 100-cc bulb was first sealed to the system through a U-type mercury cut-off, which contained a small glass check-valve in each arm. After the system had been pumped down to a pressure of 10^{-5} mm, the cut-off was closed and a definite amount of isobutene was then admitted to the system and its pressure determined. The cut-off was then opened again, and the system was allowed to stand for three hours before starting the run.

At the end of each run the system was left for two hours in order to allow diffusion to equalize the composition throughout the system. The cut-off was then closed and Dewar flasks of liquid air were placed around the sample bulb, and around a trap in the system. When the McLeod gage showed that the pressure in the system had fallen to a constant value, the sample bulb was sealed off and removed from the system. The gas, non-condensible in liquid air, present in the system was pumped into the gas burette for measurement. The hydrogen was determined by circulation through a tube containing finely-divided cupric oxide deposited on glass wool. The tube was maintained at 300°C by a small resistance heater. The residue from the hydrogen determination was identified as methane by combustion in excess oxygen over a small electrically-heated platinum spiral.

The isobutene used in the measurements was the C.P. grade manufactured by the Matheson Company, East Rutherford, New Jersey. After several trap-to-trap distillations, the middle fraction was collected and stored in a one-liter flask provided with a Warrick-Fugassi valve.[4] Mass spectrometric analysis showed that the gas had the composition shown in Table I.

RESULTS

Isobutene shows a similar behavior to propylene in that the pressure begins to fall linearly with time as soon as the cell is exposed to radiation from the mercury resonance lamp. At the same time the window of the cell gradually becomes covered with tiny colorless droplets of liquid polymer. The gas, non-condensible in liquid air, which remained in the system at the end of each run, was shown to be a mixture of hydrogen and methane. These data are sum-

[4] E. Warrick and P. Fugassi, Ind. Eng. Chem. Anal. Ed. 15, 13 (1943).

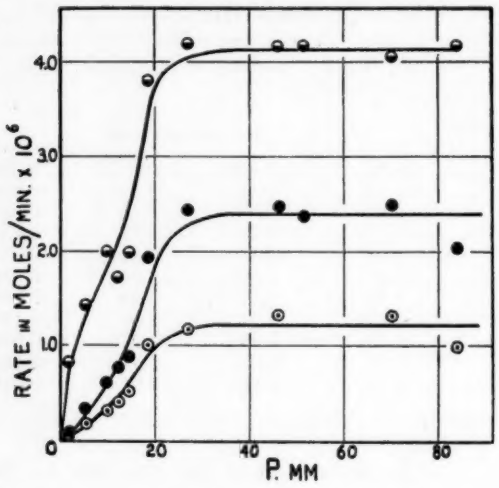

FIG. I. ◒ Rate of consumption of isobutene *vs.* initial pressure. ● Rate of formation of propylene *vs.* initial pressure. ⊙ Rate of formation of acetylene *vs.* initial pressure.

marized in Table II. From the table, it can be seen that, in contrast to propylene, the rate of pressure decrease is independent of the initial pressure, in the complete quenching region, i.e., above 15–18 mm. The rates of formation of hydrogen and methane, however, seem to fall off with increasing pressure in the same pressure region. Furthermore the ratio of these two rates, as given in the last column of Table II, appears to be constant, within experimental error. Runs were also made wherein the actual amounts of methane and hydrogen formed were determined as functions of the time, at a constant initial pressure of isobutene. Two sets of runs were made, the first set at an initial pressure of 15 mm, and the second at an initial pressure of 30 mm. 10-, 20-, 30-, 50-, and 80-minute runs were made at these pressures and the amount of methane and hydrogen determined in each case. These quantity-time curves were all straight lines passing through the origin.

The Products of the Reaction

The principal products of the reaction, condensible in liquid air, were propylene, liquid polymer, acetylene, and propane, in order of decreasing importance. Smaller amounts of a large number of other products are also present, especially at lower pressures where radical recombination reactions assume a more important role. These minor products were ethane, propadiene and/or methyl acetylene, *n*-butane, methyl butenes, neopentane, benzene, cyclohexadiene, cyclohexene, cyclohexane, toluene, heptadiene, heptanes, methyl cyclohexenes, dimethyl pentenes, dimethyl pentanes, ethyl cyclopentene, ethyl cyclopentane, trimethyl pentene, trimethyl pentanes, dimethyl hexene, dimethyl hexane, diisobutylene, and octanes. The rates of formation of these minor products were all less than 0.01 micromole per minute.

In Table III the over-all rate of consumption of isobutene, together with the rates of formation of acetylene, propylene and propane, are tabulated as functions of the initial pressure. These results are represented graphically in Fig. 1. From a study of Table III, we see that the four rates tabulated all seem to be constant and independent of the pressure, within experimental error, above 18 mm. Above this pressure there are approximately 0.54 mole of propylene, and 0.28 mole of acetylene formed for each mole of isobutene decomposed. Furthermore the ratio $(d[C_2H_2]/dt)/(d[C_3H_6]/dt)$ has a constant value over the entire pressure range of 0.51 ± 0.02.

Quantum Yield

Four determinations were made of the quantum input to the cell from the mercury resonance lamp by filling the cell with ethylene at an initial pressure of 13 mm and measuring the initial rate of production of hydrogen.

LeRoy and Steacie[1] have shown that the initial stages of the mercury photo-sensitized reaction of ethylene at room temperature can be represented by the sequence

$$C_2H_4+Hg(^3P_1)\rightarrow C_2H_4^*+Hg(^1S_0),$$
$$C_2H_4^*+C_2H_4\rightarrow 2C_2H_4,$$
$$C_2H_4^*\rightarrow C_2H_2+H_2,$$

and that the initial quantum yield is 0.37 at 13 mm. On this basis the mean quantum input to the cell was $7.0_7\times10^{-6}$ einstein per minute. The values for the over-all quantum yield of isobutene consumption, $\varphi(i-C_4H_8)$, are given for each pressure in Table IV.

Rate of Polymerization

By a carbon balance calculation, an estimation was made of the rate of polymerization of

isobutene, $-d[i-C_4H_8]$ poly./dt at the various initial pressures. These results are tabulated in Table IV. From this table, it will be seen that the rate of polymerization of isobutene seems to reach a maximum at an initial pressure of about 18 mm, and above that pressure it seems to show a slight trend downward.

The polymer formed was a clear, colorless, viscous liquid, completely soluble in benzene, in all these respects exactly similar to the polymer formed in the mercury photo-sensitized reaction of propylene.[3]

TABLE IV.

P_0 mm	$\varphi(i-C_4H_8)$	$-d[i-C_4H_8]$ poly./dt Moles/min. $\times 10^6$
1.49	0.12	0.57
5.05	0.20	0.70
9.50	0.28	0.81
11.93	0.24	0.91
14.29	0.28	0.99
18.14	0.54	1.69
26.63	0.59	1.66
45.90	0.59	1.49
51.28	0.59	
69.93	0.57	1.33
83.91	0.59	1.40

DISCUSSION

Any mechanism proposed to explain the reaction of isobutene with mercury ($^3P_1$) atoms must be consistent with the following facts:

(a) The pressure *vs.* time curve is linear even in the initial stage of the reaction.

(b) The rate of pressure decrease is independent of pressure in the complete quenching region, i.e., above 18 mm.

(c) The products of the reaction are propylene, liquid polymer, acetylene, and propane, together with smaller quantities of hydrogen, methane, and a large number of other hydrocarbons.

(d) The polymer is a viscous liquid, completely soluble in benzene and present even in the initial stages of the reaction.

(e) The rate of isobutene consumption, as well as the rates of formation of propylene, acetylene, and propane are independent of pressure in the complete quenching region.

(f) Above 18 mm there are approximately 0.54 mole of propylene and 0.28 mole of acetylene formed for each mole of isobutene decomposed. Furthermore the ratio $(d[C_2H_2]/dt)/(d[C_3H_6]/dt)$ has a constant value over the entire pressure range of 0.51 ± 0.02.

(g) The rates of formation of methane and hydrogen seem to fall off slightly with increasing pressure in the complete quenching region.

(h) The over-all quantum yield of isobutene consumption is constant above 18 mm at 0.59.

(i) The rate of polymerization seems to fall off slightly with increasing pressure in the complete quenching region.

The reactions of mercury ($^3P_1$) atoms at room temperature with ethylene,[1] propylene,[3] isoprene,[3] butadiene,[2] 1-butene,[5] and 2-butene[5] can all be explained on the assumption that an activated molecule is formed initially on the collision of a mercury ($^3P_1$) atom with the hydrocarbon molecule, the mercury ($^3P_1$) atom reverting thereby to the ground state. A similar mechanism can be proposed for isobutene. Consider the sequence

$$i-C_4H_8+Hg(^3P_1)\rightarrow i-C_4H_8^*+Hg(^1S_0), \quad (1)$$

$$i-C_4H_8^*+i-C_4H_8\rightarrow 2i-C_4H_8, \quad (2a)$$

$$i-C_4H_8^*+i-C_4H_8\rightarrow C_4H_7+C_4H_9, \quad (2b)$$

$$i-C_4H_8^*\rightarrow C_4H_7+H, \quad (3)$$

$$H+i-C_4H_8\rightarrow C_4H_9^*, \quad (4)$$

$$C_4H_7+i-C_4H_8\rightarrow C_2H_2+C_6H_{13}, \quad (5)$$

$$C_4H_9+i-C_4H_8\rightarrow C_3H_6+C_5H_{11}, \quad (6)$$

$$C_5H_{11}+i-C_4H_8\rightarrow C_3H_6+C_6H_{13}. \quad (7)$$

Proroguing for the moment, a discussion of the individual reactions, the rate of formation of acetylene, on the above scheme, using a steady-state calculation, would be given by the expression,

$$\frac{d[C_2H_2]}{dt}=Iab\left[1\Big/1+\frac{k_{2a}[i-C_4H_8]}{k_3+k_{2b}[i-C_4H_8]}\right].$$

Now, it has been found that $d[C_2H_2]/dt$ is independent of pressure in the complete quenching region, and consequently we must assume that $k_3\ll k_{2a}[i-C_4H_8]$ in the above expression in order to make the rate of acetylene formation independent of pressure. This is true, at least,

[5] H. E. Gunning and E. W. R. Steacie, J. Chem. Phys. (to be published).

so long as we assume that the initial quenching act is 100 percent efficient. Effectively this assumption would mean that the activated isobutene molecule has an extremely long life compared to the interval between collisions, and therefore that it would disappear in the main by bimolecular reactions rather than undergo unimolecular decomposition. On this basis

$$\frac{d[C_2H_2]}{dt}=\left[Iab\frac{k_{2b}}{k_{2a}+k_{2b}}\right],$$

and similarly for the rate of formation of propylene we obtain

$$\frac{d(C_3H_6)}{dt}=2Iab\left[\frac{k_{2b}}{k_{2a}+k_{2b}}\right].$$

This mechanism would account for the fact that the rate of formation of propylene is just double the rate of formation of acetylene.

Radical disproportionation reactions in general are considered to be rather slow. However there seems to be no exact precedent for a reaction of the type of (2b). Gunning and Steacie found it necessary to assume that the reaction

$$C_4H_6^*+H_2\rightarrow C_4H_7+H$$

occurred to some extent in the mercury photo-sensitized hydrogenation of butadiene.[2] In the mercury photo-sensitized reaction of 1-butene,[5] there is very good evidence for collisional reaction between activated molecule and molecule since the reaction

$$1-C_4H_8^*+1-C_4H_8\rightarrow 2-C_4H_8+1-C_4H_8$$

appears to be very fast. Certainly reaction (2b) is quite possible from an energetic standpoint, since the net effect of the reaction is merely the degradation of a C=C to a C−C, which would certainly require less energy than the 112.2 kcal. possessed by the activated isobutene molecule.

A much simpler mechanism can be devised, however, if we assume (1) that the activated isobutene molecule has a shorter life than the interval between successive collisions and (2) that the initial quenching process is very inefficient. The result would be that instead of reactions (1), (2a), (2b), and (3), we would essentially have only the single initial step

$$i-C_4H_8+Hg(^3P_1)\rightarrow C_4H_7+H+Hg(^1S_0).$$

The C−H bond split would likely occur at one of the six weak C−H bonds in isobutene in a position once-removed from a double bond.[3] The rates of formation of acetylene and propylene would then be simply

$$\frac{d[C_2H_2]}{dt}=K\cdot Iab \quad \text{and} \quad \frac{d[C_3H_6]}{dt}=2K\cdot Iab,$$

where K is a constant, less than unity, representing an inefficiency in the initial quenching process.

From Table III, we find that the rate of formation of acetylene in the complete quenching region has the average value of 1.16×10^{-6} mole per min. and similarly the average value for propylene is 2.29×10^{-6} mole per minute. Whence with $Iab=7.07\times10^{-6}$ einstein per minute.

$$K=\frac{d[C_2H_2]}{dt}\Big/Iab=\frac{d[C_3H_6]}{dt}\Big/2Iab=0.16.$$

In other words, only 16 percent of the mercury ($^3P_1$) atoms colliding with the isobutene molecules lead to decomposition. There is a good deal of evidence in support of the assumption of an inefficiency in the primary quenching process in the mercury photo-sensitized reactions of the unsaturated hydrocarbons. In the first place, the quantum yields for all the hydrocarbons that have been investigated so far are less than unity, in spite of the fact that all these reactions involve the formation of free radicals which are capable of propagating polymer chains. The assumption of an inefficiency in the primary process would clarify the situation considerably. In reference (3) the authors pointed out that the zone of reaction in the mercury photo-sensitized reaction of the unsaturated hydrocarbons must be limited to a layer a few millimeters in thickness at the window. Under these conditions it is probable that if some quenching of mercury ($^3P_1$) atoms to the metastable ($^3P_0$) state occurs, the mercury ($^3P_0$) atoms, on account of their long life, could be deactivated at the window. Another very important possibility, with the unsaturated hydrocarbons especially, is physical

quenching. The high quenching efficiency of these molecules renders it quite possible that the excitation energy transferred from the mercury ($^3P_1$) atom on collision might simply be disseminated over the various vibrational and rotational modes of the hydrocarbon molecule, without sufficient energy ever accumulating in one bond to bring about decomposition. 2-butene seems to afford an excellent example of physical quenching since the quantum yield of the mercury photo-sensitized reaction seems to be considerably lower than any of the other unsaturated molecules that have been investigated so far.[5]

Since there seems to be very good evidence for an inefficiency in the primary quenching process, the assumption of an initial C−H bond split seems to be the more plausible mechanism.

Returning now to a discussion of the individual reactions leading to the formation of acetylene and propylene, reaction (4) should be exothermic to the extent of about 30–40 kcal., by analogy with the reaction

$$C_3H_6+H\rightarrow C_3H_7,$$

which, as Rabinovitch, Davis, and Winkler pointed out,[6] is exothermic to about 40 kcal. It is therefore likely that the butyl radical formed is rich in energy by this heat of hydrogenation.

Reaction (5) should be endothermic, since the net effect of the reaction is the formation of a C≡C from a C=C, and the degradation of a C=C to a C−C. Only semi-quantitative data exist on the values for the carbon-carbon double and triple bond strengths,[7] but in general the increment in carbon-carbon bond strength in passing from single to double, appears to be greater than from double to triple. The six C−H bonds on the methyl groups in isobutene should each have a bond strength not exceeding 93 kcal. by analogy with propylene (3). And therefore it is quite probable that the C_4H_7 radical formed in the initial C−H bond split may be richer in energy by the difference between the excitation energy of the Hg($^3P_1$) state and the C−H bond strength, or, in other words, by about 20 kcal. Consequently reaction (5) may occur readily, even though it may have an activation energy of upwards of 20 kcal., owing to the activated C_4H_7 radical.

From the standpoint of steric hindrance, the C_6H_{13} radical formed in (5) would most probably have the structure $(CH_3)_2:C\cdot C_3H_7$. Such a highly branched structure would likely have a relatively long life, and since it does not possess sufficient energy to split off another acetylene molecule, it may either react further with isobutene to form a longer polymer chain or diffuse to the wall and become deactivated.

As we pointed out above the C_4H_9 radical formed in (4) should be "hot" owing to the 30–40 kcal. to which the reaction is exothermic. Consequently the C_4H_9 radical must have at least twice as much excess energy as the C_4H_7 radical formed in the initial quenching process. Now the net effects of reactions (6) and (7) from an energetic standpoint are approximately the same. Namely the formation of a C=C from a C−C, and the degradation of a C=C to a C−C. Therefore, in this case, it may be quite possible for two molecules of propylene to split off the growing polymer chain. The C_6H_{13} radical formed in reaction (7) will be sterically protected against further reaction with isobutene molecules. This radical may either diffuse to the wall or it may add on another molecule of isobutene through a favorable collision. But, in any event it will not possess sufficient energy to split off another molecule of propylene.

In Table IV, data are given for the actual rate of polymerization, $-d[i-C_4H_8]$ poly./dt, as a function of the initial reaction pressure. On the basis of the mechanism outlined above, we were led to the conclusion that the growing polymer radical, which we can represent by the formula $[i-C_4H_8]_n\cdot C_6H_{13}^-$ decreases in its rate of growth owing to steric factors. That is to say, the steric factor for the reaction

$$[i-C_4H_8]_{(n-1)}C_6H_{13} + i-C_4H_8\rightarrow[i-C_4H_8]_n\cdot C_6H_{13}$$

decreases rapidly with increasing n. And under these conditions the radical tends to diffuse to the wall where it is deactivated by some zero-

[6] B. S. Rabinovitch, S. G. Davis, and C. A. Winkler. Can. J. Research **B21**, 251 (1943).

[7] For a discussion of hydrocarbon bond strengths, see E. W. R. Steacie, *Atomic and Free Radical Reactions* (Reinhold Publishing Corporation, New York, 1946), Chapter III.

order reaction. Now we can make a rough calculation of the average value of n, i.e., $\bar{n}$, from our data, since $\bar{n}$ can be represented by the expression

$$\bar{n}=\frac{-d[i-C_4H_8]\text{ poly.}/dt}{\left[\frac{d[C_2H_2]}{dt}+\frac{1}{2}\frac{d[C_3H_6]}{dt}\right]}.$$

In the complete quenching region, the mean value of the above quantities from Tables III and IV are $-d[i-C_4H_8]$ poly.$/dt=1.5$, $d[C_2H_2]/dt=1.16$, and $d[C_3H_6]/dt=2.29$, all in micromoles per minute, and therefore $\bar{n}=0.6$. This calculation shows that the chain length of the polymer is very short, in agreement with the observation that the polymer is liquid and completely soluble in benzene. If the polymer is finally formed by a zero-order recombination at the wall, the polymer should have an average molecular weight of only 240.

If the slight falling off in the rate of polymerization with pressure is a real effect, and not just experimental error, it may indicate that chain decomposition, which should increase with the collision frequency, is a significant factor.

The rate of formation of propane seems to be the same type of function of the initial pressure as the rate of formation of acetylene and propylene. This could be explained by assuming that the reaction

$$C_4H_9+i-C_4H_8\rightarrow C_3H_8+C_5H_9 \qquad (8)$$

occurs to some extent. This reaction would probably only occur with isobutyl radicals, whereas on steric grounds reaction (4) should form predominately tertiary butyl radicals. The rate of formation of propane would then be represented by

$$\frac{d[C_3H_8]}{dt}=\frac{k_8}{2k_6}\cdot\frac{d[C_3H_6]}{dt}.$$

Hence, from Table III, we see that

$$\frac{k_8}{k_6}=\frac{1}{12}.$$

The small amounts of hydrogen and methane formed probably arise from the unimolecular decomposition of the activated butyl radicals formed in (4). This radical may decompose to some extent by the reactions

$$C_4H_8\rightarrow CH_4+C_3H_5, \qquad (9)$$

$$C_4H_8\rightarrow H_2+C_4H_7, \qquad (10)$$

whence

$$(d[H_2]/dt)/(d[CH_4]/dt)=k_{10}/k_9=2.4$$

from Table II.

These rates should both fall off with increasing pressure in accordance with our findings. The increase in the rate of formation of methane at very low pressures suggests that the reaction

$$CH_3+H+M\rightarrow CH_4+M \qquad (11)$$

is occurring at the wall.

CONCLUSIONS

The most surprising result of the present investigation is the striking difference in behavior between isobutene and the other unsaturated hydrocarbons which have been previously investigated. Ethylene,[1] propylene,[3] isoprene,[3] butadiene,[2] 1-butene,[5] and 2-butene[5] all seem to form activated molecules in the initial quenching process. These activated molecules seem to have sufficiently long lifetimes to be able to undergo deactivating collisions, as well as decomposing unimolecularly into radicals or molecules. Isobutene, on the other hand, appears to decompose, in the main, initially into C_4H_7 radicals and H atoms. If we compare isobutene with propylene, which, of all the above molecules, it should most closely resemble, we see that the substitution of a methyl group for a hydrogen shortens the lifetime of the activated state to such an extent that it becomes less than the interval between collisions. This is true, at least, up to a pressure of 80 mm. Actually the difference in behavior between propylene and isobutene is probably more a matter of degree than kind. The reactions

$$RH+Hg(^3P_1)\rightarrow R+H+Hg(^1S_0), \qquad (12)$$

$$RH+Hg(^3P_1)\rightarrow RH^*+Hg(^1S_0) \qquad (13)$$

undoubtedly occur in both cases, (12) predominating in isobutene and (13) in propylene.

The quenching efficiency of a double bond is

some six hundred times greater than that of a single bond. Now in isobutene there is a greater probability that quenching will occur at the paraffinic end than in propylene, and this should lead to reaction (12). On the other hand if quenching does occur at the olefinic end, reaction (13) may occur with propylene, whereas with isobutene, the increased number of degrees of freedom may cause the excitation energy of the mercury ($^3P_1$) atoms to be dissipated as vibrational and rotational energy without leading to reaction. This argument is supported by the fact that the initial quenching process seems to be only 16 percent efficient in isobutene.

ACKNOWLEDGMENT

It is a great pleasure to acknowledge our indebtedness to Dr. A. Keith Brewer, Chief of the Mass Spectrometry Section of the National Bureau of Standards, for his kindness in performing the mass spectrometric analyses reported in this paper.

Our thanks are also due Mr. Yves Lupien for his assistance in making the measurements.

THE JOURNAL OF CHEMICAL PHYSICS VOLUME 14, NUMBER 9 SEPTEMBER, 1946

The Mercury Photo-Sensitized Reactions of Diethyl Ether*

B. deB. Darwent, E. W. R. Steacie, and A. F. van Winckel
Division of Chemistry, National Research Laboratories, Ottawa, Canada

(Received June 28, 1946)

The mercury photo-sensitized reactions of diethyl ether have been investigated in a circulatory system at 35°C and between 9- and 193-mm pressure. The principal products are hydrogen and $C_8H_{18}O_2$; smaller amounts of CO, CH_4, C_2H_6, and aldehydes are formed. The quantum yield for ether disappearance is about 2.0 initially but decreases with the duration of the experiment. In low pressure experiments the hydrogen produced initially is consumed in the later stages of the experiment and ultimately vanishes. The decrease in rate and the consumption of hydrogen in the late stages of the reaction are not caused by the accumulation either of polymer on the wall or to hydrogen and/or CO in the system. The nature of the reaction is altered by interrupting the experiment thus indicating the occurrence of a dark reaction. The initial stages may be explained by either a C-H split followed by "atomic cracking" or by reactions involving an active ether molecule.

INTRODUCTION

THE thermal decomposition of diethyl ether has been investigated extensively and the indications[1] are that the reaction proceeds by a mixed free radical and molecular rearrangement mechanism. The only photochemical investigation of the decomposition of diethyl ether published is that of Berthelot and Gaudechon[2] who report that non-condensible gas consisting of 14.5 percent CO and 85.5 percent H_2, CH_4, and C_2H_6 (ethane predominating) was formed when diethyl ether was exposed in a quartz vessel to the light of a mercury lamp. In the same investigation they found that dimethyl ether behaved similarly but report that a liquid was formed as well as the non-condensible gas. Since both dimethyl and diethyl ethers are almost completely transparent to light of wave-length longer than about 2000A and since Berthelot and Gaudechon do not mention any precautions to remove mercury vapour from their reaction vessel and used a Hg lamp which probably gave unreversed λ2537, it seems likely that they investigated the mercury photo-sensitized reaction rather than the photolysis of diethyl ether.

Although much information is available on the

---

* Contribution No. 1412 from the National Research Laboratories, Ottawa, Canada.

[1] For comprehensive reviews see: (a) E. W. R. Steacie, *Atomic and Free Radical Reactions* (Reinhold Publishing Corporation, New York, 1946). (b) H. J. Schumacher, *Chemische Gasreaktionen* (Theodor Steinkopff, Leipzig, 1938).

[2] D. Berthelot and H. Gaudechon, Comptes rendus (Paris) **153**, 383 (1911).

photo-sensitized reactions of the simple saturated[3] and unsaturated[4] hydrocarbons, little is known about similar reactions of simple organic compounds containing oxygen. Taylor and Bates[5] carried out preliminary qualitative investigations of the reactions between $Hg(^3P_1)$ atoms and a number of compounds including methyl and ethyl alcohols, acetone, and formic acid and found that those substances reacted readily; however no information was provided on which mechanisms could be assigned to those reactions. Hence it was thought that more detailed investigation of the mercury photo-sensitized reactions of some of the simple organic compounds would be of interest, and we present below the results obtained in the reaction between diethyl ether and $Hg(^3P_1)$ atoms at 35°C and at pressures between 9 and 190 mm.

EXPERIMENTAL

The reaction was investigated in a circulatory system of conventional design[3] in which ether vapor was circulated at constant pressure, provided by the presence of liquid ether in a trap at constant temperature, over a pool of warm mercury, through a trap filled with iron pellets and kept at constant temperature to reduce the partial pressure of mercury vapor to the desired level and then through a quartz reaction vessel in which the mixture of mercury and ether was illuminated by a lamp emitting λ2537. Products of low vapor pressure were removed, more or less efficiently, by circulating through a cold trap while those of high vapor pressure accumulated in the gas phase and were circulated with the ether and mercury vapor.

The volume of the reaction system was 980 cc and the circulation rate about 400 cc $min.^{-1}$. The reaction vessel was a quartz annular cell of about 430-cc capacity. The lamp was of the usual low pressure type with neon as carrier gas, the emission of which is almost entirely λ2537. The transmitting portion of the lamp was a quartz U which fitted into the annulus of the reaction vessel. The intensity of λ2537 was measured from the rate of hydrolysis of monochloracetic acid placed in the reactor and therefore represents the amount of λ2537 entering the reaction zone; allowance was made for the contribution of the dark reaction to the rate of hydrolysis of monochloracetic acid as found by Smith, Leighton, and Leighton.[6] The type of lamp used emits very little light other than λ2537 which is active in the hydrolysis of monochloracetic acid and the λ2537 emitted is narrow enough so that no great error could be introduced from the wings of the line. Since we could detect no fluorescence in our experiments, it is likely that the quantum input measured did approximate very closely to the amount of λ2537 entering the system, and certainly represents the upper limit of the input of useful λ2537.

Stopcocks were excluded from the system because of the high solubility of ether in stopcock grease; mercury cut-offs and valves of the type described by Warwick and Fugassi[7] were used instead.

In preliminary experiments the reaction was carried out without the mercury saturator, depending on the contact of the gas with mercury in the circulating pump for saturation and it was found that the reproducibility was very poor. Concordant results were obtained only where the mercury saturator and desaturator were included in the system and when the desaturator was kept at a constant temperature. This was accomplished by placing the desaturator very near to the reaction vessel and immersing both in a thermostat at 35°C. The indications are that concentration of mercury in the reacting gases is critical. The thermostat was emptied and refilled with fresh distilled water and the reaction cell cleaned by flaming in an atmosphere of oxygen with an oxygen-gas flame before each experiment.

The ether used was a commercial product. It was purified by refluxing over and distilling from solid potassium hydroxide followed by freshly pressed sodium wire. The purified ether was stored over freshly cut sodium in a bulb attached to the apparatus through a mercury cut-off, and was freed from any hydrogen that might have

[3] (a) E. W. R. Steacie and N. W. F. Phillips, Can. J. Research **B16**, 303 (1938). (b) B. deB. Darwent and E. W. R. Steacie, J. Chem. Phys. **13**, 563 (1945).

[4] (a) D. J. LeRoy and E. W. R. Steacie, J. Chem. Phys. **9**, 829 (1941). (b) H. E. Gunning and E. W. R. Steacie, J. Chem. Phys. **12**, 484 (1944).

[5] H. S. Taylor and J. R. Bates, Proc. Nat. Acad. Sci. **12**, 714 (1926).

[6] J. O. Smith, P. A. Leighton, and W. G. Leighton, J. Am. Chem. Soc. **61**, 2299 (1939).

[7] E. Warwick and P. Fugassi, Ind. Eng. Chem. Anal. Ed. **15**, 13 (1943).

TABLE I. Effect of time and pressure on the mercury photo-sensitized reactions of diethyl ether.

Volume of system = 980 ml
Volume of reaction vessel = 430 ml
Circulation rate = 400 ml/min.
λ2537 absorbed = 2.8×10^{-6} einsteins/sec.
Reaction temp. = 35.0°C
Hg pressure = 4.2×10^{-3} mm (35.0 = C)

Run No.	Time (min.)	Ether reacted cc	Gaseous products—cc						Liquid products Found mg	Liquid products Calculated mg	Liquid products Calculated cc	Liquid products Formula $C_xH_yO_z$ X	Y
			H_2	CO	CH_4	C_2	Ald.	Et_2O					
Series (A)—Working pressure of ether = 9.3 mm													
115	1	3.2	2.0	0.2	0.0	0.2	0.3	0.78	8.0	8.0	1.4	8.6	19.0
116	2½	6.0	4.2	0.3	0.1	0.3	0.3	0.58	7.0	16.2	2.7	8.3	17.8
102	10	13.5	9.2	1.8	1.2	1.5	0.4	0.33	—	—	5.6	8.3	17.5
99	30	22.3	11.7	6.8	6.3	3.6	0.3	0.18	—	—	7.6	8.5	19.0
160(*a*)	30	—	14.2	5.7	5.7	—	—	—	—	—	—	—	—
105	60	28.5	10.6	10.6	14.4	5.0	0.1	0.12	35.0	49.0	8.9	8.4	18.8
161	60	31.1	14.0	9.6	13.0	6.1	—	0.13	—	—	—	—	—
163	60	—	15.5	9.7	12.4	—	—	—	—	—	—	—	—
169	60	21.7	8.8	8.5	11.4	4.1	—	0.09	—	—	—	—	—
103	90	35.8	8.9	15.9	21.4	5.6	0.1	0.09	45.0	60.0	9.9	8.7	20.6
165	120	48.1	11.3	15.3	26.0	8.9	—	0.10	—	—	—	—	—
167	120	34.7	8.9	18.5	24.3	6.9	—	0.07	—	—	—	—	—
104	150	43.6	5.6	20.8	33.0	8.3	—	0.07	56.0	67.0	11.2	8.5	20.0
97	300	50.0	0.0	29.9	49.8	12.2	—	0.04	—	58.0	9.5	8.8	21.4
			Aldehyde—average volume = 0.26 ml										
Series (B)—Working pressure of ether = 15.0 mm													
143	10	21.3	11.4	0.6	0.2	0.7	0.3	0.51	22.5	62	10	8.0	17.8
144	25	31.5	20.8	3.7	2.3	2.6	0.3	0.31	83.0	84	14	8.5	16.2
139	30	40.7	23.4	3.4	2.0	3.0	0.5	0.33	43.5	112	18	8.0	17.8
140	60	51.0	25.0	7.8	8.7	5.8	0.4	0.21	45.5	131	21	7.8	17.6
142	80	46.0	24.5	11.1	15.3	7.4	0.2	0.14	68.5	—	—	—	—
133	120	65.7	33.8	14.9	21.4	9.4	0.5	0.13	140.0	154	25	7.7	17.0
150	120	58.4	23.3	14.9	25.9	9.0	0.2	0.12	80.5	132	22	7.8	17.2
141	240	77.5	23.7	23.7	47.2	13.7	0.6	0.08	145.5	162	27	7.4	15.7
151	240	76.1	21.9	25.6	47.9	14.5	0.2	0.08	548.5	156	26	7.4	16.2
134	360	77.1	11.5	31.3	67.2	—	0.3	0.05	338.5	—	—	—	—
			Aldehyde—average volume = 0.35 ml										
Series (C)—Working pressure of ether = 20.0 mm													
146	30	30.2	26.6	2.0	1.1	1.7	0.4	0.24	79	84	14	8.1	17.2
149	60	59.4	39.3	7.0	7.1	5.7	0.3	0.24	101	159	26	7.6	17.2
147	120	75.4	38.7	13.6	18.9	10.7	0.3	0.20	121	188	31	7.7	16.7
148	240	67.0	27.0	25.6	46.8	14.8	0.2	0.07	135	126	21	6.8	15.2
			Aldehyde—average volume = 0.31 ml										
Series (D)—Working pressure of ether = 25.0 mm													
118(*B*)	1	8.1	2.8	0.2	0.0	—	—	1.98	—	—	—	—	—
120(*B*)	2	13.6	6.6	—	—	0.2	—	1.32	—	—	—	—	—
119	5	20.2	10.2	0.5	0.1	0.4	—	0.98	—	—	—	—	—
138	15	33.0	19.2	1.1	0.4	1.4	0.7	0.53	50	—	—	—	—
136	25	49.3	—	—	—	2.3	0.4	0.48	57	—	—	—	—
137	25	45.9	26.5	1.5	0.6	1.2	0.8	0.44	57	133	22	8.2	18.0
132	45	54.5	39.0	3.0	1.6	2.6	0.5	0.29	96	156	26	8.0	17.2
145	45	55.5	36.4	3.0	1.8	2.8	0.3	0.29	101	160	26	8.0	17.3
130	120	93.5	60.2	11.0	14.9	8.9	0.8	0.19	—	—	—	—	—
131	240	147.2	85.2	18.2	33.2	18.8	0.8	0.15	364	387	64	7.6	16.0
127	360	—	119.2	29.2	40.1	29.9	—	—	1034	525	86	7.3	15.2
129	360	196.0	119.6	22.8	48.0	26.1	1.3	0.13	323	—	—	—	—
			Aldehyde—average volume = 0.69 cc										
Series (E)—Working pressure of ether = 50 mm													
106	10	39	18	0.7	0.2	0.5	0.9	0.95	98	113	18	7.6	18.4
108	30	88	41	1.6	0.7	1.1	0.7	0.70	316	261	43	8.0	18.2
125	60	128	79	3.1	1.4	3.7	—	0.51	321	378	62	8.0	17.5
135	84	140	87	5.0	2.7	3.6	1.2	0.39	330	415	68	8.1	17.6
126	150	189	113	10.0	8.6	9.5	1.2	0.31	486	522	84	7.8	17.4
128	360	316	198	28.1	28.1	24.0	0.8	0.22	728	878	144	7.8	17.2
			Aldehyde—average volume—0.95 cc										
Series (F)—Working pressure of ether = 193 mm													
114	2.5	—	10	0.0	—	—	—	—	—	—	—	—	—
113	5.0	37	18	0.2	0.0	0.1	0.9	1.80	80	110	18	8.2	18.2
110	10.0	67	33	2.8	0.0	0.2	1.2	1.64	114	192	32	8.3	19.0
112	20.0	121	64	2.1	0.0	0.8	1.9	1.46	311	354	58	8.2	18.3

been generated by repeated freezing and melting in a vacuum. No aldehydes or other impurity could be detected by the analytical methods used. Hydrogen was taken from a cylinder of electrolytic gas and purified by passage over heated copper followed by calcium chloride, solid potassium hydroxide, and a trap in liquid air. Samples of this hydrogen were oxidized by hot copper oxide without leaving any residual gas or material volatile at −78°C. Carbon monoxide was prepared by the action of concentrated sulphuric acid on formic acid and purified by passage through "ascarite," calcium chloride, and a liquid air trap. Samples of this gas were

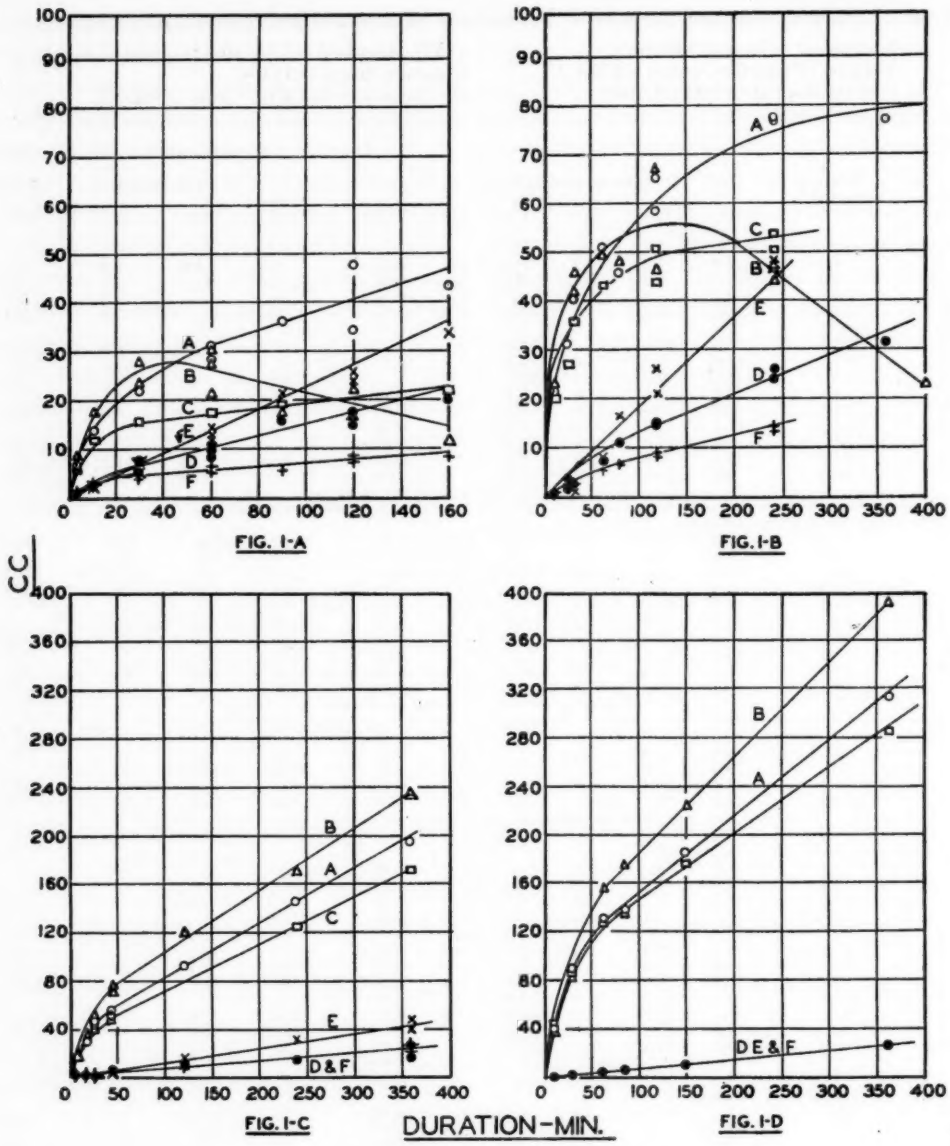

FIG. 1. Effect of time on the products.

Fig. 1-*A* Runs at 9.3 min.
1-*B* Runs at 15.0 min.
1-*C* Runs at 25.0 min.
1-*D* Runs at 50.0 min.

Curves *A* = cc Et_2O reacted
B = 2 × cc H_2 produced
C = 2 × cc liquid product (as gas) produced
D = cc CO produced
E = cc CH_4 produced
F = cc C_2 hydrocarbons produced.

completely oxidized by CuO and the gas volatile at −78°C was equal in volume to the samples taken.

The products of the reaction were analyzed by separation into four fractions and further analysis of these fractions. The fractions obtained were as follows: (1) *Non-condensible gas*—volatile at liquid air temperatures; analyzed by oxidation over copper oxide at 220°C and measurement of the CO_2 formed. The residue was characterized as CH_4 by combustion with excess oxygen on a glowing platinum wire. (2) *Volatile at −103°C—*

obtained by pumping down to 0.1 mm from traps at −80°C and −103°C (melting cyclohexene); analysis of this fraction by micro fractionation has shown that it consists almost entirely of C_2 hydrocarbon. (3) *Residual ether*—a fraction volatile at −70°C; this fraction was measured in as small a volume as possible to minimize inaccuracies caused by the possible presence of small amounts of heavy products and was analyzed for aldehydes by bisulphite titration.[8] (The volume of the residual ether was obtained by subtracting from this volume the volume of aldehyde found and by correcting the pressure for the presence of heavy products.) (4) *Residue non-volatile at −70°C*—this consisted of a heavy liquid with a vapor pressure of about 7 mm at 25°C and was weighed in a removable trap. The heavy products were also analyzed for aldehydes by bisulphite titration.

The C_2 fraction, residual ether, and the heavy product were analyzed for compounds of the ethylene oxide type by a reaction which depended on the formation of the chlorhydrin[9] and for unsaturates by bromine titration. Neither of these types of compounds was detected.

The procedure adopted for a typical experiment was as follows: Ether was condensed from the storage bulb into a calibrated volume of convenient size and the pressure measured at room temperature with a constant volume manometer. This amount of ether was then condensed in a liquid air trap in the reaction system. This trap was warmed with dry ice-acetone to the desired temperature. The lamp was turned on but separated from the reaction vessel by a cylindrical copper shutter, until the lamp and reaction system, with the circulating pump on, had attained equilibrium. The reaction vessel was illuminated, by dropping the copper shutter, for a definite period, and the lamp was turned off and the products analyzed as described above.

TABLE II. Composition of "dimer" and related compounds.

Compound	Formula	% C	% H	% O
"Dimer"	—	65.11	11.89	23.00
$(C_2H_5 \cdot O \cdot C_2H_4)_2$	$C_8H_{18}O_2$	65.8	12.3	21.9
$(C_2H_5 \cdot O \cdot CH_2)_2$	$C_6H_{14}O_2$	61.0	11.8	22.2
Ethyl ether	$C_4H_{10}O$	64.9	13.5	21.6

[8] A. Zahorka and K. Weiman, Monats. f. Chemie **71**, 229 (1938).

[9] (a) O. F. Lubatte, Trans. Soc. Chem. Ind., 361T (1932). (b) F. W. Kerchow, Zeits. f. anal. Chemie **108**, 249 (1937).

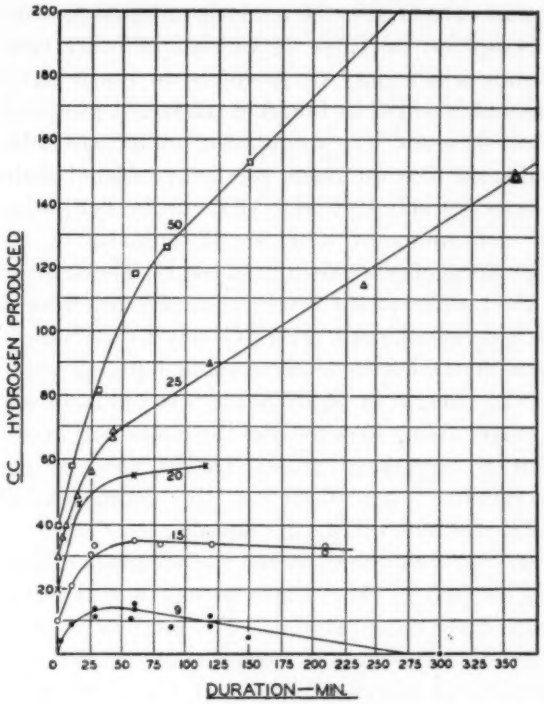

FIG. 2. Effect of time and pressure on the production of hydrogen. Working pressure of ether as indicated on graph.

RESULTS

The effect of working pressure of ether and of the duration of the experiment at constant ether pressure on the nature of the products of the reaction are shown in Table I and Figs. 1 and 2. In Table I we have given a material balance for each experiment; the amounts of C, H, and O found in the products, assuming the aldehyde to be CH_3CHO, were subtracted from the amount of C, H, and O in the ether reacted, the weight of liquid product necessary for a perfect material balance was obtained on the assumption that, on the average, each molecule of liquid product contained two atoms of oxygen. With regard to the above assumption: the aldehyde was found almost entirely in the residual ether fraction and is therefore probably acetaldehyde; the analysis of the liquid product* was:—65.11 percent C, 11.89 percent H, 23.00 percent O, which is close

* We are indebted to Dr. Léo Marion of this Laboratory for the micro C−H analysis.

to that of $C_8H_{18}O_2$; the analysis of liquid product is compared in Table II to that of other compounds which may be produced in the reaction and which would be found in the heavy products. From these results it would seem not unreasonable to assume that the liquid product consisted of the "dimer" $(C_2H_5 \cdot O \cdot C_2H_4)_2$ of diethyl ether probably contaminated with small amounts of the other compounds shown in Table II. The analysis of the portion of the products unaccounted for in the gas corresponds rather closely to $C_8H_{18}O_2$ in agreement with the analysis of the liquid product, and the weight of liquid product found is, on the average, about 70 percent of the calculated figure. This is considered reasonable in view of the uncertainties attendant on the estimation of small amounts of volatile liquids.

In Fig. 1 we have plotted the volumes of ether reacted and of the various products against the duration of the experiment. The sections of Fig. 1 refer to experiments carried out at different working pressures of ether. In Fig. 2 we have replotted the volumes of hydrogen produced against time so as to make easier the comparison of the effects of time and pressure on the production of hydrogen.

From the results shown in Table I and Fig. 1 it is evident that the volume of ether reacted and of H_2, CO, CH_4, C_2 and liquid products (calculated) varies in a rather regular manner with the duration of the experiment, the volume of aldehyde produced is reasonably constant at constant ether pressure and we have given the average "steady-state" concentration of aldehyde in Table I, Section A to E.

The decrease in the rate of reaction (cc of ether reacted per minute) and of the production of hydrogen and liquid product as well as the consumption of hydrogen produced initially in the runs at low pressures, with the duration of the experiment (Fig. 1) is an important point in deciding on the mechanism of the mercury photosensitized reactions of ether. The effect of time on these rates may be caused either by the accumulation of liquid product on the incident face of the reactor, leading to the formation of "polymer" by subsequent reaction at the wall and so to a decrease in light intensity, or by the accumulation of some product which inhibits the reaction. The results of experiments carried out to obtain information on this point are given in Table III. These experiments were carried out with ether at 9.3 mm, since the above-mentioned effects are most pronounced at low pressures. To determine the possible effects of the accumulation of polymer on the wall, the reaction was conducted in the normal way for 60 minutes at 9.3 mm pressure; the non-condensible gases, C_2 hydrocarbons and residual ether were removed and measured as usual and the liquid products removed by sealing off a small bulb at the bottom of the cold trap. Fresh ether was then measured, introduced in the reaction system and reacted for 60 minutes at 9.3 mm pressure (Run No. 169(b)). In this way no air was admitted to the system between experiments, and it is likely that most of the polymer formed in the first experiment would remain on the wall for the second reaction. The results do not indicate that the accumulation of polymer has any appreciable effect on the nature of the reaction.

Information on the effect of hydrogen and carbon monoxide on the rate of the reaction is obtained from the results of runs 158 and 159 in which H_2 and H_2+CO were added at the start of 30-minute runs in the amounts in which they are present at the end of the first 30 minutes of the reaction. The volumes of ether reacted and of products in these runs therefore should be the same as found during the second thirty minutes of reaction if H_2 and/or CO were responsible for altering the nature of the reaction. From experiment 158 it may be seen that the only effect of hydrogen is to reduce the initial rate of production of hydrogen from 13 to 9 cc in the first 30 minutes and that neither the rate of reaction nor the rate of formation of other products is affected significantly. The additional effect of CO (Run 159) is negligible. The rates found in these experiments do not correspond to those expected in the second half of a 60-minute run. A similar experiment of 60-minute duration (Run No. 162) confirmed that the addition of H_2 reduces only the rate of production of H_2 but not to the extent necessary to explain the disappearance of that product in the 9.3-mm runs and that the rates of disappearance of ether and of the production of CO, CH_4, and C_2 hydrocarbons are unaffected. Hence the presence of some other products as well as hydrogen and/or CO must be responsible for the re-

TABLE III. Effect of H_2, CO, and polymer on the reaction at 9.3 mm. Conditions as in Table I.

Run No.	Duration min.	Ether reacted cc	Products—cc H_2	CO	CH_4	C_2	Remarks
A	30	22	13±1	6±1	6±1	4	Average of "normal" 30-min. runs 99 and 160(a).
B	60	27±4	12±4	10±1	13±1	5±1	Average of "normal" 60-min. runs 105, 161, 163, 169.
C	120	41±7	10±2	17±1	25±1	8±1	Average of "normal" 120-min. runs 165, 167.
D	—	5	0	4	5	1	Production during second 30 min.
E	—	14	0	7	14	3	Production during second 60 min.
158	30	19	9	5	6	4	12.0 cc H_2 added at start.
159	30	20	8	5	7	4	12.0 cc H_2+7 cc CO added at start.
160(b)	30	—	6	4	6	6	12.0 cc H_2+7 cc CO added to condensible residue from "normal" 30-min. run (160(a)).
169(b)	60	31	21	8	10	5	Experiment carried out after a "normal" 60-min. run (169) without cleaning cell.
162	60	26	5	8	14	4	15 cc H_2+6 cc CO added at start.
163(b)	60	—	6	7	13	10	14 cc H_2+6 cc CO to condensible residue from a "normal" 60-min. run (163).
166	120	46	17	18	24	10	Runs stopped after 60 min.; nonconds. removed from liquid air trap and experiment resumed after 60-min. interruption.
168	120	45	17	17	24	9	
170	120	54	19	13	16	9	Run stopped after 60 min. for 45 min.; products warmed to room temperature, and experiment resumed.

moval of hydrogen from the later stages of the reaction at 9.3 mm. This possibility was tested by adding the requisite amounts of hydrogen and CO to the condensible products, after removal of the non-condensible gases, from experiments of 30-minutes (Run 160(b)) and 60-minutes (Run 163(b)) duration. Again it was found that the rate of production of hydrogen was reduced to about the same extent as when H_2 and CO were added at the start of the experiment. Hence, if some product, other than hydrogen and CO, is responsible for the consumption of hydrogen in the runs at low pressures, it is either removed or changed during the period in which the condensible gases were being frozen out in liquid air. To test this possibility experiments were conducted in which (a) the products after 60-min. reaction at 9.3 mm were frozen out in liquid air for 45 min. and the reaction resumed for a further period of 60 min. after readjusting the trap temperature (Runs 166, 168) and (b) same as (a) but instead of freezing out the products the trap was allowed to warm up to atmospheric temperature while the experiment was interrupted for 45 min. (Run 170). Both experiments (a) and (b) showed similar trends but the effect in (b) is more marked. By interrupting a 120-min. experiment after 60 min. (Run 170) the volume of ether reacted was increased from 41(±7) to 54 cc and the volume of hydrogen produced increased from 10±2 to 19 cc whereas significant decreases were noted in the volumes of CO and CH_4 produced. These effects can only be explained by the disappearance of some relatively unstable intermediate during the interval between the two halves of the experiment.

DISCUSSION

The following facts brought out by this investigation are of importance in devising a mechanism to account for the observed results of the mercury photo-sensitized reactions of diethyl ether:

(1) The initial products of the reaction are principally hydrogen and the "dimer" of ether with minor amounts of CH_4, CO, C_2 hydrocarbons and acetaldehyde.

(2) Initially half a mole each of hydrogen and "dimer" are produced per mole of ether reacted.

(3) The rates of production of CO, CH_4, and

C_2 hydrocarbons are equal in the early stages of the reaction.

(4) The rate of production of methane is independent of time but decreases with increasing ether pressure.

(5) The rates of production of CO and C_2 hydrocarbons decrease with time and with increasing ether pressure; the time dependence of these rates is more pronounced in the experiments at low ether pressure.

(6) The volume of acetaldehyde found in the products is independent of time, indicating that the "stationary" concentration is rapidly attained, but increases with increased working pressure of ether.

(7) The rate of decomposition of diethyl ether decreases with time and eventually attains a constant value. The initial rate of ether decomposition is independent of pressure but the constant rate eventually attained increases with increasing ether pressure.

(8) The rates of production of hydrogen and "dimer" also decrease with time and, at high ether pressures, reach constant values. In experiments at low pressures (9.5 and 15 mm) the hydrogen produced in the early stages is consumed in the later stages of the experiment and, at 9.5 mm, actually disappears entirely from the products.

(9) The decrease in the reaction rate and in the rate of production of hydrogen with time is not caused by the accumulation of polymer on the incident face of the reactor.

(10) The addition of hydrogen either to pure ether at the start of the reaction or to a mixture of ether and the condensible products of the reaction decreases the rate of production of hydrogen but does not lead either to the consumption of hydrogen nor does it affect significantly the rates of either the decomposition of ether or of the production of the other products of the reaction.

(11) By interrupting the experiments at low pressures the consumption of hydrogen in the later stages is prevented and the rate of decomposition of ether increased.

The fact that approximately $\frac{1}{2}$ mole each of hydrogen and "dimer" ($C_8H_{18}O_2$) are produced per mole of ether reacted indicates that the principal primary act is:

$$Hg(^3P_1)+(C_2H_5)_2O\rightarrow C_2H_5\cdot O\cdot C_2H_4+H+Hg(^1S_0). \quad (1)$$

This reaction is in complete accord with the primary step proposed for the similar reactions of the lower paraffin hydrocarbons.[3]

Since the quantum yield for ether decomposition approaches 2.0 at zero time the reaction,

$$H+(C_2H_5)_2O\rightarrow C_2H_5\cdot O\cdot C_2H_4+H_2 \quad (2)$$

probably occurs with relatively high efficiency. The production of "dimer" is explained satisfactorily by recombination of the radicals produced in reactions (1) and (2),

$$2C_2H_5\cdot O\cdot C_2H_4\rightarrow \text{"Dimer"}\ (C_8H_{18}O_2). \quad (3)$$

The recombination of the radicals in reaction (3) is probably fast and occurs without real activation energy.

The formation of CO, CH_4, C_2 hydrocarbons and acetaldehyde indicates that C—C bonds are broken and it has been customary in these reactions to explain C—C splitting as the result of "atomic cracking" reactions first suggested by Rice and Teller.[10] According to the Rice-Teller principle, atomic cracking will occur by the following process:

$$H+C_2H_5OC_2H_4\rightarrow C_2H_5\cdot O\cdot CH_2+CH_3, \quad (4)$$

or

$$\rightarrow C_2H_5\cdot O+C_2H_5, \quad (4')$$

depending on whether the structure of the radical in question was $C_2H_5\cdot O\cdot CH_2\cdot CH_2$ (leading to (4)) or $C_2H_5\cdot O\cdot CH\cdot CH_3$ (leading to (4′)). Since the secondary[11] and tertiary[12] hydrogen atoms are removed more easily than the primary in these reactions, it is likely that the radical would be $C_2H_5\cdot O\cdot CH\cdot CH_3$ and so reaction (4′) is likely to be the first stage in the atomic cracking chain. The activation energy of reactions of this type is probably small and may be zero[3(b)] so atomic cracking may be responsible for the early formation of C_2 hydrocarbons and methane. For a rapid formation of acetaldehyde the reaction

$$C_2H_5O\rightarrow CH_3\cdot CHO+H \quad (5)$$

[10] F. O. Rice and E. Teller, J. Chem. Phys. 6, 489 (1938).
[11] E. W. R. Steacie and D. J. Dewar, J. Chem. Phys. 8, 571 (1940).
[12] B. deB. Darwent and C. A. Winkler, J. Phys. Chem. 49, 150 (1945).

may be postulated. There is no information available about the speed of this reaction but the reaction

$$CH_3CH_2O \rightarrow CH_3 + CH_2O$$

has been estimated to have an activation energy of 28–34 kcal.[13] So by analogy it is likely that the activation energy for reaction (5) is high and therefore this reaction will not be noticeable at 35°C in a system such as the present.

The decomposition of C_2H_5O by further reaction with H,

$$H + CH_3CH_2 \cdot O \rightarrow CH_3 \cdot CHO + H_2, \quad (6)$$

$$\rightarrow CH_4 + CO + H_2, \quad (6')$$

may be the source of aldehyde CO and CH_4 if reactions (5) and/or (4′) are responsible for CH_4 and C_2 hydrocarbons.

The stationary concentration of acetaldehyde has been found to be a direct linear function of the working pressure of ether, hence acetaldehyde probably disappears by a second-order process in which it is in competition with ether for the second reactant. The decomposition of acetaldehyde has been shown to lead to the formation of CO and CH_4 and the following reaction:

$$CH_3CHO + X \rightarrow CH_4 + CO + X \quad (7)$$

preceded by reactions (4′) and (6) can account for the products obtained initially and for the pressure dependence of the rates of production of CO, CH_4, C_2 hydrocarbons and stationary concentration of acetaldehyde. In the above reaction X may be H or $Hg(^3P_1)$. If the acetaldehyde disappeared by direct photolysis involving λ2537, then the stationary concentration of acetaldehyde would not depend on the ether pressure since the aldehyde would be in competition only with $Hg(^1S_0)$ for λ2537 and, since a large excess of mercury was used, the concentration of $Hg(^1S_0)$ is not dependent on the pressure of ether in the reaction vessel under conditions where quenching is reasonably complete. The ratio of the pressure of aldehyde to the working pressure of ether is constant at 0.020 ± 0.004, hence X must react considerably faster with acetaldehyde than with ether.

The above mechanism accounts for some of the characteristics of the reaction and is in accord with the mechanisms postulated for the similar reactions of the lower paraffin hydrocarbons,[3(a), 11, 12] however it seems likely that the unsaturated hydrocarbons[4] and even the saturated hydrocarbons[3(b)] react at least in part by the formation of an active molecule and the reactions

$$C_2H_5OC_2H_5 + Hg(^3P_1) \rightarrow C_2H_5OC_2H_5^* + Hg(^1S_0), \quad (8)$$

and

$$C_2H_5OC_2H_5^* \rightarrow C_2H_6 + CH_3CHO, \quad (9)$$

followed by further rapid reaction of acetaldehyde by reaction (7) could also account for the formation of the minor products of the reaction. The possibility that the "dimer" and hydrogen are also formed by second-order reactions of active ether,

$$C_2H_5O \cdot C_2H_5^* + C_2H_5OC_2H_5 \rightarrow \text{Dimer} + H_2, \quad (10)$$

cannot be discredited by our results and would explain the high quantum yield as well as the pressure dependence of the rates of production of CO, CH_4, and C_2H_6.

The secondary effects, such as the decrease in rate and consumption of hydrogen with time are indicative of complications in the later stages of the reaction. We have shown that these effects are not caused by the accumulation of hydrogen and carbon monoxide in the system, and, since the aldehyde and the "dimer" must rapidly attain their steady-state concentrations in the gas phase they cannot be responsible for those effects which occur over a considerable period. The experiments in which the runs were interrupted show that a dark reaction occurs and it is likely that this is connected in some way with the removal of hydrogen in the later stages of the experiments. It seems impossible to account for the above phenomena at the present stage of this problem but it is hoped that investigations of similar reactions of simpler compounds of the same type now in progress will throw some light on the subject.

[13] F. O. Rice and E. L. Rodowskas, J. Am. Chem. Soc. 57, 350 (1935).

THE JOURNAL OF CHEMICAL PHYSICS VOLUME 14, NUMBER 9 SEPTEMBER, 1946

Electron Diffraction Investigation of the Molecular Structure of Thioacetic Acid

WALTER GORDY*
Gates and Crellin Laboratories, California Institute of Technology, Pasadena, California
(Received May 21, 1946)

The structure of thioacetic acid has been investigated by the method of electron diffraction. The molecule was found to have very little resonance interaction between bonds. The interatomic distances found are: C=O=1.24±0.04A; C−S=1.78±0.02A; C−C=1.54±0.06A. The angle CCO was found to be 125°±5° and angle CCS, 110°±5°. The distances assumed are: C−H=1.09A and S−H=1.34A. Angle OCS was assumed to be 125°.

THE structure of thioacetic acid in the vapor state has been investigated through its electron diffraction patterns. High speed electrons, of wave-length 0.0615A, were employed. This substance gave good electron diffraction pictures which showed ten measurable rings. Measurements were made of ten different photographs. A description of the electron diffraction technique and of the instrument used for the present investigation has been made by Brockway.[1]

The values of $q_{obs.}$, listed in Table I, were obtained from the scattering angle and electron wave-lengths by use of the relation,

$$q=40/\lambda(\sin\phi/2).$$

Two radial distribution curves were made using the formula,

$$lD(l)=\sum_k C_k \sin\frac{\pi}{10}q_k l,$$

and the Schomaker method[2] of estimating intensities. In one the C_k's were used as the estimated intensities of the maxima and minima of the rings multiplied by the damping factor, $\exp(-aq^2)$. The other was a radial integral made from a curve drawn to represent the scattering pattern of the molecules as nearly as it could be estimated from the pictures. The intensities were read from this curve at intervals of $0.05q$ and were multiplied by a damping factor, $\exp(-aq^2)$, to obtain the intensity constants, C_k's, in the above equation. The two radial distribution curves agree in that the essential peaks come in the same places on each. The radial integral curve shown in Fig. 1 is the only one given here.

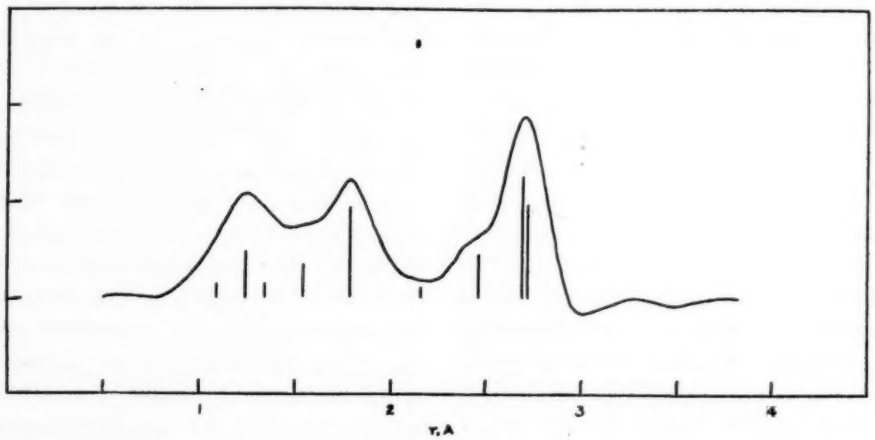

FIG. 1. Radial distribution curve for thioacetic acid. Bars are for Model *A* of Table II.

* Present address: Department of Physics, Duke University, Durham, North Carolina. The experimental work reported here was done while the author was a National Research Fellow in Physics, 1941.

[1] L. O. Brockway, Rev. Mod. Phys. **8**, 231 (1936).

[2] V. Schomaker, American Chemical Society Meeting, Baltimore, Maryland, April, 1939.

Theoretical intensity curves for several models were plotted (Fig. 2), using the formula,

$$I(q)=\sum_i \sum_j (Z_iZ_j/l_{ij}) \sin \frac{\pi}{10} q l_{ij}.$$

In these the scattering factors are assumed to be proportional to the atomic numbers of the atoms. For the terms containing hydrogen, temperature corrections were applied.[3]

All calculations were made with International Business Machines.

DISCUSSION OF RESULTS

In interpretation of results the following assumptions were made: C−H distances were taken as 1.09A, and S−H ones as 1.34A; angle SCO was assumed to be 125°; all atoms of the molecules except those of hydrogen were considered in a single plane. A certain amount of resonance might be anticipated between the C−S and C=O. Such interation, however, would be unlikely to affect measurably angle SCO. As the C−S bond takes on double bond character, the C=O bond correspondingly approaches a single bond. This would tend to keep the bond angle constant and to keep the bonds to the central carbon coplanar.

In the radial distribution curve there are three well-defined peaks, at 1.24A, 1.78A, and 2.70A, respectively; one not completely resolved occurs at about 2.44A. Those at 1.24A and 1.78A can be identified with the C=O and C−S distances, respectively. The peak at 2.70A, strong and rather sharp, is assumed to be due to the non-bonded S−O and S−C scattering terms which are too close together to be separated. The peak at about 2.44A may be identified with the non-bonded C−O scattering. The C−C term, because of its low scattering power and because of its occurrence between the strong peaks at 1.24A and 1.78A, is not resolved.

Of the several models listed in Table II, Model *A* is the one suggested by the peaks of the radial distribution curve. The other models, for which the distances vary as much as 0.03A from those of Model *A*, produce slightly less satisfactory agreement than does Model *A* with the observed scattering curve as well as with the radial distribution curve. The values for the various parameters are thus determined as: C=O =1.24±0.04A; C−S=1.78±0.02A; C−C=1.54 ±0.06A; angle CCS=110°±5°; angle CCO

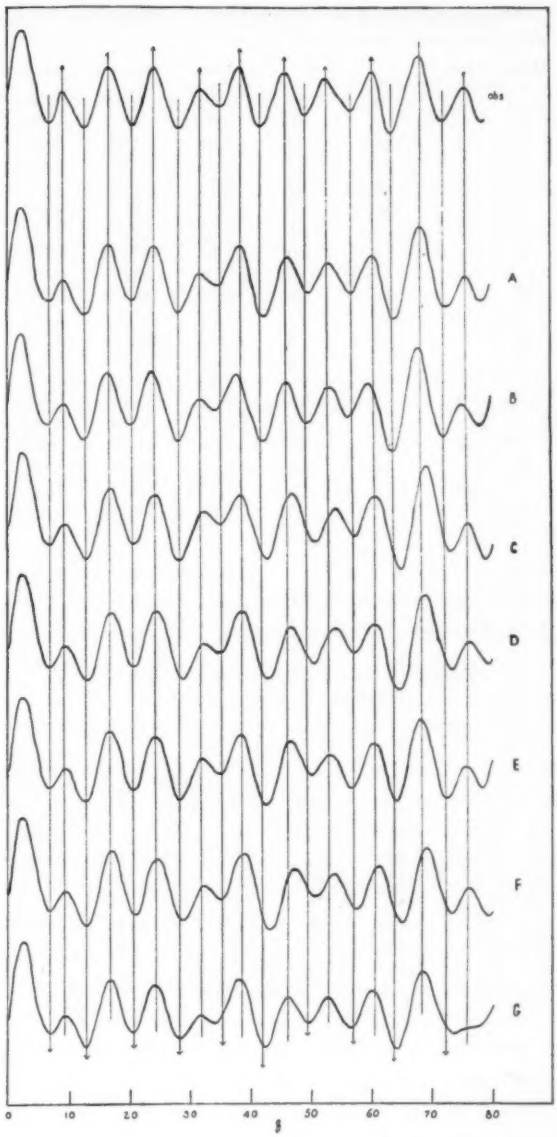

FIG. 2. Curve (marked obs.) drawn to represent the appearance of diffraction pictures, and theoretical scattering curves for models listed in Table II.

[3] D. P. Stevenson, H. D. Burnham, and V. Schomaker, J. Am. Chem. Soc. 61, 2922 (1939).

TABLE I. Electron diffraction data for thioacetic acid.

Max.	Min.	I	C	$q_{obs.}$	$q_{calc.}$[a]	$q_{calc.}/q_{obs.}$
	1	− 8	−80	7.05	6.95	0.986
1		3	30	9.28	9.30	1.002
	2	−10	−92	12.99	12.90	0.993
2		10	87	16.83	16.80	0.998
	3	− 9	−73	20.71	20.70	1.000
3		10	75	24.31	24.30	1.000
	4	− 9	−61	28.33	28.40	1.002
4		3	20	31.84	32.00	1.005
	5	− 3	−16	35.39	35.00	0.989
5		10	48	38.58	38.40	0.995
	6	−10	−42	41.88	42.50	1.015
6		8	28	46.12	46.50	1.008
	7	− 6	−24	49.37	49.95	1.012
7		6	16	52.90	53.30	1.008
	8	− 5	−10	57.03	57.00	0.999
8		8	13	60.56	60.50	0.999
	9	−12	−16	63.59	64.10	1.008
9		12	12	68.36	68.40	1.001
	10	− 8	− 6	72.17	72.75	1.008
10		4	2	75.90	75.75	0.998
					Average	1.001
					Average deviation	0.006

[a] For Model *A* of Table I.

TABLE II. Distances and bond angles for thioacetic acid models.

Model	C=O	C−C	C−S	Angle OCS	Angle CCO	Angle CCS	Average deviation of $q_{calc.}$ from $q_{obs.}$
A	1.24A	1.54A	1.78A	125°	125°	110°	0.006
B	1.24	1.54	1.81	125°	125°	110°	0.015
C	1.24	1.48	1.78	125°	125°	110°	0.014
D	1.21	1.54	1.78	125°	125°	110°	0.012
E	1.27	1.54	1.78	125°	125°	110°	0.012
F	1.24	1.54	1.75	125°	125°	110°	0.015
G	1.24	1.54	1.78	125°	121°	114°	0.017

$=125°\pm5°$; angle OCS $=125°$ (assumed). Though the photographs were excellent and Model *A* agrees closely with the observed features of the rings, the bond distances and angles could not be determined with great accuracy because none of the qualitative features of the computed curves are particularly sensitive to variations of the parameters in the neighborhood of the chosen values.

From a consideration of resonance effects in other molecules, a small amount of double bond character would be expected to shorten measurably the C−S bond distance. The fact that the C−S distance, 1.78A, found for this molecule is only slightly less than the sum of the single bond covalent radii of S and C, 1.81A, indicates that there is very little resonance of the C−S bond with the carbonyl group. The amount of double bond character of C−S computed from the observed distance using Pauling's rule[4] is only six percent. In contrast, similar compounds in which the S is replaced by the more electronegative N and O atoms, the amides or esters for example, show appreciable interaction[5] with the C=O.

The author is indebted to Professor Linus Pauling for his helpful advice, also to Doctor Verner Schomaker and Doctor Robert Spurr for their assistance.

[4] Linus Pauling, *Nature of the Chemical Bond* (Cornell University Press, Ithaca, New York, 1939), p. 164.
[5] Linus Pauling, reference 4, p. 130.

Note on the Conditions of Equilibrium for Systems of Many Constituents[1]

STUART R. BRINKLEY, JR.[2]
Central Experiment Station, U. S. Bureau of Mines, Pittsburgh, Pennsylvania

(Received July 12, 1946)

An analytical criterion is given for the choice of independent components. An inclusive discussion of equilibrium in systems of many constituents is thereby achieved. By reason of symmetry, the resulting conditions are particularly suited to form the basis of a calculation of the equilibrium composition of the system.

IT is well known, and has been clearly stated by Gibbs,[3] that the components selected from a system containing many constituents for describing the composition of the system must be independent and sufficient in number to describe the composition completely; however, it is not customary, to provide an analytical criterion for that choice. Such a criterion is developed in the present communication. In systems containing comparatively few constituents, a proper choice of components is usually intuitively obvious, but in more complicated systems, the criterion has a practical utility.

In terms of this criterion, the discussion in the manner of Gibbs[4] of the conditions for equilibrium of such systems becomes particularly simple and inclusive. The conditions formulated are found to possess a high degree of symmetry and to be especially well suited to form the basis for calculating the concentrations of the several constituents in the different phases of the system at equilibrium.

THE COMPONENTS

The number of constituents of any system depends upon the accuracy with which it is desired to describe its composition. The constituents to be considered must be chosen *a priori*, and this choice will usually imply the neglect of certain equilibria that may be expected to exert a negligible effect on the composition of the system at equilibrium.

Consider a closed system containing s different substances, which are assumed to be in chemical equilibrium. The molecular formula of the ith substance may be represented by

$$Y^{(i)} = X_{\alpha_{i1}}{}^{(1)} \cdots X_{\alpha_{il}}{}^{(l)} \cdots X_{\alpha_{im}}{}^{(m)}, \qquad (1)$$

$i = 1, 2, \cdots s$, where $X^{(l)}$ is the symbol of the lth element, α_{il} is the subscript (which may be zero) to this symbol in the formula of the ith substance, and m is the total number of elements represented in the system. For every i, the array of subscripts $\alpha_{il}, l = 1, 2, \cdots m$, may be said to define a vector,

$$y_i = (\alpha_{i1}, \cdots \alpha_{il}, \cdots \alpha_{im}), \qquad (2)$$

which may be called the *formula vector* of substance i. If the rank of the matrix of the vector elements α_{il} is c, it follows from a well-known theorem of algebra[5] that there are c linearly independent vectors, and if $c < s$[6] there are $s-c$ linearly dependent vectors which may be expressed as linear combinations of the independent vectors. It may be assumed that the independent vectors are designated by the values 1, 2, $\cdots c$ of their index. Then the dependent vectors may be expressed as linear combinations of the form,

$$\sum_{j=1}^{c} \nu_{ij} y_j = y_i, \qquad (3)$$

$i = c+1, c+2, \cdots s$. To Eq. (3) there correspond $s-c$ conceivable chemical reactions,

$$\sum_{j=1}^{c} \nu_{ij} Y^{(j)} = Y^{(i)}, \qquad (4)$$

[1] Published by permission of the Director, Bureau of Mines, U. S. Department of the Interior.
[2] Physical chemist, Bureau of Mines, Central Experiment Station, Pittsburgh, Pennsylvania.
[3] *Collected Works of J. Willard Gibbs* (Longmans, Green and Company, New York and London, 1928), Vol. 1, p. 63.
[4] Reference 3, pp. 63–82.
[5] See, for example, M. Bôcher, *Introduction to Higher Algebra* (The Macmillan Company, New York, 1907), Chap. III.
[6] Note that $c \leqslant m$ if $m \leqslant s$, or that $c \leqslant s$ if $m \geqslant s$.

resulting in the formation from the c substances with linearly independent formula vectors of the $s-c$ substances with linearly dependent formula vectors. It follows that the specification of c substances such that their formula vectors are linearly independent is sufficient for a description of the composition of the system. Therefore, the number of components of the system equals the rank c of the matrix of the subscripts to the symbols of the elements in the formulae of the substances comprising the system.[7] It may be noted that the choice of independent vectors is not, in general, unique, and that, in consequence, the choice of c substances as components and the expression of the remaining $s-c$ substances as products of reactions involving only the chosen components is usually not unique.

THE CONDITIONS FOR EQUILIBRIUM

The discussion of equilibrium in systems of many constituents assumes a particularly simple and symmetrical form in terms of the definitions that have been introduced. We consider the general case where the s substances are distributed among p co-existing phases. The conservation of mass in the system as a whole requires that

$$\sum_{k=1}^{p}\{\sum_{j=1}^{c} n_j^{(k)}M_j+\sum_{i=c+1}^{s} n_i^{(k)}M_i\}=\sum_{j=1}^{c} q_jM_j, \quad (5)$$

where $n_i^{(k)}$ and $n_j^{(k)}$ are the number of gram-moles in the kth phase of the ith and jth substances, respectively, M_i and M_j are the corresponding weights of one gram-mole, and the q_j are obtained by solution of the linear equations,

$$\sum_{j=1}^{c} \bar{\alpha}_{lj}q_j=Q_l, \quad (6)$$

$l=1, 2, \cdots m$, with $\bar{\alpha}_{lj}=\alpha_{jl}$ and with Q_l denoting the number of gram-atoms of the lth element available to the system. Since mass is conserved by each of reactions (4), one may substitute

$$M_i=\sum_{j=1}^{c} \nu_{ij}M_j \quad (7)$$

into Eq. (5). On equating the coefficients of M_j, there are obtained

$$\sum_{k=1}^{p}\{n_j^{(k)}+\sum_{i=c+1}^{s} \bar{\nu}_{ji}n_i^{(k)}\}=q_j, \quad (8)$$

$j=1, 2, \cdots c$, where $\bar{\nu}_{ji}=\nu_{ij}$.

It may be noted that these results lead immediately to the phase rule. Equations (9) and (10) constitute $c(p-1)+p(s-c)=ps-c$ relations between the chemical potentials. The chemical potentials in a given phase depend upon the common values of the state variables, which we assume to be only the temperature and pressure, and, since they are homogeneous functions of degree zero in the mole numbers, upon the mole fractions of the constituents of the phase, a total (because of the identity relation between mole fractions) of $p(s-1)+2$. In order that the system of equations be compatible, it is necessary that

$$ps-c\leqslant p(s-1)+2 \text{ or } p\leqslant c+2, \quad (11)$$

which is a statement of the phase rule of Gibbs[8] for systems depending upon only two state variables.

Together with Eq. (8), Eqs. (9) and (10) provide, by reason of their symmetry, the simplest basis for calculating the concentrations at equilibrium of the several constituents of the system. In particular, if the substances are limited to a single phase, the equations become

$$n_j+\sum_{i=c+1}^{s} \bar{\nu}_{ji}n_i=q_j,$$

$$\mu_i-\sum_{j=1}^{c} \nu_{ij}\mu_j=0, \quad \nu_{ij}=\bar{\nu}_{ji} \quad (12)$$

for equilibrium at constant temperature and pressure. A computational procedure utilizing these relations will be presented in a subsequent communication.

[7] Compare Gibbs, reference 3, pp. 63, 67.

[8] Gibbs, reference 3, pp. 96, 97.

Letters to the Editor

THIS section will accept reports of new work, provided these are terse and contain few figures, and especially few halftone cuts. The Editorial Board will not hold itself responsible for opinions expressed by the correspondents. Contributions to this section should not exceed 600 words in length and must reach the office of the Managing Editor not later than the 15th of the month preceding that of the issue in which the letter is to appear. No proof will be sent to the authors. The usual publication charge ($3.00 per page) will not be made and no reprints will be furnished free.

Tyndall Spectra, Their Significance and Application

WILFRIED HELLER
Chemistry Department, Wayne University, Detroit, Michigan
AND ETIENNE VASSY
Laboratoire d'Enseignement de Physique à la Sorbonne, Paris, France
June 24, 1946

"TYNDALL spectra," i.e., the variation of light scattering with the wave-length, λ, were determined by spectrographic investigations of the resulting apparent (conservative) absorption. The value of the "wave-length exponent," n, in the formal equation

$$k = c\lambda^{-n}$$

(k, absorption coefficient, c, a factor which is constant if light scattering particles and medium have equal optical dispersion) and, in addition, the variation of n with λ were found to provide two types of significant information on light scattering systems. n was either calculated or determined graphically from the slope of log k (log λ)-curves.[1]

(1) The $n(\lambda)$ functions of exclusive apparent absorption, $n_a(\lambda)$, and of exclusive true absorption, $n_t(\lambda)$, are characteristically different. A consideration of their difference greatly facilitates the detection and delimitation of absorption bands in such complex spectra where bands of true absorption are suspected, but indistinct because of a background of strong conservative absorption.

The differences, which follow from theoretical considerations and which are illustrated in part by the juxtaposed spectra in Fig. 1, are

(a) n_t may vary between 0 and $\pm\infty$, whereas n_a can only vary between 0 and 4.0, except for large microscopic particles, where small negative values are conceivable. n-values in excess of 4.0 are, therefore, generally indicative of the presence of true absorption.

(b) n_t changes rapidly with λ, whereas n_a changes so slightly (unless the particles are microscopic) that log k (log λ) curves are, in the latter case, practically straight lines over a spectral range of 1000A or more. The spectral approach of true absorption can thus easily be recognized.

The wave-length at which n changes sign characterizes the exact peak of an absorption band in systems free from light scattering. In light scattering systems, the approximate location of the peak is possible from considerations of the $dn/d\lambda$-values, although the magnitude and wave-length characteristics of light scattering are altered in the spectral range of true absorption.

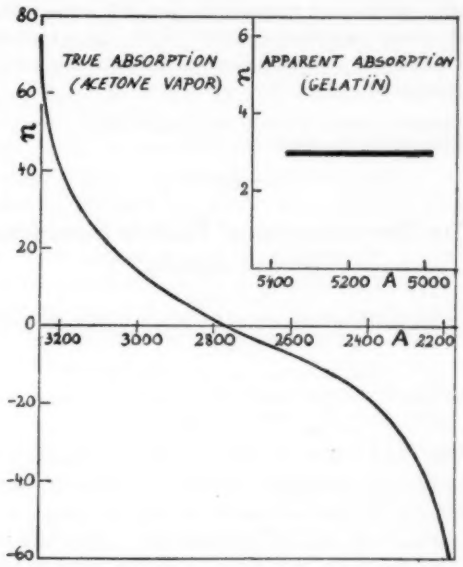

FIG. 1. Variation of n with wave-length. Main figure: Calculated from data taken from Landolt-Börnstein. (Peak of absorption: 2777±5A.) Inset: Six percent aqueous solution of Nelson photographic gelatin at 21.00°C (equilibrated gel).

The application of this type of spectral analysis to strongly light scattering inorganic colloidal solutions made it possible, as will be shown elsewhere, to characterize and to define chemically the light scattering material.

(2) In absence of true absorption, n has a constant value of 4.0 as long as the diameter of spherical particles (or the longest axis of non-spherical particles) is $<\frac{1}{10}$ of the wave-lengths used (Rayleigh radiation). With an increase of the diameter (long axis) beyond this limit, the value of n decreases for reasons which follow from the theory of Mie.[2] This opens the possibility of determining particles sizes (or axial ratios, if the size is known) from n-measurements.

This principle of size analysis was tested in extensive spectrographic investigations on light scattering of gelatin solutions. The objective was limited to determining relative sizes and to studying the kinetics of changes in size of gelatin particles. The results were encouraging and seemed to warrant the development of the method into a quantitative method. As an example, the following table gives the variation of n in a 3 percent, 3:2 water-ethanol solution of Nelson photographic gelatin containing 100 millimoles of NaCl, with the time, t, elapsed since the solution, in equilibrium for 35°C, was brought to the lower constant temperature of 18.0°C.

t (hours):	0.17	2.25	7.5	12.75	25.0	47.5
n:	4.0	3.5	2.5	2.0	2.0	2.0

The change in size here is, as shall be explained elsewhere, caused by a reversible aggregation of molecules to so called

"geloids" which are responsible for gel formation. The size of these aggregates varies with the experimental conditions, such as temperature, protein concentration, and composition of the solvent.

[1] W. Heller and E. Vassy, Phys. Rev. **63**, 65 (1943).
[2] G. Mie, Ann. d. Physik **25**, 377 (1908).

The Determination of Particle Sizes from Tyndall Spectra*

W. HELLER
Chemistry Department, Wayne University, Detroit, Michigan
AND
H. B. KLEVENS† AND H. OPPENHEIMER
Chemistry Department, University of Chicago, Chicago, Illinois
June 24, 1946

TYNDALL spectra in light scattering systems without selective absorption furnish a hitherto neglected principle for the determination of particle sizes within an important range of ultramicroscopic dimensions. The principle, based on the decrease of the wave-length exponent, n, with increasing particle diameter, above dimensions of $\sim\frac{1}{10}$ of the wave-lengths used, was outlined in a previous paper[1] and it has now been used for a quantitative method. For this purpose, particle size determinations were carried out with the slit ultramicroscope, using model systems described below. The data obtained were correlated with the wave-length exponent which was obtained, on the same systems, from spectrophotometric measurements of the conservative absorption, the latter being equivalent to spectrophotometric measurements of the global Tyndall effect. Two instruments, the visual Pulfrich spectrophotometer and the Beckman photoelectric spectrophotometer were used for the experiments. The range of wave-lengths covered was 4000–6500A for the latter and about 1000A less for the former. Using the principle outlined previously,[1] true absorption—which would interfere with the measurements—was found to be practically absent above 3800A. The calibration curves, obtained on the variation of n with particle size, depend slightly on the amount of Tyndall light radiated in the direction of the primary beam. The respective solid angle was defined for the Pulfrich instrument, under the conditions used, by $\leqslant 4°$, depending on the slit width (turbidity). The angle is larger for the Beckman instrument where it is constant by virtue of the standard construction of the apparatus. The wave-length exponent obtained for a given particle size decreases slightly with increasing concentration of the particles. This effect was excluded by compiling n in each instance for a series of concentrations and by extrapolating to infinite dilution. The latter value generally differs by not more than 5 percent from the lower value obtained at a concentration of 0.1 percent, the latter being approximately the highest concentration used in all experiments.

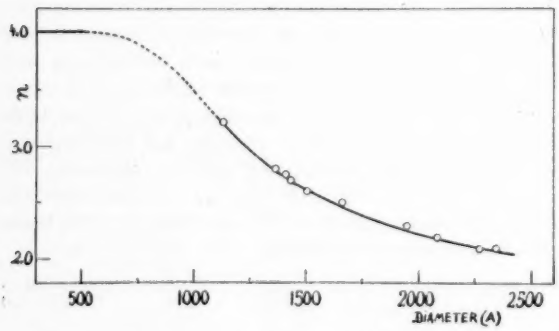

FIG. 1. Variation of wave-length exponent with the diameter of spherical dielectric particles.

The model systems used were aqueous emulsions of polystyrene, polyisoprene and styrene-isoprene copolymer. Ultramicroscopic observations showed that these particles were spherical (in contradistinction to the molecules of which they are composed). Extensive optical investigations of the authors on the locus and mechanism of emulsion polymerization, by means of a spectrophotometric-interferometric method,[2] and with the ultramicroscope—selected results have already been published[3]—showed that the size of these particles can be varied and controlled by varying the reaction time and temperature, and the nature and concentration of the emulsifier used. The information thus gained made it possible to vary the average particle diameter systematically between <500 and ~ 3000A, the size range desired for calibrations of n against particle sizes. Because of the courtesy of the United States Rubber Company, electron-microscopic material could be examined which showed that the size distribution curve in systems as those used is—if prepared in the presence of a stabilizer—generally fairly symmetrical and has a half-width of approximately 200A. The results obtained for the calibration curves, therefore, do not differ appreciably from those to be expected from strictly monodisperse systems.

Figure 1 represents the calibration curve obtained with a series of polystyrene emulsions. It is valid for a refractive ratio $m = n_P/n_M$ (n_P, refractive index of the light scattering particles, n_M, refractive index of the medium) of 1.23–1.25. The total range of m covered thus far in the various series extends from 1.18–1.25. Since light scattering is, in absence of true absorption, wholly independent of the chemical nature of the particles, the data obtained may be applied for particle size determinations in any type of dispersed system with spherical particles and refractive ratio 1.24 ± 0.01. (These refractive ratios were determined interferometrically from the refractive indices of the emulsion and of the medium, using, for the calculation of n_P, a mixture rule given recently.)[4]

TABLE I.

Reaction time (hours)	Percent conversion	n	Diameter (A)
6	<0.5	4.0	500**
9	<0.5	4.0	570**
11	<0.5	3.95	~700**
14	~0.5	3.8	800
18	1.0	3.5	900
36	2.3	2.85	1150
60	3.0	2.5	1500
360	13.8	2.1	2300
540	44.0	2.05	2550
660	59.5	2.0	~2700

** Determined from the quantitative value of light scattering itself, reference 2.

An example of the practical application of the method for rapid particle size determinations is given in Table I which contains data on the variation of the particle diameter of polymer with percent conversion of monomer to polymer in agitated styrene-isoprene reaction mixtures which were kept in bombtubes at 50°C, in presence of 0.2 percent of potassium caprylate as emulsifier. The calibration curve differs here from that in Fig. 1 (in <1.23).

* The work reported in this abstract was done at the University of Chicago in connection with the Government Research Program on Synthetic Rubber under contract with the Office of Rubber Reserve, Reconstruction Finance Corporation. Details of the method and results are given in the restricted reports Comptes rendus 87, 124, 237 (1943); 470 (1944); 845, 846, 858, 888 (1945).

† Present address: Firestone Tire and Rubber Company, Akron, Ohio.

[1] W. Heller and E. Vassy, J. Chem. Phys. **14**, 565 (1946).
[2] W. Heller and H. B. Klevens, Phys. Rev. **67**, 61 (1945).
[3] W. D. Harkins, J. Chem. Phys. **13**, 381 (1945); **14**, 47 (1946).
[4] W. Heller, Phys. Rev. **68**, 5 (1945).

Spectrophotometric Studies on Solubilization of Hydrocarbons*

W. HELLER
Chemistry Department, Wayne University, Detroit, Michigan
AND H. B. KLEVENS†
Chemistry Department, University of Chicago, Chicago, Illinois
July 16, 1946

A STRONGLY light scattering emulsion is formed on exceeding the limiting concentration of hydrocarbon, c_1, which defines its solubility in a soap solution. A quantitative spectrophotometric method for studies on solubilization was based on this known fact. c_1 is characterized by a minimum in light scattering which facilitates the measurements. Special joint studies with H. Oppenheimer showed that the minimum is caused by a decrease in size of molecular aggregates of soap, with increasing oil concentration, at concentrations $<c_1$. Solubilization studies on ethylbenzene gave the following results valid at 20°–25°C.

(1) c_1 increases with time, particularly in concentrated solutions where a practically final value is reached only after 60 hours.

(2) The number of moles of ethylbenzene, dissolved per mole of soap, R_m, increases for a given soap concentration, with increasing chain length of the soap molecules. R_m, implicitly, increases with a decrease in the "critical soap concentration," c_{cr}, above which micelles are formed. Considering 15 percent soap solutions, the following R_m (c_{cr}) values were found: KC_6: 0.0031 (1.62); KC_8: 0.080 (0.395); KC_{10}: 0.207 (0.100); KC_{12}: 0.433 (0.023); KC_{14}: 0.870 (0.007). The c_{cr} values, in moles of soap per liter were determined in supplemental experiments by other methods.

(3) With an increase in concentration of a given soap, R_m first decreases, reaches a minimum, and then increases nearly linearly without definite indication of approaching saturation at a 15 percent concentration. The minimum value of R_m, is reached at c_{cr}, providing thereby a new method for determining c_{cr} from solubilization measurements. c_{cr} thus found for KC_{12} is 0.025 mole per liter.

(4) Adopting the concept of the lamellar micelle structure,[1a,1b] using cross-sectional areas of soap molecules as obtained from x-ray measurements and assuming that the density of ethylbenzene absorbed in the micelles is, in the first approximation, identical with that of liquid ethylbenzene, one can calculate from R_m—corrected for oil dissolved by micelles only—the thickness (spacing) of the individual intermicellar ethylbenzene layers. For KC_{12}, one thus finds, by interpolation, that the oil layer is equivalent to a completed monomolecular layer and a bimolecular layer at a soap concentration of 0.09 and 0.50 mole per liter, respectively. According to extrapolation, a trimolecular layer would be completed at a concentration of 1.08 moles per liter. The corresponding spacings are $2.7+2\epsilon$, $5.4+2\epsilon$, and $8.1+2\epsilon$A, respectively, where ϵ, a fraction of one A, represents the unknown distance, at a minimum of potential energy between the hydrophobic ends of the oriented soap molecules and the neighboring ethylbenzene molecules.

* The work reported in this abstract was done at the University of Chicago in connection with the Government Research Program on Synthetic Rubber under contract with the Office of Rubber Reserve, Reconstruction Finance Corporation. The methods used were developed early in 1943.

† Present address: Firestone Tire and Rubber Company, Akron, Ohio.

[1] a: J. W. McBain, in *Advances of Colloid Science* (Interscience Publishers, New York, 1942), Vol. 1, pp. 99–143; b: several recent papers by W. D. Harkins and co-workers, e.g., W. D. Harkins, R. W. Mattoon, and M. L. Corrin, J. Am. Chem. Soc. **68**, 220 (1946).

Refractive Indices of Soaps and Detergents*

H. B. KLEVENS†
Department of Chemistry, University of Chicago, Chicago, Illinois
June 28, 1946

ACCORDING to Hess, Philippoff, and Kiessig,[1] the variation in the refractive indices with the concentration for various soaps is characterized by an intersection of two linear functions. The authors believe that this intersection represents the critical micelle concentration above which micelles are formed. These experiments were repeated and expanded using a Haber-Loewe type of interferometer (layer thickness, 160.290 mm, $T=23.5$°C) using both cationic and anionic soaps or detergents; a few preliminary data are given below.

The results reported here are those obtained with lauryl amine hydrochloride (LA-HCl) and with potassium laurate (KC_{12}). The former was kindly supplied by the Research Laboratories of Armour and Company and was subsequently recrystallized five times; the latter was prepared by multiple fractionation of the methyl ester of lauric acid, followed by saponification and repeated recrystallizations.

The refractive indices change in the case of LA-HCl between 1.332849 and 1.336065 and for KC_{12} between 1.332828 and 1.335640 over a concentration range from 0.10 percent to 2.00 percent. Plotting of this data gives two straight lines for each series which intersect at 0.29–0.30 percent for the LA-HCl and at 0.61–0.62 percent for the KC_{12} solutions. The refractive increment, $(n_i-n_m)/c$, where n_i is the refractive index of the solution, n_m the refractive index of the medium, and c the concentration in grams per hundred grams solution, reaches a maximum value at 0.29–0.30 percent and at 0.61–0.62 percent for LA-HCl and KC_{12}, respectively.

More significant is the change with concentration in the refractive index of the solute itself (n_s). These values were obtained by use of the new mixture rule reported recently by Heller.[2] These results are plotted in Fig. 1. In both cases,

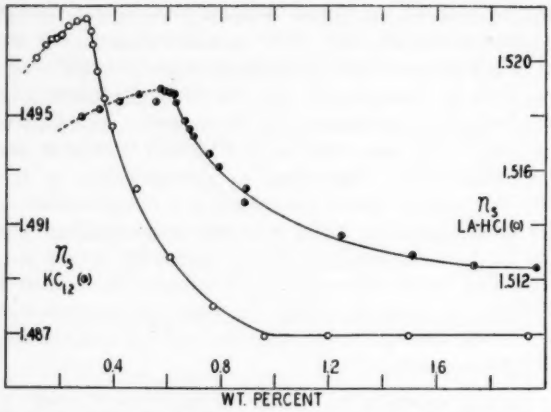

FIG. 1. The change in the refractive indices of lauryl amine hydrochloride (LA–HCl) and potassium laurate (KC_{12}) with concentration. The dotted portion of the curve is the region in which there is as yet no certainty that the equation used here is valid.

n_s increases slightly and then decreases suddenly, apparently then approaching a constant value at concentrations above 1.2–1.3 percent. Ralston and Hoerr[3] reported a discontinuity in the equivalent conductivity curve at a concentration of 0.29 percent for the LA-HCl. This agreement between the two methods regarding the concentration at which a discontinuous change in the properties of soap and detergent solutions occurs, is significant. In the case of KC_{12}, the values obtained by Bury and Parry[4] from density measurements indicate that this discontinuity occurs at about 0.9 percent at 25°C. Recently, from measurements of the spectral shifts of cyanine dyes, a value of 0.54–0.57 percent has been reported as the critical micelle concentration for KC_{12}.[5]

If one were to consider these and other similar discontinuities as indicative of a formation of a new phase in soap solutions, then the value of n_s at concentrations below the break point would represent the refractive indices of molecularly dispersed soaps or detergents or of a simple micelle, and the asymptotic values of n_s at concentrations above the maximum, the refractive indices of micellar soap or of aggregates of micelles. The values between these two regions may be caused by mixtures of these various forms, or by a gradual change in form or aggregation. Further, it may prove possible, if the first hypothesis is correct, to determine the relative amounts of molecular and micellar soap present in this intermediate region when more data are available.

Comparison of the discontinuities observed for various properties of soap solutions shows that the discontinuity observed in n_s is particularly interesting because it is characterized by a considerable change in the slope, whereas in most other experimental results there is only a small change in slope.

* The work reported in this paper was done in connection with the Government Research Program on Synthetic Rubber under contract with the Office of Rubber Reserve, Reconstruction Finance Corporation.
† Present address: Firestone Tire and Rubber Company, Akron, Ohio.
[1] K. Hess, W. Philippoff, and H. Kiessig, Kolloid Zeits. **88**, 40 (1939).
[2] W. Heller, Phys. Rev. **68**, 5 (1945).
[3] A. W. Ralston and C. W. Hoerr, J. Am. Chem. Soc. **64**, 772 (1942).
[4] C. R. Bury and G. A. Parry, J. Chem. Soc. (London) 626 (1935).
[5] M. L. Corrin, H. B. Klevens, and W. D. Harkins, J. Chem. Phys. **14**, 216 (1946).

On the Dissociation Energies of CO, N_2, NO, and CN

J. G. VALATIN
Institute of Experimental Physics, Hungarian University for Technical and Economic Sciences, Budapest, Hungary
July 18, 1946

GAYDON and Penney tried to obtain dissociation schemes with respect to CO, N_2, NO, CN by a systematic application of the non-crossing rule of the energy eigenvalue curves of the two-center problem to the potential curves of the molecule.[1] Their paper shows that even their correlation leads to contradictions with such a non-crossing rule for the excited states since they consider the correlation of the molecular ground state to the atomic ground states as a necessary consequence of this rule. For instance in Herzberg's CO dissociation scheme there are also crossings of the same species with respect to the potential curves of the states $a\ ^3\Sigma^+$ and $A\ ^1\Pi$ with the corresponding repulsive curves. Moreover, the dissociation schemes given by Gaydon and Penney do not seem to be reconcilable with other spectroscopic arguments.

Schmid and Gerö have pointed out several times that the non-crossing rule cannot be applied to the correlation of molecular terms to the atomic term combinations, strong spectroscopic arguments being adducible both in the use of the molecules mentioned and in the case of diatomic hydride and deuteride molecules.[2] In addition, theoretical considerations show,[3] that from the non-crossing of the energy eigenvalue curves of the two-center problem one cannot deduce the sequence of the discrete energy levels of the molecule, and the possibility of the violation of a non-crossing rule does not have to be specially postulated. The potential curves of unperturbed electronic states, resulting by an averaging of the interactions with respect to the electronic motions which can also be influenced by the nuclear motion, cannot, in general, be identified with the energy eigenvalue curves of the two-center problem.

Table I shows the dissociation energies and dissociation products of CO, N_2, NO, CN as given by Schmid and Gerö. The corresponding dissociation schemes can be regarded as taking into consideration all the spectroscopic data. The bond energies are to be counted from the atomic term

TABLE I.

Molecular ground state	Dissociation products	Bond energy cm^{-1}	Lowest atomic term combination	Dissociation energy cm^{-1}
CO $X^1\Sigma^+$	$C(^1D)+O(^1D)$	81,660	$C(^3P)+O(^3P)$	55,600[a–e]
N_2 $X^1\Sigma_g^+$	$N(^2D)+N(^2D)$	78,750	$N(^4S)+N(^4S)$	40,350[d,e]
NO $X^2\Pi$	$N(^2D)+O(^3P)$	53,800	$N(^4S)+O(^3P)$	34,600[d–f]
CN $X^2\Sigma$	$C(^1D)+N(^2D)$	61,100	$C(^3P)+N(^4S)$	31,700[g]

[a] R. Schmid and L. Gerö, Zeits. f. physik. Chemie **B36**, 105 (1937).
[b] R. Schmid and L. Gerö, Zeits. f. Physik **106**, 205 (1937), **112**, 676 (1939).
[c] R. Schmid and L. Gerö, Physik. Zeits. **39**, 460 (1938).
[d] R. F. Schmid and L. Gerö, Csillagászati Lapok **6**, 101, 102 (1943). Short English communication.
[e] R. Schmid and L. Gerö, "Matematikai és Természettudományi Értesitö," Communications of the Hungarian Academy of Sciences, **62**, 408, 416 (1943). In Hungarian with German abstract.
[f] L. Gerö, R. Schmid, and F. K. v. Szily, Physica **11**, 144 (1944).
[g] R. Schmid, L. Gerö, and J. Zemplén, Proc. Phys. Soc. **50**, 283 (1938).

combination corresponding to the dissociation of the molecular state, whereas the thermochemical dissociation energies are the lower values counted from the lowest atomic term combination. In thermochemical calculations concerning organic compounds generally energy values corresponding to the tetravalent ^5S state of carbon are to be taken into account, the energy values given for CO, CN having to be modified according to $C(^5S)=C(^3P)+33800\ cm^{-1}$.[4] The heat of sublimation of carbon into ^5S carbon atoms calculated from these results is 170 kcal.

[1] A. G. Gaydon and W. G. Penney, Proc. Roy. Soc. **A183**, 374 (1945).
[2] L. Gerö and R. Schmid, Zeits. f. Physik **111**, 588 (1939), **115**, 47 (1940).
[3] J. G. Valatin, in the course of publication.
[4] R. Schmid and L. Gerö, Zeits. f. Physik **105**, 36 (1937).

The Crystal Structure of Polonium

WILLIAM H. BEAMER AND CHARLES R. MAXWELL
Santa Fe, New Mexico
September 12, 1946

PRELIMINARY results of the investigations of various physical properties of polonium in this laboratory indicate that polonium undergoes a phase transformation at about 75°C. This was first discovered in experiments by one of the writers (C.R.M.) in measuring the thermal coefficient of electrical conductivity of thin polonium films. A plot of these data exhibits an abrupt decrease of electrical conductivity which is attributed to a phase change. This transformation has been further identified by x-ray diffraction powder photographs. For this work about 100 micrograms (0.5 curie) of pure polonium were vacuum distilled into a capillary about 0.3-mm diameter and 0.01-mm wall thickness at residual gas pressure below 10^{-5} mm of mercury. The metal was concentrated in a short length of the capillary by two successive vacuum distillations in a closed system under a thermal gradient. The capillary was outgassed before use for about 20 hours at 425°C at 10^{-6} mm of mercury pressure. Diffraction patterns have been obtained of three samples using copper and iron radiation. Because of the load formed by the radioactive disintegration of the polonium, the patterns change with time. This change is being followed in an effort to obtain knowledge of the Po-Pb system. The rate of formation of lead is approximately 0.5 percent per day. The photographs used for structure determination were taken from freshly prepared samples so that the lead content was less than 2 percent.

The crystal structure of polonium was studied by electron diffraction by Rollier, Hendricks, and L. R. Maxwell.[1] These workers interpreted the pattern obtained by transmission of thin films of polonium about 100A thick as that of a monoclinic structure. Table I shows a comparison of their data with those of this investigation. Column 1 gives the ring number, columns 2 and 3 give $1/d^2$ and the intensity estimate for the ring as reported by Rollier, Hendricks, and Maxwell, columns 4 and 5, 6 and 7 give $1/d^2$ and intensity of the low temperature and high temperature forms of polonium, respectively. It appears that the earlier investigation was carried out on a mixture of the two phases.

TABLE I.

Ring No.	Reported in reference (1) Intensity	Reported in reference (1) $1/d^2$	Low temperature form Intensity	Low temperature form $1/d^2$	High temperature form Intensity	High temperature form $1/d^2$
1	*VS*	0.0890 to 0.0940	*VS*	0.0897	*VS*	0.0932
2	*M*	.1580			*S*	.1550
3	*MS*	.1804	*S*	.1791		
4	*W*	.2175			*MS*	.2169
5	*MW*	.2481			*MS*	.2489
6	*W*	.2642	*MW*	.2692		
7	*W*	.3634	*W*	.3560		
8	*VW*	.370			*M*	.3735
9	*M*	.4068			*MS*	.4047
10	*M*	.4480	*M*	.4486		
11	*VW*	.46			*W*	.4669
12	*S*	.5310	*MW*	.5364	*MS*	.5279
13	*W*	.7170	*VW*	.7177	*W*	.7155
14	*VW*	.8000	*W*	.8062		
15	*W*	.8465			*MW*	.8396
16	*W*	.8953	*W*	.8978	*VW*	.8714
17	*MW*	.9920	*VW*	.9860	*VW*	.9947
18	*VW*	1.149	*F*	1.164	*VW*	1.151
19	*VW*	1.248	*VW*	1.253		
20	*W*	1.473	*VW*	1.519	*VW*	1.458
					F	1.489
21	*VW*	1.627	*F*	1.607	*F*	1.613
					F	1.638

The high temperature form is present in the capillary when the surroundings are at room temperature. The polonium is maintained above the transition temperature by the heat evolved in stopping its alphas (theoretically 27.42 calories/curie/hour). The low temperature form was found after the capillary had been cooled for several hours in an air stream at about −10°C.

Complete structures have not yet been worked out for the two forms of polonium. Preliminary calculations show that the low temperature form fits a simple cubic lattice with $a=3.34$A. It has been pointed out to us by Dr. W. H. Zachariasen that the high temperature form can be indexed as a simple rhombohedron with $a=3.36$A and $\alpha=98°13'$. A rough density determination is being made.

This work is being carried out under contract between the University of California and the Manhattan District, Corps of Engineers, War Department.

[1] Rollier, Hendricks, and Maxwell, J. Chem. Phys. **4**, 648 (1936).

The Superficial Density of the Energy of Natural Vibrations

A. BRAGER AND A. SCHUCHOWITZKY
Moscow, Russia
July 26, 1946

WHEN solving different physical problems one is often confronted with the necessity of summing up the energy of natural vibrations of a restricted body.

The solution of this problem for the case of the electron gas is known to correspond to Sommerfeld's theory of metals. A calculation of the energy of acoustic vibrations gives according to Debye the thermal energy of a solid body. Finally, Planck's law of the blackbody radiation corresponds to a summation of the energy of electromagnetic vibrations. In all the above-mentioned cases, however, this summation has always been carried out without taking into account the boundary conditions,

i.e., neglecting the effect due to the superficies of the vibrating body.

Our having taken into account this effect[1,2] leads to a calculation of the superficial density (in Gibbs's sense of the term) of the energy of natural vibrations. For the first of the above problems this superficial density gives a correct idea of the main features of the surface tension of metals. For the second problem a calculation of this kind results in establishing the dependence of the specific heat of dispersed bodies and the surface tension of solid bodies on the temperature. By considering the third problem along the same lines the surface tension of the radiation has been calculated.

While solving the first problem[1] it was essential to bear in mind that the electrons when fixed on the boundaries of the body cannot occupy energy levels with quantum numbers equaling zero. It was also important to estimate the error due to the substitution of the integration for a summation of the energy of natural vibrations. The latter process requires a determination of the number of whole points in the sphere. By effecting these calculations on the basis of Vinogradoff's paper[3] we derived the following equation for the calculation of the surface tension of metals

$$\sigma = 56{,}400(\gamma/A)^{4/3}\ \text{dyne}\cdot\text{cm}^{-1}, \qquad (1)$$

where A is atomic weight and γ is density of the metal, g. cm^{-3}.

A comparison with experimental data has shown that Eq. (1) expresses the order of magnitude and the dependence of the surface tension on the density of the electron gas.

An important factor in the solution of the second problem[2] is the fact that for an entirely free surface, account should be taken of the presence of the Rayleigh and transitional (from ordinary to Rayleigh) waves. This could be only done by considering a vector problem.

By making use of Lamb's[4] solution of the problem of the vibrations of the infinite thin plate, we derived the following equation for the specific heat of a non-compressible solid body:

$$c_v = 9Nk\left[\frac{4}{x^3}\int_0^x \frac{\xi^3 d\xi}{e^\xi - 1} - \frac{x}{e^x - 1}\right] + \frac{4.26 N^{2/3} k F^{2/3} l^{2/3}}{V^{2/3}}\left[\frac{6}{x^2}\int_0^x \frac{\xi^2 d\xi}{e^\xi - 1} - \frac{2x(e^x-1)+x^2e^x}{(e^x-1)^2}\right] \qquad (2)$$

which at low temperature passes into:

$$c_v = \frac{467.56}{V_m \cdot x^3} + \frac{61.3F}{V_m^{2/3} x^2 \cdot N_A^{1/3}}. \qquad (3)$$

In these equations N is the number of atoms contained in the body in question, with volume V, surface F, and length of edge of base l; x and ξ have the same meaning as in the Debye theory: $x = h\nu_{max}/kT$; $\xi = h\nu/kT$; V_m is molecular volume; N_A is Avogadro's number.

The first terms in Eqs. (2) and (3) are the usual expressions for the specific heat of a solid body according to the Debye theory. An estimation of the second term in Eq. (3) shows that a measurement of the specific heat of dispersed bodies (catalysts and activated charcoal, for example) at low temperature may serve as a method for determining their specific surface. The difference in the specific heat of activated charcoal and graphite, for example, as established by Simon and Swain,[5] corresponds to the specific surface of charcoal in its order of magnitude.

The authors wish to express their gratitude to Professor I. E. Tamm and Professor M. A. Leontovitch for a number of valuable suggestions made by them while discussing the results of the present investigation at the different stages of its progress.

[1] A. Brager and A. Schuchowitzky, Acta Physicochimica U.S.S.R. 21, 13 (1946).
[2] A. Brager and A. Schuchowitzky, Acta Physicochimica U.S.S.R. (in press).
[3] I. Vinogradoff, Trans. (Trudy) Stekloff Math. Inst. Acad. Sci. U.S.S.R. 9, 17 (1935).
[4] H. Lamb, Proc. Roy. Soc. **A93**, 114 (1917).
[5] F. Simon and R. Swain, Zeits. f. physik. Chemie **B28**, 189 (1935).

Upper and Lower Bounds to Rayleigh's Frequency for a Vibrating System

WILLIAM J. TAYLOR[1]
National Bureau of Standards, U. S. Department of Commerce, Washington, D. C.
April 18, 1946

THE variation method of quantum mechanics has been extended by D. H. Weinstein[2] to yield upper and lower bounds for the eigenvalues of the wave equation. The method of Weinstein may be extended to the frequencies of a system of coupled harmonic oscillators. The characteristic equation of the system may be written as

$$Vk_i = \lambda_i T k_i,$$

where V and T are the real symmetric potential and kinetic energy matrices, respectively, k_i is a real eigenvector (normal mode), and λ_i is the corresponding real positive eigenvalue ($\lambda_i = 4\pi^2\nu_i^2$, where ν_i is the frequency). The secular equation for vibrations thus contains two non-commutable symmetric (real Hermitian) matrices, and in this respect differs from the wave equation of quantum mechanics, which contains a single Hermitian operator (the Hamiltonian). However the secular equation may be made isomorphic with the wave equation by transforming to a representation in which T is reduced to the unit matrix and V remains symmetric. The method of Weinstein may then be applied. Alternatively, the method with modifications may be applied directly to the secular equation in its original form. In either case the following result is obtained.

At least one eigenvalue, λ_i, lies within the range

$$\mu_1 \pm (\mu_2 - \mu_1^2)^{\frac{1}{2}},$$

where

$$\mu_1 = (k'Vk)/(k'Tk),$$
$$\mu_2 = ((Vk)'T^{-1}(Vk))/(k'Tk).$$

k is an arbitrary (variation) vector. Primed and unprimed vectors are row and column vectors, respectively. $\mu_1 = 4\pi^2\nu^2$, where ν is the frequency of the system when it is forced by means of constraints to vibrate in a non-normal mode k.[3] μ_1 and μ_2 are positive or zero. If k is an eigenvector, k_i, $\mu_1 = \lambda_i$, and $(\mu_2 - \mu_1^2) = 0$. If k is not an eigenvector,

$(\mu_2-\mu_1^2)>0$. Therefore, at least in principle, the minimization of $(\mu_2-\mu_1^2)$ provides a method of obtaining all the eigenvalues and eigenvectors.

G. Kron[4] has recently made use of Rayleigh's estimate of the frequency in connection with electric circuit models for the vibration of polyatomic molecules.

[1] Research Associate on the American Petroleum Institute Research Project 44 on the "Collection, Analysis, and Calculation of Data on the Properties of Hydrocarbons," at the National Bureau of Standards.
[2] D. H. Weinstein, Proc. Nat. Acad. Sci. **20**, 529 (1934); J. K. L MacDonald, Phys. Rev. **46**, 828 (1934).
[3] Lord Rayleigh (J. W. Strutt), Proc. London Math. Soc. **4**, 357 (1873).
[4] G. Kron, J. Chem. Phys. **14**, 19 (1946).

The Preparation of Mixed Thallium Bromide-Iodide for Infra-Red Transmission

O. F. Tuttle and P. H. Egli
Naval Research Laboratory, Washington, D. C.
July 25, 1946

MIXED thallium bromide-iodide crystals were synthesized in Germany for use in military infra-red optical instruments. Superior chemical and mechanical stability and the increased range of infra-red transmission of these crystals make them appear promising for a variety of infra-red applications.

The composition of the material was reported in a foreign technical mission report by Dr. Wallace Brode, but the method of preparation was not discussed. Crystals of 42 mole percent TlBr-58 mole percent TlI, having properties similar to those reported for the German material, have been synthesized at the Naval Research Laboratory by crystallization from a melt of the same composition.

Transmission measurements of a plate of the material 2 mm thick over the spectral range 0.5 to 14μ were kindly furnished by Dr. J. A. Sanderson of this laboratory. The observed transmission rose rapidly from approximately 0 percent at 0.5μ to 50 percent at 1μ and to approximately 67 percent from 10 to 14μ. Although precise transmission measurements have not been performed beyond 14μ on the present specimens, the German results reported by Brode showed constant transmission factors of about 67 percent from 2μ to 30μ with transmission decreasing at longer wavelengths to zero percent at 70μ. The light loss is caused largely by reflection, since the index of refraction of the crystal is nearly 2.4 at 10μ.

The crystals were grown from a melt using a modification of the technique developed by Bridgman[1] for growing single crystals of metals. The furnace is a vertical tubular resistance type similar to that used by Stockbarger[2] for growing single crystals of lithium fluoride. The upper section and the lower section are separated by an insulating baffle, and the temperature in the two sections is independently controlled, the baffle serving to increase the gradient in the region where growth takes place.

A mixture of the desired composition is melted in a cylindrical platinum or Pyrex crucible with a conical bottom, for which an angle of 60° has been found satisfactory. A single crystal will result provided only one nucleus is formed in the tip of the crucible; or if several nuclei form, if only one is favorably oriented to grow along the axis of the crucible.

The growth process is controlled by the temperature gradient maintained, and the rate at which the crucible is lowered through the furnace. For homogeneous growth, relatively free of strains, a sharp temperature difference is needed, and the rate of passage through the gradient must be sufficiently slow that crystallization takes place at the point of the temperature gradient in a plane across the whole surface of the solid-melt interface. Too rapid lowering causes crystallization to proceed up the sides of the boule leaving the center molten, and results in multi-crystalline formation. For this material the temperature in the upper section of the furnace is held at approximately 470°C with variations of 5°C not noticeably affecting the quality of the crystal. No heat is used in the lower section of the furnace which is open at the bottom. A lowering rate of 7 hours per inch has given excellent crystals one inch in diameter, and 32 hours per inch has proved satisfactory for two-inch diameters.

The system TlBr-TlI is characterized by a complete solid solution with a minimum temperature at a composition close to 50 mole percent. The region of minimum temperature is relatively broad, and the properties of the crystal appear not to change rapidly with small changes in composition. With sufficiently pure material, single crystals form very readily.

[1] P. W. Bridgman, Proc. Am. Acad. Sci. **60**, 305 (1925).
[2] D. C. Stockbarger, Rev. Sci. Inst. **7**, 133 (1936).